Tissue Engineering Simplified: Biodegradable Polymers and Biomimetic Scaffolds Made

Easy, Tailorable, and Economical for Tissue Engineering

by

Renato Samuel Navarro

A dissertation submitted in partial fulfillment
of the requirements for the degree of
Doctor of Philosophy
(Macromolecular Science and Engineering)
in The University of Michigan
2020

Doctoral Committee:

Professor Jinsang Kim, Co-Chair
Associate Professor Kenichi Kuroda, Co-Chair
Professor Y. Eugene Chen
Professor Joerg Lahann
Associate Professor Bo Yang

Renato S. Navarro

snavarro@umich.edu

ORCID iD: 0000-0001-5949-8251

Dedication

This work is dedicated to the memory of my father, Pedro Navarro. Your dreams and aspirations live in me.

friends and family I made have helped me grow as a scientist and person. Reminding me why I we do this. Thank you to everyone who I have met as part of the institute but in particularly to Gordon Palmer, Channing Matthews, Lydia Mensah, Laura Motta, Asya Harrison, Steven Moore.

I would like to thank my family from the bottom of my heart. Thank you for all the love and support. Especially to my father and mother who brought us to this country and worked whatever job available to pay the bills. Thank you for every fruit you picked, every house you cleaned, and odd job you took to provide for us. Mostly thank you for suffering every indignation that migrants endure in this nation to give me a chance at a brighter future. To my father, who unfortunately is not here with us any longer. Thank you for all your math lessons as a child, most importantly, thank you for believing in me. It was your voice I heard whenever I began to doubt myself. I did not become the type of doctor you imaged me, but I have made the most of your sacrifice. Again, thank you both for your love and support.

To my Daughter, **Izabela**. Thank you for your patience, love, and support.

Lastly, I would like to thank my wife **Kaela Navarro** for all her support and love during this process. Thank you for putting up with me during this process and always being there to offer your love and support. Thank you for coming with me to lab most Saturdays and Sundays so the we can spend time together and thank you for all the glassware you helped clean over the years.

Table of Contents

List of Tables

List of Figures

Abstract

Modifying scaffolds with regulatory signals has been shown to enhance the scaffold's biomimetic properties (hydrophilicity, degradation, and biocompatibility) resulting in improved regeneration. However, most polymers available for scaffolding lack chemical functionality in the backbone, limiting our ability to modify scaffolds through the conjugation of regulatory signals (growth factors, biomolecules, and peptides). Therefore, synthesizing polymers that can be fabricated into scaffolds with biomimetic physical architecture (porous, interconnected, and nanofibrous) and can be easily conjugated with these molecules through the polymers chemical functionality would result in enhanced regeneration conditions.

Poly(spirolactic-co-lactic acid) (PSLA), a derivative of poly(L-lactic acid) (PLLA), is an attractive candidate for scaffolding in tissue engineering due to its tailorable functionality and PLLA-like properties. However, traditional polymerization methods have resulted in low molecular weight PSLA copolymers (<30 kDa) unsuitable for tissue engineering (< 150 kDa). To mitigate these effects and develop lactone polymers containing high molecular weight (HMW) suitable for scaffolding in the laboratory, we developed a method of using cold polymerization (-80 ℃) and triazabicyclodecene organocatalyst in solution polymerization. In this manner, we can mitigate the viscosity and water effects that plague traditional polymerizations, thereby producing polymers suitable for scaffolding (< 350 kDa).

To demonstrate the utility of the PSLA copolymer for tissue engineering, small diameter (< 6 mm ID) biomimetic tubular scaffolds were developed for in situ implantation in female rat models. Through the PSLA's highly reactive norbornene ring, an anticoagulant molecule (heparin) was conjugated into the backbone to mitigate the effects of thrombosis. Thus, by modulating the amount of heparin, we were able to increase the biocompatibility as well as tune the hydrophilicity and degradation rate. The viability of the

scaffolds modified with heparin was tested in vivo by implanting the scaffolds as replacement vessels (1 cm) in the descending aorta below the renal arteries. The patency and viability were confirmed through dynamic ultrasound and histological analysis of the explanted tissue, demonstrating excellent tissue reconstruction with a laminar cellular arrangement and no sign of hyperplasia, aneurysm, or thrombosis. Furthermore, we achieved complete endothelization of the vessel lumen and enhanced extracellular matrix decomposition (collagen & elastin). Through the use of PSLA, we developed a biocompatible vascular graft that can mitigate thrombosis and generate small-diameter blood vessels in animal models.

To improve current post-modification methods, we have developed a copolymer derived from L-lactide, poly(exomethylene-co-lactic acid) (PELA), with click-chemistry reactivity under physiological conditions in the absence of catalyst, heat, or organic solvents and without producing toxic byproducts. The copolymer itself (exomethylene lactide segment) can be rapidly (seconds) conjugated with amine-containing molecules, forming a stable and enzymatically cleavable amide bond. The polymer can be processed into biomimetic tissue engineering scaffolds with excellent mechanical properties. Taking advantage of the facile conjugation method, we were able to demonstrate that we can tune properties such as wettability, degradation rate, and biocompatibility. Finally, we demonstrate biocompatible and enhanced cell penetration into the PELA scaffolds through the use of in vitro and in vivo (subcutaneous implantation) assessment.

This original work provides insightful molecular design and development strategies that can be readily adapted by researchers in tissue engineering and regenerative medicine research due to the simplicity, cost-effectiveness, and effectiveness.

Chapter 1. Biodegradable Polymers for Biomedical Applications Scaffolds in Tissue Engineering

1.1 Tissue Engineering Scaffolds

1.1.1 Tissue engineering for tissue regeneration

Tissue engineering is exciting interdisciplinary approach to supply tissue and organs after injury or disease [1-6]. The goal of tissue engineering is to restore, maintain, and improve tissue function after critical loss of tissue [2, 7-9]. Through the combination of material science and engineering and life sciences novel approaches are developed to address the need of vital tissues that at times can prevent death. At the core of tissue engineering, polymers fashioned into tissue engineering scaffolds are an invaluable tool to provide support for tissue regeneration [10-14]. Scaffolds don't only provide a supporting environment in which cells are able to occupy but can also be involved in promoting cellular processes and response [2, 10-15]. Specifically, scaffolds are able to guide cell growth, promote natural extracellular matrix formation, which can lead to formation of functional tissues and organs [4, 16-18]. In the absence of such scaffolds, where the body is unable to regenerate itself after disease or injury the body can experience *i*) scar tissue formation leading to loss of function *ii*) improper repair and regeneration *iii*) and extreme cases death[18]. Therefore, depending on the tissue that is injured or diseased it is crucial to identify means in which to optimize regeneration. Beyond providing structural support scaffolds that have experienced the best success also include support for cell attachment, proliferation, and differentiation [11, 16, 19-21]. Therefore, scaffolds play an equal part in combination with regulatory

1

signals and cells that lead to the best tissue formation possible. This thought has led to the development of the tissue engineering triad, a scheme to illustrate how biomaterials can be utilized in combination with cells and regulatory signals for tissue engineering [**Figure 1.1**] [22-24].
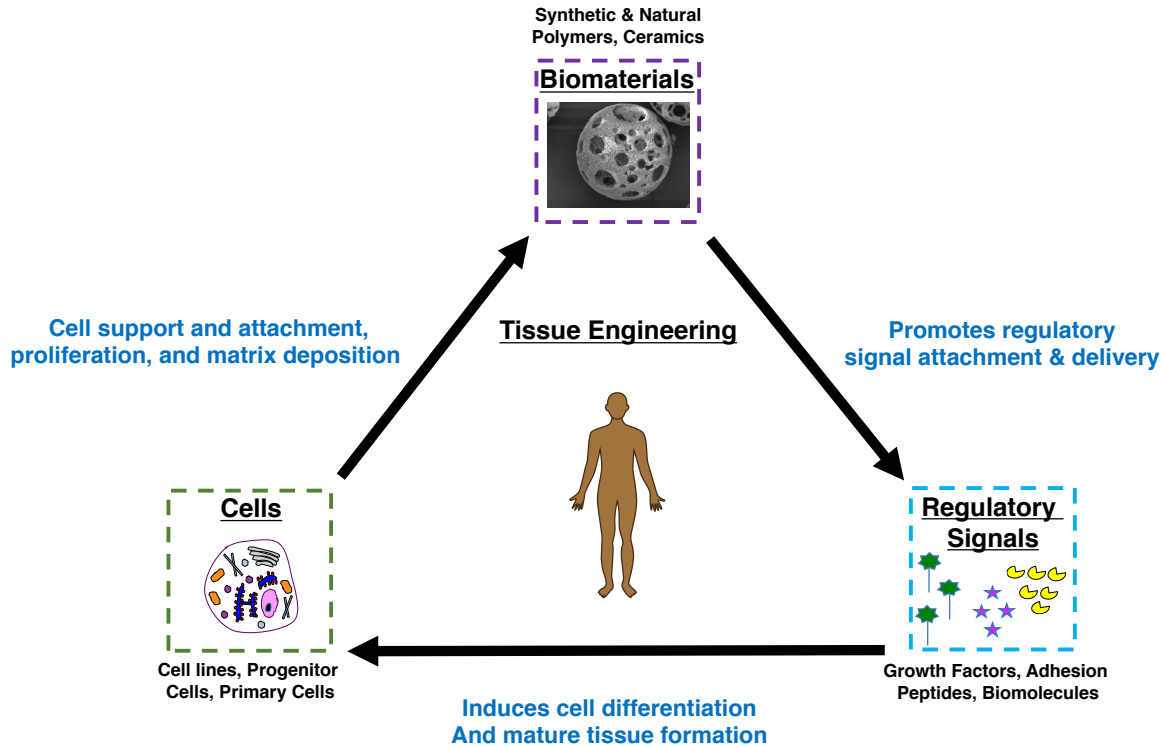
Figure 1.1 Tissue engineering triad depicting the interplay of cells, regulatory signals, and biomaterials in tissue engineering.

When discussing the favorable scaffold properties, it is important to mention that scaffolds derive their characteristics from the polymers that they are fabricated from [2, 15, 25-27]. The polymers inherit properties – hydrophobicity, biocompatibility, mechanical properties – will directly translate into the retention/degradation rate, biocompatibility, and mechanical properties exhibited by the scaffolds. For this reason, polymers for tissue engineering will be discussed in depth in a later section. The work presented in this document will focus on the development of biodegradable polymers to fabricate the best scaffolds possible, therefore it is imperative that we define what basic criteria scaffolds should exhibit i) biocompatible ii) biodegradable iii) three-

dimensional structure iv) mechanical integrity to support handling and regeneration [3, 4, 11, 16].

Particularly, biodegradation is important as tissue engineering scaffolds should be remodeled to produce tissue similar to the natural tissue found [28-31]. Another important factor that has been shown to improve tissue formation is the geometry that scaffolds are fabricated in order be match the tissue need [12, 21, 32-36]. Scaffolds can be fabricated through various process and methods. Currently, the most favorable approaches utilize molds, electrospinning, or templates (porogen). Through these methods scaffolds can be fabricated in an array of shapes such as disk, tubular, and sphere to name a few[34-38]. What is important to note is that with current approaches we are able to fabricate scaffolds for specific tissue applications which have made a tremendous difference in the resulting tissue. This has been of particular importance in vascular tissue engineering as we are able to fabricate specific inner and outer diameter tubular scaffolds that fit the vasculature which is being replaced.

1.1.2 Imparting biomimetic properties through physical architecture

To this point, we have discussed the basic requirements of tissue engineering scaffolds; however, since they were first utilized, scaffolds have been optimized to contain biomimetic features [17, 39, 40]. These biomimetic features are defined as the development of facets of the natural environment in which cells find themselves and can range from topography, the inclusion of regulatory signals, mechanical properties, matching degradation to cell proliferation, and tissue formation, among others [41-48]. It has been demonstrated that as scaffolds most closely mimic the natural environment in which cells occupy the regenerated tissue more closely resembles the natural tissue. Therefore, it has become the material scientist's goal and objective to replicate both the macro and microenvironment.

In an attempt to accomplish this goal, much effort has been devoted to imparting biomimetic cues through the physical architecture of the scaffold. The use of porous and interconnected scaffolds has been of particular interest since they allow excellent mass flow, as well as cellular penetration and migration; therefore, the scaffold provides for faster remodeling and improved tissue formation[3, 12, 38, 49-51]. It has been shown that scaffolds fabricated with these features prevent sieving of the cells on the top layer when seeded and can lead to faster reconstruction in vitro and in vivo. The formation of this architecture can be achieved through the use of a porogen, such as salt or sugar that is slightly annealed [12, 14, 52-57]. When removed by washing away, a template of the spheres is left behind, providing the porous and interconnected structure. Additionally, techniques such as thermally-induced phase separation (TIPS) in combination with polymers such as PLLA have been extensively studied since they produce nanofibrous morphology that mimics the native extracellular matrix (ECM) environment both in size of fiber and mechanical forces exuded on the cell [4, 27, 33, 38, 49, 55, 56, 58-61]. This technique is particularly useful due to the ease and reproducibility, and it requires only to dissolve the polymer in a hot solvent solution such as tetrahydrofuran (THF) and quickly cool it down with best results at − 80 ºC [14, 51, 55, 62]. As the solution cools, the solvent quickly leaves, creating a polymer-rich area with fibers and pores that closely mimic the ECM proteins collagen and elastin. When combined, TIPS and porogen leaching, we can produce a biomimetic scaffold that is nanofibrous, porous, and interconnected that is conducive to an array of tissue engineering applications such as bone, vascular, cartilage, and muscle regeneration [4, 27, 33, 38, 40, 42, 49, 50, 58, 59, 63-68].

1.1.3 Polyesters for tissue engineering

Polyesters make up the primary bulk of degradable polymers utilized for tissue engineering [15, 69-72]. The mode of degradation is through biological and hydrolytic cleavable of the ester bond as it reverts to the starting materials. Their primary advantage is that they typically comprise natural molecules found in the body, and therefore when they are introduced as a biomaterial in the body and degrade, they do so without any adverse effects [26, 73]. Additionally, polyesters can be tailored in molecular weight, degradation rate (hydrophobicity), and composition, which will be discussed in this section to highlight the positive attributes of polyesters and demonstrate why they have been utilized broadly in tissue engineering [70, 74].

Polyester are fabricated from the condensation reaction between a carboxylic acid and a hydroxyl group traditionally under heat [**Figure 1.2A**] [69, 75-79]. Although, the polycondensation reaction seems simple enough, as they only require the addition of starting material under a heat source. In reality, synthesizing polyesters that can be used for tissue engineering is difficult and require precise control of polymerization conditions. The primary obstacle to overcome in polycondensation reactions is the removal of water in the reaction vessel [80]. As the reaction proceeds, water molecules are produced from the condensation reaction that can terminate the reaction. Additionally, polycondensation reactions are carried out in a bulk reaction and therefore experience viscosity issues preventing the continued chain growth addition, further amplifying the accumulation of water molecules by trapping them in the viscous glob. When produced in the industrial level, these issues can be adequately addressed through powerful reactors that can continuously stir the viscous polymer and vacuums to remove the water.

This has resulted in various polyesters that are commercially available with a varying composition (homo, copolymers, block polymers, linear, star), molecular weight, hydrophobicity

A

B
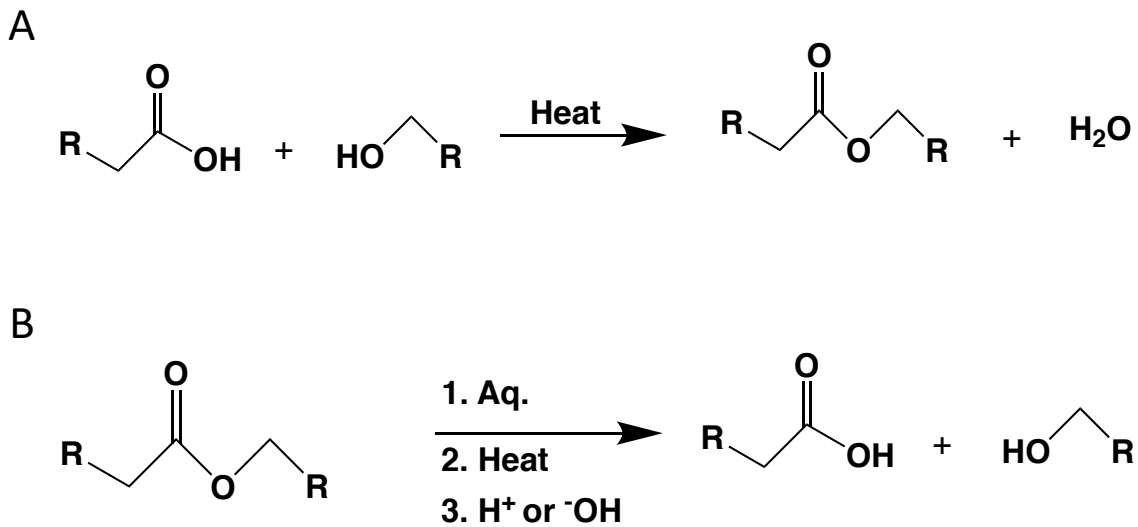
Figure 1.2 Polyester condensation and dissociation.

A) Ester condensation reaction between carboxylic acid and hydroxyl under heat leads to the release of water B) Hydrolytic cleavage of ester bonds results into dissociation back to carboxylic acids and hydroxyl group.

such as fast degrading polyesters (more hydrophilic) to slow degrading polyesters (less hydrophilic) [15, 74, 79]. The range of hydrophobicity can vary significantly with polyesters, which translates into a varying retention time both *in vitro* to *in vivo*. This time can differ from degradation as early as three weeks in (poly(glycolic acid) (PGA) and poly(glyceral-co-sebacate) (PGS) to delayed degradation of 3 years with polymers such as poly(caprolactone) (PCL) [47, 81-87]. Another method to effects retention and degradation rate is to modulate the polymer's molecular weight. Through the use of higher molecular weight, we can directly affect the degradation rate and mechanical properties of the resulting biomaterial. Lastly, polyester can be tailored by including various compositions such as adding segments of slow degrading polymers with fast degrading polymers or changing the geometry of the polymers from linear to star-shaped polymers [8, 25, 81, 88-90]. Changes that can affect the resulting biomaterials properties and retention time.

1.1.4 Lactones for tissue engineering

Of all the polyesters available and currently used as biomaterials for tissue engineering, lactones derived polymers are the gold standard. Particularly of all the lactones, PGA, PLLA, and PCL are the most widely utilized for scaffold fabrication for tissue engineering [26, 91, 92]. This is due to their ease of synthesis through ring-opening polymerization in a bulk reaction, properties (hydrophobicity, mechanical, degradation rate) can be easily tailored, and their biocompatibility [**Figure 1.3**][15, 69, 70, 79]. Similarly, to the polycondensation described in the previous chapter, lactones are polymerized through the use of heat that provides the energy and drives the reaction. However, the ring-structure is stable in the absence of water, base/acid, and catalyst; therefore, a tin catalyst is utilized to coordinate the ring-opening by cleaving the ester bond [**Figure 1.3**] [93, 94]. Once the ring is cleaved, the polycondensation can proceed, as previously discussed in section 1.1.2. The reaction is rapid and can grow polymers efficiently in the laboratory using basic systems (without the use of expensive reactors or vacuums) to mid-range molecular weight (MW) (50-60 k Da) and HMW polymers in industrial settings (>100 k DA). Like the polyesters described in the previous section, lactone polyesters degrade through hydrolytic cleavage. Most importantly, it has been noted that these polymers experience bulk degradation – meaning we get equal degradation of the biomaterial fabricated from these lactone polymers [95, 96].

What makes these polymers and why they have remained the gold standard for several decades is their versatility, tunability, and defined properties. Each of the polymers has a range of degradation that has been thoroughly investigated, and predictions on retention rates can be carefully determined. Traditionally, we have seen degradation times of 1-3 months for PGA, 6-12 months for PLLA, and 2-3 years for PCL[15, 69, 70, 79]. These retention times can be extrapolated
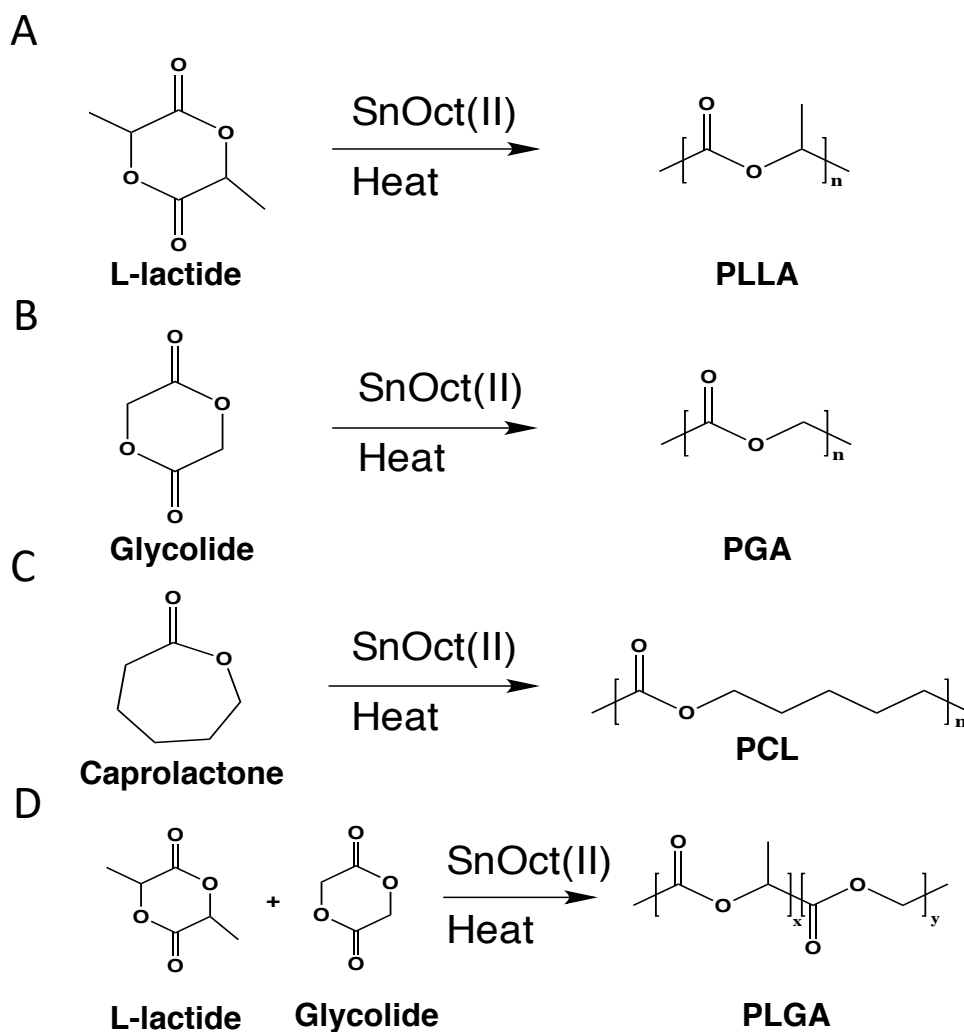
Figure 1.3 Synthesis of lactone monomers to produce biodegradable polymers.

A) Ring-Opening polymerization of L-lactide to produce poly(L-lactic acid) utilizing tin catalyst B) Ring-Opening polymerization of glycolide to produce poly(glycolic acid) utilizing tin catalyst C) Ring-Opening polymerization of ε-caprolactone to produce poly(caprolactone) utilizing tin catalyst D) Ring-Opening polymerization of L-lactide and glycolide to produce poly(L-lactic-co-glycolic acid) utilizing tin catalyst.

to both in vitro and in vivo studies. Additionally, the retention time is directly related to the

hydrophobicity of the resulting polymer. In the case of between PGA and PLLA, the defining

difference is a single methyl group that projects out from the backbone in PLLA and results in

increased hydrophobicity and retention rate. In the case of PCL, this polymers repeat unit contains 6 methylene groups that increase the hydrophobicity resulting in prolonged time retention times and increased hydrophobicity. The physical structure of the polymer repeat unit also gives us an indication of the polymers varying levels of crystallinity, with PGA being highly crystalline, PLLA semi-crystalline, and PCL containing a very low crystalline structure. The latter polymer also exhibits a low Tg at around - 60 ºC and demonstrates elastic properties, which expands the uses of the lactone polymers[93].

Although all three polymers have been extensively utilized as biomaterials for tissue engineering due to their unique properties – fast degradation, elasticity, etc, PLLA has been shown to provide the most beneficial biomimetic properties of the three when fabricated into tissue engineering scaffolds [36, 49, 56, 58, 65]. This is due to how it can be processed to produce nanofibers that mimic the natural extracellular matrix proteins such as collagen and elastin. Additionally, PLLA has an average retention rate (6-12 m) that, for most applications, becomes beneficial as it provides structural support by not degrading fast like PGA, but it also does not a linger beyond when it's needed as seen with PCL[28, 69, 97]. Furthermore, PLLA can be fabricated into tissue engineering scaffolds with less toxic and cost-effective solvents compared to PGA, which requires the use of highly fluorinated solvents [47, 85]. Likewise, PLLA can be processed into tissue engineering constructs more broadly than PCL. This is due to PCLs elastic properties that make it difficult to yield biomimetic physical architecture [62, 83, 98]. Therefore, the preferred method to fabricate into biomimetic fibrous architecture is through the use of electrospinning[62, 99]. Limiting its utility and substantiating the broader use of PLLA for tissue engineering scaffold.

1.1.5 Functionalization of polymers leads to post fabrication

In the previous section, we highlight encouraging aspects that have made PLLA one of the most highly used polymers in tissue engineering scaffolding – can be fabricated into biomimetic physical architecture, tailorable (mechanical properties, hydrophobicity, and retention), biocompatible [38, 100]. However, as we try and fabricate scaffolds with enhanced biomimetic features, it is useful to conjugate regulatory signals (growth factors, peptides, biomolecules) that elicit response cellular response – whether it is differentiation, proliferation, or enhanced tissue formation [101-103]. However, since scaffolds derive their properties from the polymers in which they are fabricated from (hydrophobicity, retention, biocompatibility), and many polymers such as the lactone-based polymers lack chemical functionality in the polymer backbone it is problematic to conjugate these signals unto the polymer under normal circumstances.

Chemical functionality or backbone functionality is being defined in this work as the presence of chemical groups that quickly and efficiently permit the modification of the polymer or resulting tissue engineering construct by chemical attachment of the desired regulatory signal. Meaning that the molecule introduced is not only fouling the surface by entanglement, hydrophilic, ionic, or Van Der Waals interactions, but a chemical bond has formed between the two molecules. Specifically, we highlight the preference of polymers and resulting biomaterials that contain the primary (traditional) chemical groups such as amines (NH2), double bonds (C=C), thiols (SH), or carboxylic acids (COOH) that are more reactive and yielding a greater conjugation efficiency over hydroxyl groups [64, 101, 104, 105]. Furthermore, there is an array of newer and more efficient chemical groups, such as click-chemistry tools, which will be discussed in the following section. Nonetheless, to efficiently modify the polyesters, such chemical groups are a

10

necessity to conjugate the desired molecules. Unfortunately, like PLLA, many of the polyesters that are favorable in tissue engineering scaffolding lack these groups and can be considered "chemically inert" as we can't easily chemically conjugate regulatory signals. We do acknowledge that, especially when using polyesters, carboxylic acids are present; however, they are the least reactive of the groups mentioned, and the MWs of the polymers utilized dramatically reduces the density of these groups in the fabricated scaffold. Therefore, conjugation of desired molecules is diminished based on the amount of COOH present and their low reactivity.

A facile method to introduce these chemical groups into the polymer would be to initiate the reaction with an initiator containing the desired chemical group [**Figure 1.4**] [106, 107]. The polycondensation reaction can occur in the same fashion as described in the previous section, except that the resulting polymer will now contain one of the favorable chemical groups [**Figure 1.4**]. However, as mentioned in the earlier sections, polycondensation reactions in the laboratory without specialized equipment are challenging to control when producing polymers for tissue engineering scaffolds (> 100 k Da). In our experience, creating polyester in this manner only produces medium weight polymers due to the accumulation of water and high viscosity issues. Without achieving these high molecular weights (HMWs), the tissue engineering scaffolds will suffer from low mechanical properties resulting in a fragile scaffold that breaks apart when handling. A facile method to solve this would be to blend a HMW polymer with the lower molecular weight (LMW) end-functionalized polymer. However, this can lead to deleterious effects on the scaffold from poor mechanical properties that lead to fragile scaffolds to scaffolds with little to none favorable biomimetic nanofibrous architecture[65]. Of note, is that commercially, HMW polymers that have been end-functionalized are not readily available.
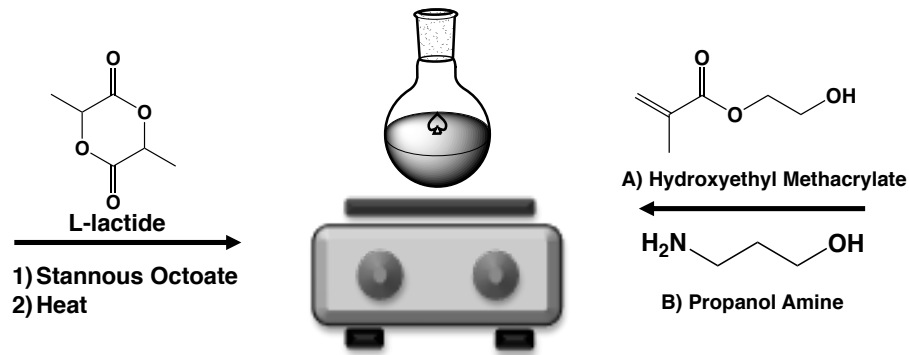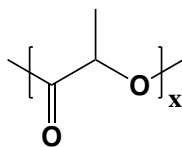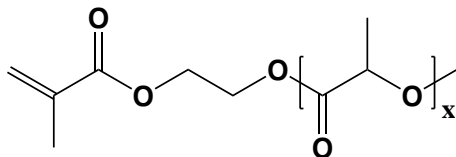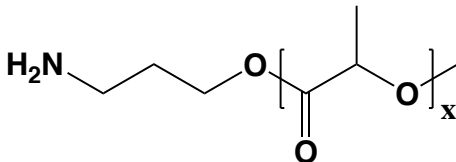
Figure 1.4 Synthesis of end-functionalized PLLA.

Bulk polymerization of PLLA and end functionalized PLLA via tin catalyst and initiator A) synthesis of HEMAPLLA using hydroxyethyl methacrylate to initiate the polymerization resulting in acrylate functional group for post modification B) synthesis of Amine-PLLA using propanol amine to initiate the polymerization resulting in amine functional group for post modification.

Likewise, custom orders are costly and unattainable for most groups wishing to conduct basic

research. Additionally, as mentioned previously, as the polymer grows in MW, the density of the functional groups available becomes less, which can affect the conjugation efficiency and the effect the regulatory signals have on the cells.

Therefore, the polyesters that would produce the best outcome are those in which all the polymers utilized are equal and made out of HMW polymers, contain chemical functionalization, and can provide favorable nanofibrous architecture [65]. Ideally, the polymers produced would have a higher degree of functionalization beyond a single point of conjugation. Various polyesters, such as poly(spiro-co-lactic acid) (PSLA), can fit these criteria. However, current polymerization methods have failed to produce these polymers with MWs required for tissue engineering purposes. For this reason, novel synthesis methods that can produce HMW polyesters such as PSLA could provide new tools in tissue engineering scaffolding by providing polymers with tailorable backbone functionality density that can be quickly and conjugated with regulatory signals. Development of the method of synthesizing HMW polymers easily, rapidly, and a cost-effective manner and developing tissue engineering scaffolds is the focus of Chapter 2 and Chapter 3 and will be discussed in detail in those chapters.

1.2 Click-Chemistry for scaffold optimization

1.2.1 Click chemistry

Traditionally click-chemistry is defined as the ring formation between an azide and alkyne. This cycloaddition follows the described 3+2, addition of azide (3) to alkyne (2), with the reaction being coordinated by copper [**Figure 1.5A**][108-112]. This is made possible by the active Cu(I) that can coordinate the electron exchange between the alkyne and the azide effectively yielding a cycloaddition very rapidly and with a high yield[111]. This work was first introduced by the German chemist Huisgen in 1963 at the University of Munich, since then certain parameters

have been set for click-chemistry reactions 1) rapid 2) high yield 3) stereospecific 4) nontoxic by product 5) broad solvent to include aqueous environments [113, 114]. Although, these parameters set a bar for click-chemistry reactions, since it was first discovered by Huisgen there has been a large expansion of reactions that fall under click reactions that push some of these parameters [115-121]. Therefore, it can be said that the method is ever expanding allowing for a variety of chemistries to be highlighted under the click-chemistry umbrella.

1.2.2 Copper-free click chemistry

For all the perceived benefits of the copper catalyzed click reaction, this proved problematic when carrying out in biological systems due to toxicity of the catalyst as it can interfere with cellular processes [122-124]. Therefore Click-chemistry did not shine again until 2001 when Karl Sharpless rediscovered the work and expanded the use of click reactions by highlighting the use of cyclooctynes in the reactions [113, 125]. Through the use of these highly ring-strained rings the reaction can be carried out in the absence of the copper-catalyst. This is made possible by the use of the ring-strain to drive the reaction [108, 113, 125] [**Figure 1.5 B-C**]. Most importantly, this reaction became wide known and useful across many disciplines as it could be carried out in an aqueous environment at various temperatures without being pH dependent. Specifically, in the field of polymer science and biomaterials researchers have made this click reaction the gold standard, following on the footsteps of Carolyn Bertozzi in 2007, as it allows for facile, high yield conjugation of biomolecules in a biorthogonal fashion at physiological conditions [126].

1.2.3 Hydrazone and Oxime click-chemistry

Since Sharpless work in 2001 and Bertozzi bringing click-chemistry *in vivo* copper free click chemistry has expanded to additional substrates beyond azides and alkynes. In this section

we will discuss two click-reactions, hydrazone and oxime click-chemistry, that highlight the need to rethink the stringent notion of an orthogonal reaction when addressing click reactions [114]. In the case of these reactions a ketone or aldehyde and a hydrazide (amine bound to amine) or aminooxy (amine bound to oxygen) come together to form an imine adducts [**Figure 1.5 D-E**]. In these reactions the heteroatom-bound amine becomes more nucleophilic which promotes the attack of the carbonyl carbon causing the water to be expelled and a bond formation between the carbonyl carbon and the hydrazide/aminooxy agent[127-131]. Although these reactions naturally occur in biological systems the imine is usually transient and easily dissociates. Additionally, these reactions are thermodynamically unfavorable and require low pH to proceed efficiently [127-131]. Nevertheless, these click-chemistry reactions have been utilized for various tissue engineering and biomedical applications such as hydrogels, biosensors, drug delivery systems [90, 132-137] However due to their limited selectivity for aldehydes and ketones that are naturally present this has limited their used *in vivo*, nevertheless these reactions are labeled as semi-biorthogonal and classified as click-chemistry [114]. Thereby broadening our interpretation of click-chemistry reactions and can be applied to the work in chapter 4. Where in this case we have weaker nucleophilic amine but a much more reactive ketone driving the click-chemistry reaction by ring-strain.

1.2.4 Thiol-ene click chemistry

The conjugation of alkenes to thiols is another class non biorthogonal click-chemistry reaction that has been widely explored [Figure 1.5F] [104, 138-143]. These reactions fulfill the requirements set forth by Sharpless and coworkers – producing high yielding coupling – that is widely utilized in tissue engineering to post-modify biomaterials with cysteine containing molecules [144-148]. The reaction is catalyzed by base or UV light with a photo initiator that
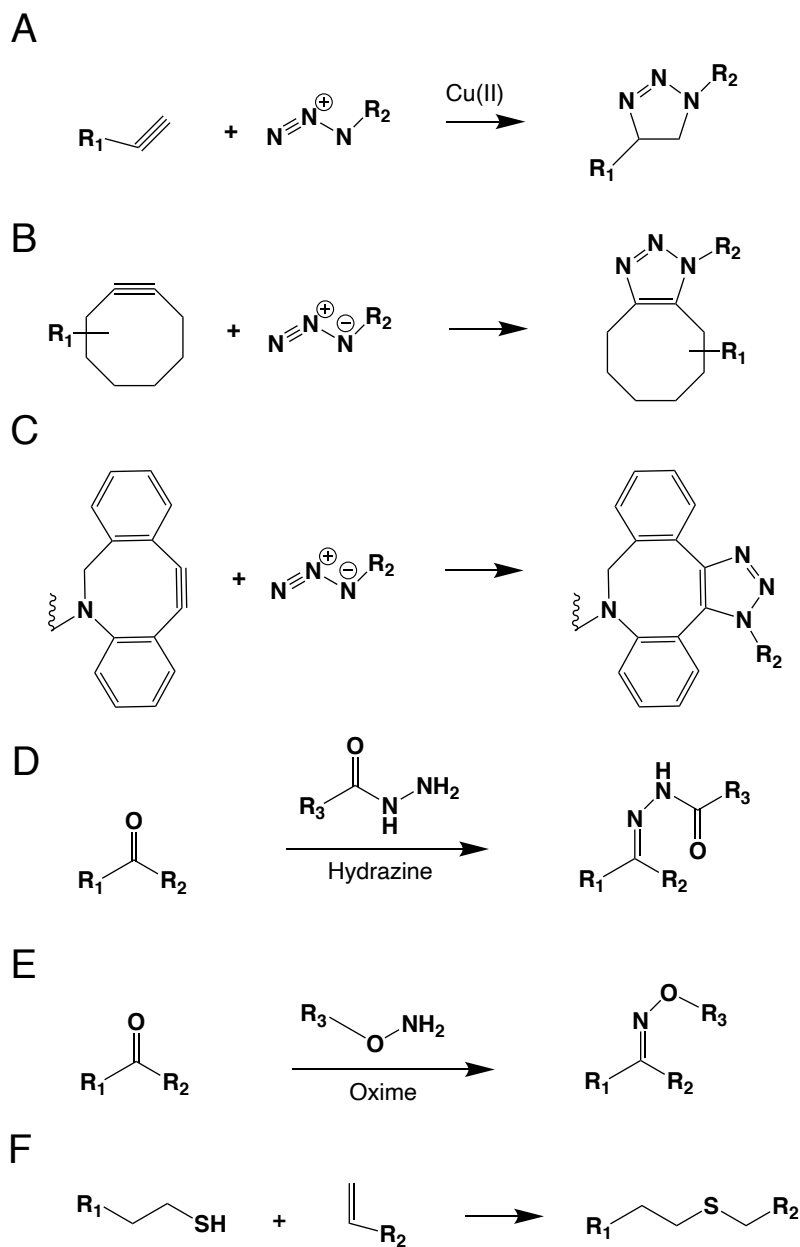
Figure 1.5 Modes of click-chemistry reported in the literature.

A) Copper catalyzed click-chemistry as reported by Huisgen and coworkers B - C) Demonstration of copper-free click chemistry via ring strain provided by the cyclooctyne and DBCO as described by Sharpless D – E) Expanding the notion of click-chemstry to form imine bonds through the use of hydrazine and oxime groups with aldehydes or ketones.

proceeds rapidly to conjugate the molecules together. Most importantly, this is one of the less

cost-effective system which when coupled with the efficiency and ease makes it popular among

biomaterial scientist [138]. In the work described in chapter 2 we focused on this method due to its

ease and low-cost of the thiol reactive groups which can be conjugated to biomolecules.

1.3 Vascular tissue engineering for cardiovascular disease

1.3.1 Cardiovascular disease a global pandemic

Cardiovascular diseases (CVDs) has become the leading cause of death in the U.S. and

internationally accounting for over for 17.7 million deaths, almost a third of all global deaths, in

2015[149]. As this figure is predicted to increase to over 23 million deaths by 2030, CVD has

become a pandemic that will continue to be a key health issue for the foreseeable future[149, 150]. In

addition to CVD's impact on human health and life, the monetary cost of CVD has been

estimated to be around $530 billion in direct and indirect costs[150]. Of all the deaths caused by

CVD, over 50 percent have been attributed to vascular damage induced by accumulation of

vascular plaque, which leads to blocked and hardening vessels that deteriorate over time and may

cause lesions[151]. This is known as atherosclerosis, when plaque builds up in the arteries, made up

of fat, cholesterol, and calcium leads to narrowing in the blood vessel. As the cholesterol and

other molecules accumulate the disease progresses to stenosis which is a much more serious

condition that requires surgical intervention. If left untreated the accumulation leads to hardened

walls and lesion calcification forming a necrotic core that weakens the vasculature, plaque

rupture that exposes the accumulated materials to blood causing thrombus formation, as well as

the walls becoming leading to vasculature to rupture [149, 152-157].

1.3.2 Current therapeutics for cardiovascular disease

Currently, early treatments for vascular disease include changes in diet, exercise, and pharmacological therapy such as from statins. Statins are a type of drugs which target cholesterol in the vasculature and reduce the amount of lipids produced in the liver in an attempt to reduce the amount accumulated [56, 158, 159]. However, as the severity of the disease progresses surgical intervention is often necessary. Most commonly these cases require replacement of the damaged vessel[9, 160, 161]. Due to the lack of readily available grafts, physicians are forced to utilize inefficient replacements. As of now, autologous blood vessels derived from the saphenous vein have served as the gold standard in these treatments[1, 37, 162-168]. However, this is not ideal for most patients because harvested autologous vessels often do not embody the same properties as the vessels, they replace[4-6]. Additionally, for patients who have exhausted the number of useful vessels that may be harvested or who suffer from widespread atherosclerotic vascular disease which has damaged suitable vessels, this treatment is simply not an option. In these cases, allografts from cadavers and xenografts from pigs have been widely used as replacement vessels, but they have been shown to elicit an undesirable immune response in some patients and there are not enough allografts available to treat everyone who needs one[85, 169, 170].

1.3.3 Synthetic materials as vascular grafts

The shortage of grafts available and the issues of immune response with currently available treatments has led to the development of synthetic materials that may be used to create grafts that can meet the clinical demands for the replacement of blood vessels[165, 167, 168]. While synthetic grafts made from Dacron® or Teflon® have made a major impact on helping mitigate the effects of vascular disease and loss of life due to shortage of suitable replacements, these grafts also suffer from several limitations: thrombosis has been observed in small diameter (<6

mm) grafts, limiting their use to large arterial blood vessels [169, 171-174]. Additionally, these grafts are made from bioinert polymers that are not biodegradable which prevents cellular migration, proliferation and remodeling, thereby the implanted material becomes susceptible to wear and tear over time and cannot be regenerated as the body might regenerate a vessel with minor injury[172-175].

1.3.4 Tissue engineering scaffolds as vascular engineer grafts

Due to these limitations with synthetic grafts, tissue engineering is a promising approach to address these problems and to create a vascular graft that is biocompatible, biodegradable, and promotes mature native tissue formation [17, 57, 160, 165, 167, 169, 176-179]. Currently, small diameter tissue engineered scaffolds used as vascular grafts have been successful in meeting the mechanical properties necessary for surgical implantation and physiological conditions in rat models [4, 177, 180-182]. Additionally, much work has gone into identifying ideal scaffold morphology and architecture, such as creating nanofibrous and porous scaffolds which optimize cell infiltration and proliferation[49, 161], determining the effect of the supportive structure on vascular muscle reconstruction[182, 183], and the conjugation of biological molecules to improve the patency of implanted scaffolds[,20, 184, 185]. However, these parameters still require further work and methods to implement and optimize more than one of these are absent in the literature. This has led to limits in cellular infiltration and proliferation and has had deleterious effects in small diameter blood vessels, yielding poor cell-scaffold interactions, cellular migration, extracellular deposition and scaffold remodeling, and thrombus and aneurism formation[1, 162, 163, 186]. Therefore, it is essential to optimize the scaffold design before tissue engineering reaches its full potential as an alternative for vascular grafts.

1.3.5 Acellular scaffolds as "in situ" vascular grafts

The last decade has seen the development of highly efficient biomimetic acellular scaffolds that can serve as vascular grafts. More recently, researchers have sought to avoid time consuming in vitro bioreactor-assisted vascular reconstruction and take advantage of the body's capability to regenerate using *in situ* implementations of tissue engineered scaffolds [164, 166, 167, 179, 187].

The goal for *in situ* vascular tissue engineering is to create a functional blood vessel that is regenerated by the body through a cell-free off-the-shelf scaffold that is biodegradable, biocompatible, and tailored for patient-specific application. In doing, the method of *in situ* cell-free vascular tissue engineering demonstrates a promising method to address the critical need for readily available vascular grafts caused by the ongoing shortage by shortening the time necessary to produce a graft[8,15] The use of cultured cells to create small-diameter TEBV for cardiac and peripheral revascularization procedures is not suitable for most clinical applications due to the immediacy in which the vessel is commonly needed; therefore cell-free tissue engineered vascular grafts allow for elimination of the time required for cell culture/harvest and immediate implantation [166, 167]. Since the first polymer scaffold was fabricated for blood tissue engineering, numerous platforms have been developed using three main fabrication methods - molds, templets, and electrospinninng[49, 160, 177, 188 1, 163, 186, 189]. This has led to synthesis of sheets that are rolled or sutured together, single layer tubular scaffolds, or bilayered tubular scaffolds to promote rapid host vascular cell invasion as well as scaffold-supported vascular reconstruction after implantation into animal models[49, 177]. Through these methods suitable scaffolds have been developed repeatedly that are able to evenly match the physical characteristic in diameter and length of the replacement vessel.

1.3.6 Polymers used in scaffold fabrication for tissue engineering

There has been a large variance in the polymers utilized for development of vascular tissue engineered scaffolds. Both slow degrading polymers, such as polycaprolactone (PCL), and faster degrading polymers, such as poly(urethane), poly(glycolic acid), and poly(glycerol sebacate) have been used in scaffold designs [62, 99, 160, 190]. Polycaprolactone is a polymer frequently used in the fabrication of mono-layer scaffolds since it is easily incorporated into tubular scaffolds via electrospinning and provides excellent mechanical properties[98, 190, 191]. However, it degrades very slowly (1.5 to 3 years) and development of calcification within the formed tissue has been observed in long term studies[192]. These observations were confirmed by Sugiura, T. and coworkers who assessed long-term studies of a bilayered scaffold containing a layer of slow degrading PCL and a layer of PLCL, a faster degrading copolymer, and then compared the level of calcification within the layers. From this work, we can conclude that the issue of calcification could be avoided if faster-degrading materials are used[97]. Fast degrading polymers such as PGS and PGA have also been utilized in scaffold fabrication and have been shown to provide rapid degradation of the scaffolds leading to faster infiltration, proliferation and matrix production[5]. However, rapid degradation has also led to formation of aneurysms and also results in the need for a slower degrading polymer to provide structural support[160, 177, 178]. For this reason, slow-degrading polymers such as PCL still prove to be useful due to their elasticity and continue to be used to improve the durability of tissue engineered scaffolds.

1.3.7 Optimization of vascular tissue engineered scaffolds

In order to increase the compatibility of the tissue engineered scaffolds, much effort has been devoted to imparting biomimetic cues through the physical architecture of the scaffold as well as incorporating biomolecules. The use of porous and interconnected scaffolds has been of

particular interest since they allow excellent mass flow, as well as cellular penetration and migration from the points of anastomosis [49, 160, 177]. Techniques such as TIPS and electrospinning have been extensively studied since they produce nanofibrous morphology that mimics the native extracellular matrix environment both in size of fiber and mechanical forces exuded on the cell[9, 49, 68, 177, 188, 193]. Previously, Ma and coworkers developed large diameter nanofibrous scaffolds fabricated from a sugar leaching template and TIPS from PLLA that showed superior cellular attachment, proliferation, and migration[49]. Additionally, the nanofibrous architecture of the scaffold was shown to be conducive for mature vascular tissue formation through the differentiation of cardiovascular progenitor cells into smooth muscle cells with contractile phenotype both *in vitro* and in subcutaneous implantation in mouse models [50, 54, 161, 194].

Recently, in an attempt to increase the biomimetic nature of the tissue engineered scaffolds regulatory signals, biological motifs, and anticoagulant molecules have been introduced unto the vascular engineering scaffolds to enhance the microenvironment and biocompatibility [181, 185, 191]. Specifically, heparin has a desirable molecule to be added as it has antithrombogenic properties and enhances the scaffolds biocompatibility [181, 184, 191, 195]. The prefer method to introduce the heparin unto the scaffold is through conjugation directly unto the polymer. However, due to the chemical structure of the polymers most widely utilized, there is no backbone chemical functionality and the only points of attachment are at the ends of the polymers. Therefore, very little heparin can be attached to the scaffold[160, 170, 181, 184, 191, 195]. To work around the low chemical functionality, researchers have taken to dipping the scaffold in a heparin solution in an attempt to foul the surface. However, due to heparin's hydrophilic nature and high solubility, retention of heparin is minimal after scaffold implantation and therefore many systems experience thrombosis issues[177, 192, 196-198]

1.4 Introduction and thesis outline

This dissertation will be used to advance the development of polymers used in the fabrication of biomimetic scaffolds for tissue engineering and regenerative medicine. Polyesters such as those synthesized from lactones, poly(caprolactone) (PCL), poly(L-lactic acid) (PLLA), and poly(glycolic acid) (PGA), are currently the gold standard used for scaffolding material. Due to their favorable properties such as processability, degradability, and biocompatibility (FDA approved). However, these polymers lack functionality in the backbone, and therefore platforms fabricated from them are limited in the manner in which they can be conjugated with regulatory signals (growth factors, biomolecules, peptides). For this reason, polymers with increased functionality that can incorporate these signals post-fabrication would be beneficial in enhancing the microenvironment. Currently, there is a lack of such polymers which are suitable for scaffolding due to the polymerization efficiency (MW which can be attained), how they can be processed, and biocompatibility. In this work, two novel polymers are explored as possible biomaterials for the fabrication of tissue engineering scaffolds. These polymers are poly(spirolactide-co-lactic acid) PSLA, a polymer with tunable functionality in the polymer backbone that demonstrates properties similar to PLLA, and poly(exomethylene-co-lactic acid) a novel copolymer with *click-chemistry like* reactivity with amine-containing molecules. These polymers were used to develop three-dimensional scaffolds, and we demonstrate how the functionality of the polymers is beneficial in enhancing the scaffolds biomimetic properties.

1.4.1 HMW Polymerization of PLLA and PSLA using extreme temperature

Chapter 2 will provide essential background on polyesters used in tissue engineering, specifically focusing on PLLA, which is the most commonly used polymer due to it's retention time and the unique architecture that can be formed via processing techniques (smooth,

nanofibrous, textured surface). We describe methods of synthesis and modification to add functionality to the platforms developed from PLLA. We describe different properties that are required of polymers to be used to create scaffolds with biomimetic physical properties as well as scaffold design and previous models used in vasculature engineering and bone formation.

1.4.2 Tubular scaffold from PLLA/PSLA for vascular engineering

In chapter 3, we will describe a novel method to synthesize high molecular weight PLLA through cold temperature-induced polymerization. Here we describe how the cold temperature can be used to polymerize HMW PLLA using organocatalyst DBN (1,5-Diazabicyclo[4.3.0]non-5-ene) and TBD (1,5,7-Triazabicyclo[4.4.0]dec-5-ene) with living polymerization like properties and MW > 300 k Da. We implemented this cold technique to synthesize the copolymer PSLA, which previously has only been shown at low MW < 30 K Da (size not suitable for scaffold fabrication) and demonstrated for the first time an HMW PSLA copolymer with a MW > 300 k Da. This copolymer displayed PLLA like characteristics with the added benefit of tunable backbone functionality (controlled by modulating the feed ratio of L-lactide and spirolactide used) was fabricated into biomimetic scaffolds with porous, interconnected, and nanofibrous architecture.

1.4.3 PELA polymer with click-chemistry like reactivity

Chapter 4 focuses on using the HMW PSLA copolymer to develop biomimetic tubular scaffolds that are porous, interconnected, and nanofibrous for *in situ* implantation in rat models. Due to the tailorable backbone functionality of the PSLA copolymer, we can conjugate heparin unto the scaffolds and modulate the microenvironment. In doing so, we can control the hydrophilicity, degradation, with anti-thrombogenic properties. The scaffolds developed where implanted *in situ* in rat models (> 45) and observed post-operative for up to 3 months. We

determined the scaffolds to be patent with zero thrombi leading to death, no aneurysm formation, and fully remodeled mature vascular tissue. Thereby demonstrating the utility of HMW PSLA in the development of biomimetic scaffolds that can be modified to enhance the microenvironment and alter the physical properties.

1.4.4 PELA polymer with click-chemistry like reactivity

Chapter 5 delves into the novel synthesis of the PELA copolymer with click-chemistry like reactivity. In this chapter, we explored the facile and rapid method of modification that leads to a peptide bond formed between the amine-containing molecule and the tissue-engineered platformed developed. The conjugation can occur in water, buffer, or media, as well as polar protic (methanol & ethanol) and polar aprotic solvents (dimethyl sulfoxide). Thereby making it possible to broadly modify the copolymer and platform fabricated with a variety of regulatory signals such as protein, peptides, or small hydrophobic molecules. The copolymer was used to develop a three-dimensional nanofibrous scaffold that is porous and interconnected via thermally induced phase separation (TIPS) and sugar leaching method. These scaffolds were shown to contain the same "click-chemistry" like reactivity towards amine-containing molecules and can promote bone formation.

1.4.5 Summary of Work and Proposed Future Work

Chapter 6 will summarize our findings, detailing how the surface modification of tissue engineering scaffolds enhances the biomimetic properties and allow us to tailor the material for a specific purpose. These favorable properties attained and modifications made possible through the development of two highly reactive polymers never before used for tissue engineering. Lastly, **Chapter 7** will detail future directions which these polymers are currently being applied in tissue engineering purposes as well as provide possible new research avenue

Chapter 2. Facile and Rapid Cold Synthesis of High Molecular Weight Biodegradable Polymers

R. Navarro, P.X. Ma., "Biodegradable polymers and nanofibrous scaffold thereof," U.S. Patent Application No. 63/014,484, Filed April 2020. Patent Pending

R. Navarro*, A. Adiwidjaja, P.X. Ma., "Facile and rapid cold synthesis by guanidine organocatalyst leads to HMW PLLA and PSLA." In Process.

2.1 Introduction

2.1.1 Synthesis of lactones into biodegradable polymers for biomedical applications

Biodegradable polymers are widely used in biomedical applications, such as tissue engineering scaffolds, drug-releasing micro-/nano-particles, and implants. Traditionally, lactones such as L-lactide are cheaply and easily polymerized via ring-opening polymerization (ROP) through the use of a tin catalyst such as stannous octoate in a reaction vessel that has been purged and heated (120 – 150 °C) [67, 94, 199]. The reaction quickly proceeds in a step-growth fashion producing water molecules as the condensation reaction occurs between adjoining lactic acid molecules. As the polymer grows, the viscosity of the growing polymer increases until you reach a point in which no more stirring is possible. Thereby limiting the interactions between chains and preventing continued growth. Likewise, the water molecules released will become entrapped in the viscous polymer and can either quench the reaction or hydrolytically cleave the polymers formed, resulting in polymers with a small molecular weight. In our experience, polymers produced in this fashion only reach an average of 50 k Da due to the viscosity and water issues mentioned.

2.1.2 The need for high molecular weight polymers in tissue engineering

Yet, for many applications, a reasonably high molecular weight (HMW) is often necessary for such polymers to be processed into the desired biomimetic physical forms or/and to possess the desired mechanical and nanofibrous properties. Such fibers are unique in that they mimic the fibrillar structure of natural extracellular proteins such as collagen and elastin and have been shown to facilitate cell attachment, proliferation, differentiation, and tissue regeneration. To develop scaffolds with this preferred nanofibrous architecture, PLLA should contain HMW due to the increased crystallinity observed and the resulting mechanical properties. Unfortunately, synthesizing HMW polymers (such as above 100 k Da) often requires high temperature, extended reaction periods, and specialized reaction vessels that are costly. Thereby limiting the access to HMW PLLA for scaffolding purposes and forcing researchers to outsource production to external vendors, at considerable cost and time.

2.1.3 Synthesis of functional polymers for scaffold fabrication with enhanced biomimetic properties

Beyond imparting tissue engineering scaffolds with biomimetic architecture such as porous, interconnected, and nanofibrous architecture, considerable effort has been expended to introduce regulatory signals into the scaffold. The preferred method of introducing these signals is to conjugate them directly into the scaffold and thereby prevent the diffusion and washing away of the regulatory signals that can be costly and limited in quantity. To prevent this, the polymers used should contain the preferred functional groups NH_2, SH, or alkene. These groups allow for a wide range of flexibility in post-modification, and the coupling reactions have a high level of efficiency. However, lactone polymers such as PLLA lack any of these functional groups, and therefore we are limited to the degree in which we can impart biomimetic properties.

2.1.4 Guanidine organocatalyst used to induce ring-opening polymerization

Previously, catalyst derived from guanidine has been shown to polymerize lactides with a very narrow polydispersity (PDI) in a facile and cost-effective manner leading to medium size polymers (50 - 70 k Da) [92, 93, 200, 201]. The catalyst which include 1,5,7 Triazabicyclo [4.4.0]dec-5-ene (TBD), 7-Methyl-1,5,7-triazabicyclo[4.4.0]dec-5-ene (MTBD), 1,5-Diazabicyclo[4.3.0]non-5-ene (DBN), and 1,8-Diazabicyclo[5.4.0]undec-7-ene (DBU) are strong basic organo-catalyst which coordinate the ring-opening and esterification through an amidine base. Unlike tin-based ROP reactions, which are traditionally performed as bulk polymerizations, the reactions performed in solution reduces viscosity problems. The solution polymerization is usually carried out in DCM at room temperature producing polymers with narrow distribution but with varying kinetics based on the catalyst used. Typically, TBD is reported as a fast-acting catalyst that is able to quickly consume > 99 % of the monomers and produce polymers within 5 min. MTBD, DBU, and DBN have been reported as less efficient (90 - 98 %) and slower compared to TBD [92, 200]. However, the efficiency changes between lactones polymerized and therefore warrant further investigation. The organocatalyst works by initiating the ring opening polymerization and simultaneously coordinating the esterification with a hydroxyl group [**Figure 2.1**]. Unlike in traditional polymerization where heat can help drive this process (esterification) and causes a more random esterification of monomer to monomer, monomer to polymer, and/ or polymer to polymer the TBD catalyst can produce the esterification in the absence of heat. Therefore, in the absence of the TBD catalyst (i.e. catalyst degrades), we expect the lactone ring will not be cleaved and the esterification (polymer growth to also not occur).

In this work, we surprisingly discovered a facile, rapid, and low-cost method to polymerize HMW polymers from lactones and other cyclic monomers by utilizing extremely low
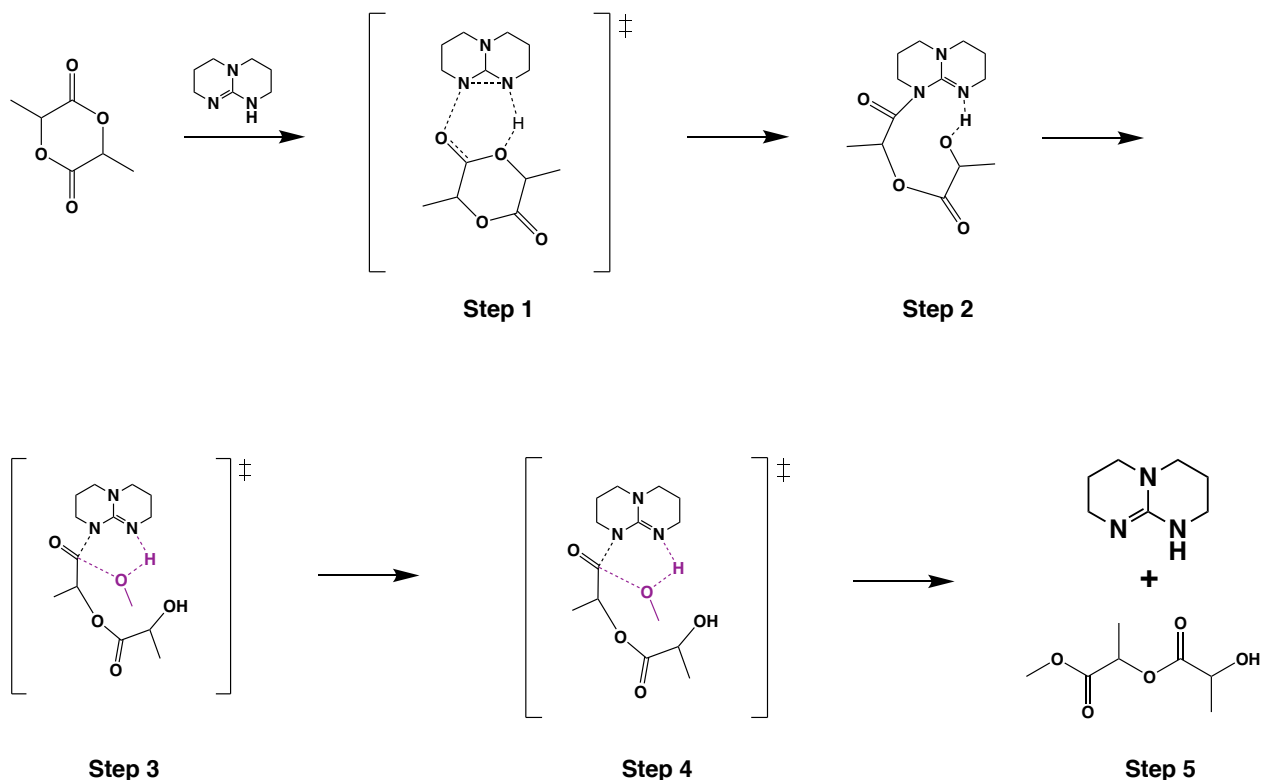
Figure 2.1 TBD catalyst mechanism of polymerization.

Ring opening of L-lactide by TBD catalyst and polymerization with hydroxyl group (step 4) coordinated by the organocatylist. Step 6 yields the catalyst and growing molecule.

temperatures and guanidine derived catalysts. Further investigating the extreme cold

polymerization while changing the following conditions: solvent utilized, solvent concentration,

catalyst concentration, and using/ not using an initiator. The latter having the effect of allowing

us to control the molecular weight of the resulting polymers and producing polymers with

defined MWs. Applying the most favorable conditions discovered, we can extend this technique

to synthesize HMW PLLA, and polymerizing other lactone-based polymers, as well as the

synthesizes of HMW PSLA for the first time. Furthermore, we showed the utility of the cold

polymerization to produce HMW copolymers such as poly(lactic-co-spirolactic acid) (PSLA)

that can be processed into desired physical forms such as nanosized fibers, which could not be

achieved before using current polymerization methods. Most importantly, in this work, we demonstrate that compared to the conventional polymerization conditions, the extreme cold polymerization does not require large equipment investment and can yield HMW polymers, including functionalized specialty polymers with low costs.

2.2 Materials and methods

2.2.1 Materials

L-lactide was purchased from Altasorb® and recrystallized two times in ethyl acetate before use. Glycolide (recrystallized in ethyl acetate), 2-hydroxyethyl methacrylate (HEMA), 3-chloropropanol, propargyl alcohol, benzyl alcohol, anhydrous acetone (AT), anhydrous tetrahydrofuran (THF), anhydrous dichloromethane (DCM), and anhydrous ethyl acetate (EA) were purchased from Sigma. The catalysts methyl-1,5,7-triazabicyclo[4.4.0]dec-5-ene (MTBD), 5,7-Triazabicyclo[4.4.0]dec-5-ene (TBD), 1,8-diazabicyclo[5.4.0]undec-7-ene (DBU), 1,5-Diazabicyclo[4.3.0]non-5-ene (DBN) were purchased from Sigma and stored under an inert environment.

2.2.2 General procedure for ring-opening polymerization using cold polymerization and TBD organocatalyst

In a reaction flask L-lactide was purged three times via a standard vacuum/nitrogen gas treatment before dissolving in anhydrous DCM. The flask was cooled to -80 °C for 1 h and then injected with catalyst dissolved in DCM. The reaction was monitored via gel permeation chromatography and the polymer formed was precipitated in ethyl ether, re-dissolved in DCM, then precipitated in ethyl ether and stored under vacuum for two days before use. All reactions performed in subsequent experiments were performed with an n = 3.

2.2.3 General procedure for the ring-opening polymerization with a change in concentration

In a reaction flask L-lactide was added and purged three times via a standard vacuum/nitrogen gas treatment before dissolving in anhydrous DCM. The reaction was dissolved at 5, 10,15, and 20% w/v concentrations. The flask was cooled to -80 °C for 1 h and was then injected with 0.01 % mol initiator followed by 0.5 % mol of catalyst dissolved in DCM. The reaction was monitored via gel permeation over a week at designated times.

2.2.4 General procedure for the ring-opening polymerization change in catalyst concentration

In a reaction flask L-lactide was added and purged three times via a standard vacuum/nitrogen gas treatment before dissolving in anhydrous DCM. The reaction was dissolved at 5, 10, 15, and 20% w/v concentrations. The flask was cooled to -80 °C for 1 h and was then injected with either 0.05 %, 0.1. %, 1.0 %, and 2.5% mol catalyst dissolved in DCM. The reaction was monitored via gel permeation over a week at designated times.

2.2.5 General procedure for the ring-opening polymerization with benzyl alcohol initiator

In a reaction flask L-lactide was added and purged three times via a standard vacuum/nitrogen gas treatment before dissolving in anhydrous DCM at 5% w/v. The reactions were then injected with initiator (benzyl alcohol) dissolved in DCM and added to the L-lactide to synthesize polymers of 10k, 25k, 50k, and100k molecular weight. The flask was cooled to -80 °C for 1 h and was then injected with 0.5% catalyst dissolved in DCM. The reaction was monitored via gel permeation chromatography and the polymer formed was precipitated in ethyl ether, re-dissolved in DCM, then precipitated in ethyl ether and stored under vacuum.

2.2.6 General procedure for the ring-opening polymerization in diverse solvents used

In a reaction flask L-lactide was added and purged three times via a standard vacuum/nitrogen gas treatment before dissolving in anhydrous solvents. The reactions were dissolved at a concentration of 5 % and 10 % w/v in anhydrous DCM, THF, AC, and EA. The flask was cooled to -80 °C for 1 h and was then injected with 0.5 % mol of catalyst dissolved in the respective solvent. The reaction was monitored via gel permeation over a week at designated times.

2.2.7 General procedure for the ring-opening polymerization of PLGA

In a reaction flask L-lactide and glycolide were added in a 1:1 ratio and purged three times via a standard vacuum/nitrogen gas treatment before dissolving in anhydrous DCM at 5% w/v. The flasks were cooled to -80 °C for 1 h and were then injected with 0.5% catalyst dissolved in DCM. The reaction was monitored via gel permeation chromatography and the polymer formed was precipitated in ethyl ether, re-dissolved in DCM, then precipitated in ethyl ether and stored under vacuum.

2.2.8 General procedure for the ring-opening polymerization of PCL

In a reaction flask ε-caprolactone was added and purged three times via a standard vacuum/nitrogen gas treatment before dissolving in anhydrous DCM at 5% w/v. The flask was cooled to -80 °C for 1 h and was then injected with 0.5% catalyst dissolved in DCM. The reaction was monitored via gel permeation chromatography and the polymer formed was precipitated in ethyl ether, re-dissolved in DCM and precipitated in ethyl ether and stored under vacuum.

2.2.9 Spiro[6-methyl-1,4-dioxane-2,5-dione-3,2'-bicyclo[2.2.1]hept[5]ene] synthesis

L-Lactide was modified based on a method reported by Hillmyer *et. al.*[202]. Briefly, L-Lactide was combined with NBS (1.1 eq.) in benzene (20 % w/v) and heated to reflux. Benzoyl peroxide dissolved in benzene was added dropwise and the reaction was monitored by thin layer chromatography (TLC) until completion. The reaction was vacuum filtrated and condensed and the resulting solid was dissolved in DCM, washed in sodium thiosulfate solution, and concentrated. The solid was recrystallized from ethyl acetate and hexane twice to yield white crystals, (3S, 6S)-3-Bromo-3,6-dimethyl-1,4-dioxane-2,5-dione (bromo-lactide) **(1)**. The white crystals were dissolved in DCM in a flask under nitrogen and cooled in an ice bath. TEA (1.1 eq) was added in dropwise and allowed to react for 1 h at 0° C and 1 h at 25° C. The reaction was washed with 1M HCl three times and condensed. The crystals were further purified by liquid chromatography on silica gel and recrystallization in ethyl acetate to yield white crystals, (6S)-3-Methylene-6-methyl-1,4-dioxane-2,5-dione (methylene lactide) **(2)**. To freshly distilled cyclopentadiene (2.2 eq.) **2** was added (1 eq.) and refluxed overnight in benzene under argon. The reaction was condensed and purified by liquid chromatography in 50/50 hexane:DCM ($r_f =$ 0.31) followed by recrystallization in ethyl acetate to yield white crystals, Spiro[6-methyl-1,4-dioxane-2,5-dione-3,2'-bicyclo[2.2.1]hept[5]ene] (spiro-lactide) **(3)**.

2.2.10 General procedure for the ring-opening polymerization of PSLA

In a reaction flask L-lactide and spirolactide were added in a 1:0, 1:1,1:2,1:3,1:5, 1:10,1:20 mol ratio and purged three times via a standard vacuum/nitrogen gas treatment before dissolving in anhydrous DCM at 5% w/v. The flasks were cooled to -80 °C for 1 h and then injected with 0.5% catalyst dissolved in DCM. The reaction was monitored via gel permeation

chromatography and the polymer formed was precipitated in ethyl ether, re-dissolved in DCM, then precipitated in ethyl ether and stored under vacuum.

2.2.11 Nanofibrous Film Fabricated from PSLA Polymer using TIPS

A two-dimensional film with a thickness of 200 μm with nanofibrous architecture was fabricated using thermal induced phase separation (TIPS). TIPS was carried out according to procedures developed by Ma *et. al.*[4, 33, 61, 203]. Briefly, a 10 % w/v polymer solution consisting of PSLA was dissolved in THF by heating to 60 °C and casting onto a glass surface. The solution was then quickly cooled to - 80 °C and maintained at this temperature for 48 h in order to allow for phase separation. The films were brought to room temperature by placing them in an ice bath and allowing the bath to reach RT before removing the film. The films were dried and stored under vacuum until ready for use.

2.2.12 Nanofibrous scaffold fabricated from PSLA polymer using TIPS

The porous, interconnected and nanofibrous scaffolds are fabricated using a sugar leaching method and TIPS as previously reported by Ma *et. al.*[20, 61, 68, 204, 205]. Briefly, the sugar template spheres are fabricated through an emulsion method and sieved to collect spheres ranging between 250 to 425 μm. The sugar is deposited in cylindrical molds and is heat treated to achieve the desired interconnected structure and then vacuum dried. A solution of PELA or PLLA was dissolved in THF to a concentration of 15% and 10% respectively and heated to 60 °C. The solution was then added to the dry sugar template and treated to reduced pressure to force the polymer solution into the template. TIPS was then induced at -80 °C for two days followed by submerging in excess hexane overnight to remove residual THF and maintain the scaffolds free of moisture. The scaffolds were then submerged overnight in DDH$_2$O to leach away the sugar template and the scaffolds cut to the desired diameter and width.

2.2.13 Fibrous Mesh Fabricated from PSLA Polymer Through Electrospinning

In a 20 mL vial PCL (MW 60-80 k), L-lactide (viscosity of 1.6 dl/g), and PSLA (MW 50, 100, and 300 k) were each dissolved in a mixture of 90:10 chloroform and methanol and allowed to stir for 24 h. The viscous solutions were then electrospun (15 kV, 10 cm, 2 mL/h) onto a flat surface covered in aluminum foil for 5 min to create a fibrous mesh. The mesh was then placed in hexane for 24 h to remove unevaporated solvent and stored under vacuum until use.

2.2.14 Nanofibrous scaffold and mesh modified via thiol-ene click chemistry

Scaffolds were modified through UV-light induced thiol-ene click-chemistry with the desired molecules to be conjugated. Briefly, thiol containing molecule and tetramethylethylenediamine (TEMED) were dissolved in DDH_2O. The UV-initiator, Irgacure 2959, was dissolved in 100 µL of dimethyl sulfoxide (DMSO) and added to the solution. The scaffolds were quickly soaked in ethanol then added to the PEG/Heparin solution prior to being exposed UV-light. The scaffolds were then washed in methanol and DDH_2O to remove excess TEMED and Irgacure 2959 before being lyophilized. The scaffolds were then sterilized with ethylene oxide (Anproline Gas Sterilizer) and stored at -20 °C.

2.2.15 General techniques and strategies

Nuclear magnetic resonance characterization: All monomers (L-lactide, exomethylene lactide and spirolactide) and polymers formed were characterized via 500 MHz ^{1}H and ^{13}C (Varian Inova 500) by dissolving in $CDCl_3$.

Ultraviolet–visible spectroscopy: All monomers and polymers formed were characterized by first dissolving in DCM and using a quartz cuvette to obtain spectrum from 200 - 700 nm (up to 350 shown) (Hitachi U-2910).

Fourier-transform infrared spectroscopy: Monomers, polymers, and modified tubular scaffolds were characterized by directly placing the sample on the diamond crystal sample holder to obtain the spectrum from 600 – 4000 nm (Thermo-Nicolet IS-50).

Scanning electron microscopy (SEM) observation: Empty scaffolds were sputter-coated with gold for 150 seconds and observed under a scanning electronic microscope (JEOL JSM-7800FLV).

Gel permeation chromatography: Polymers formed were dissolved in anhydrous tetrahydrofuran and the molecular weight of the polymers were determined by comparing to polystyrene standards *(*Shimadzu GPC).

Figure 2.2 Synthesis of lactone monomers through the use of TBD organocatalyst. Through the use of extreme cold temperature lactones such as PLLA, PLGA, and PCL.

2.3 Results

2.3.1 Cold polymerization of HMW PLLA using TBD organocatalyst

PLLA polymer was successfully synthesized using extreme temperature (-80 °C) and
TBD organocatalyst. We were excited by the speed, efficiency, and reproducibility of results
achieved with synthesis of PLLA with TBD as an organocatalyst via a solution polymerization.
The polymerization occurred rapidly and efficiently with most of the monomer consumed in 15
min. The polymer also grew to ~ 80% of its maxed MW within 1 h of polymerization [**Figure
2.2**]

2.3.2 Effects of low temperature on the molecular weight of polymerized PLLA

To demonstrate the effects that the extreme temperature has on the polymerization
efficiency, the polymerization was conducted at RT, 0 °C, - 20 °C, and - 80 °C monitoring the

10 % w/v in DCM, 1.0 % [Initiator]
R^2= 0.9497; P value < 0.0001
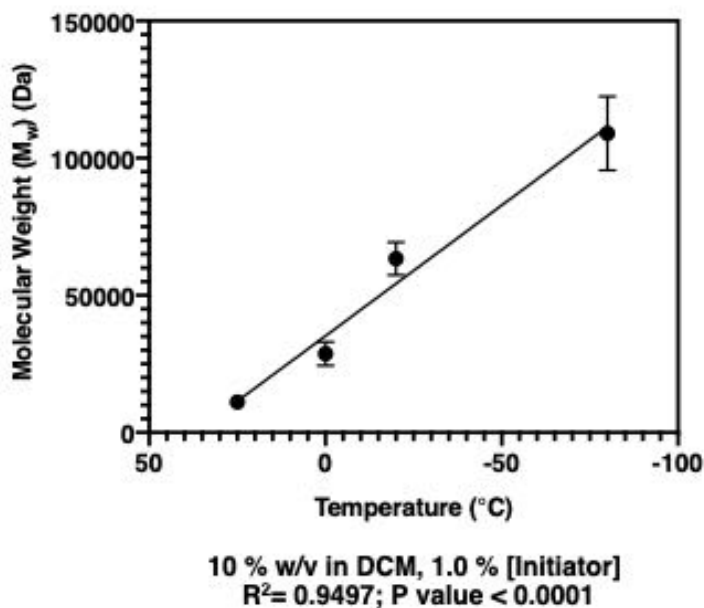
Figure 2.3 Growth of polymer M_w based on change in temperature.

Observation in change in molecular weight after 24 h due to the change in temperature.
Polymerizations where observed at RT, -4 °C, -20 °C and -80 °C.

reaction over 7 days at predetermined times (24h reported). As previously described, we observed high efficiency in the consumption of L-Lactide monomer and synthesis of PLLA. The M_w of PLLA observed at -80 °C after 15 min exceeded over 90 k Da M_w compared to approximately 20 k Da, 30 k Da, and 50 K Da M_w for the reactions at RT, 0, and - 20 °C, respectively. We continued to observe the change in M_w reporting a change of approximately 20 % increase at 24 h and no change by day 7, reaching a M_w of ~ 110 k Da and a PDI of 1.3. This is a 57 % increase in M_w over the - 20 °C reaction and 440 % increase when compared to the reaction at room temperature. This observation shows a clear correlation between the reaction temperature and the growth of the polymer [**Figure 2.3**].

2.3.3 TBD catalyzed polymerization of PLLA in diverse solvents

In the literature PLLA synthesis using the organocatalyst TBD has utilized DCM as the solvent of choice[92, 200]. This solvent was shown to perform the reaction at a fast rate while maintaining the polymer solubilized as it grew in molecular weight. Previously, our experiments in this study utilized this solvent due to its extremely low melting point (MP) (- 96.7 °C). Additionally, the solvent demonstrated extremely high solvation for PLLA at the extreme reaction temperature (- 80 °C). In order to investigate if DCM was the optimal solvent for this reaction at this temperature, we chose 4 additional solvents with low MPs in which PLLA was soluble: acetone (-95 °C), THF (-108.4 °C), ethyl ether (-116.3 °C), and toluene (-95 °C). All the solvents maintained the L-Lactide in solution before the polymerization and allowed for the polymerization of PLLA using TBD. However, as the polymer grew in MW in these 4 solvents the solubility at these extreme temperatures caused the polymer to precipitate in 3 out of the 4 solvents (Acetone, Toluene, Ethyl Acetate) resulting in low molecular weight polymers. In this study, we noticed that acetone polymerized the smallest PLLA polymers with a range between

10 – 15 k Da, followed by Toluene ~ 15 k da, ethyl acetate 30 – 45 k Da, and THF 50 – 70 k Da. Of these solvents, we postulated that THF would be able to match the molecular weight achieved using DCM since we did not observe precipitated polymer. However, we postulate that at these temperatures the solubility affected the polymer growth based on the results seen in the additional solvents. With this information going forward we utilized DCM as the solvent to conduct all polymerizations.
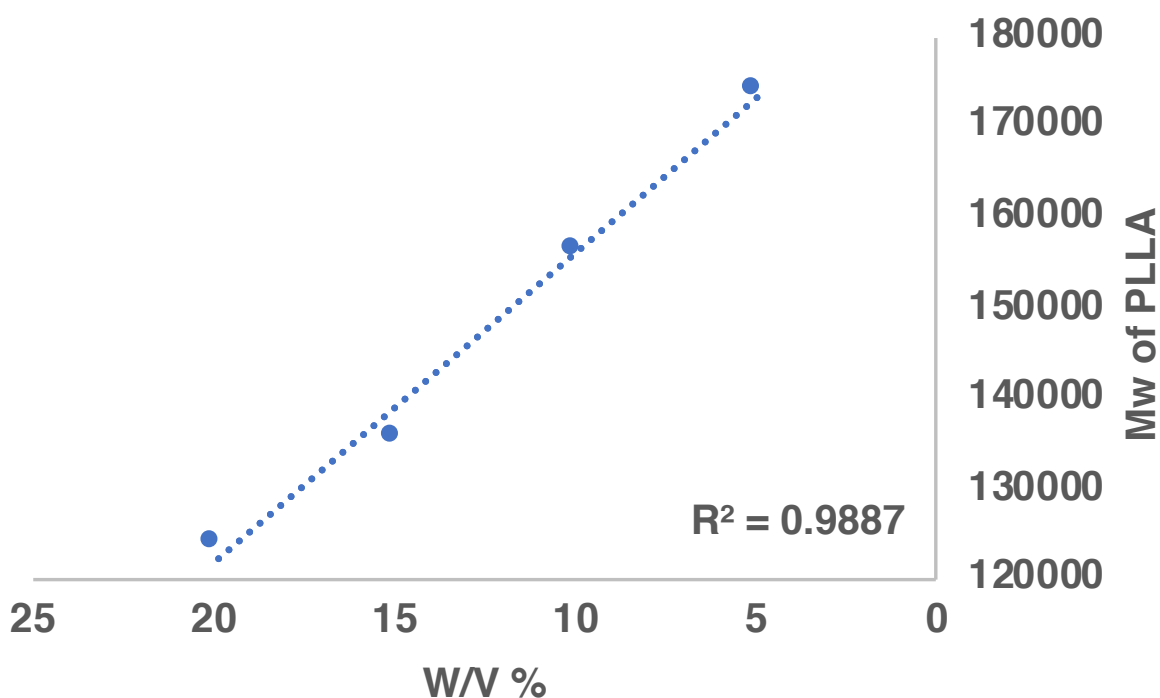
Figure 2.4 Growth of polymer M_w based on change in polymerization concentration.

Effects of polymerization concentration of molecular weight of PLLA polymer after 24 h at 5, 10, 15, 20 % weight by volume conducted at extreme cold temperature of - 80 °C in DCM.

2.3.4 Effects of the solution concentration (w/v %) on polymerization MW

The effects of polymerization concentration at 5 %, 10 %, 15 %, and 20 % where tested with a catalyst concentration at 1 % and excluding an initiator. To our knowledge we are the only group to report the polymerization of PLLA using the TBD organocatalyst without the use of an

initiator. We discovered that under these conditions we are able to achieve molecular weights exceeding > 170 K Da M_w with a PDI of 1.9 for the reaction with 5% w/v. The polymers collected showed a clear trend of increasing M_w as the concentration of the reaction went from 20% to 5% with an "R" value of 0.987. Additionally, all other reactions reached a minimum of > 130 k Da with a PDI ~ of 1.9 after 24 h. It is important to note that we attempted to polymerize the reaction at 1% weight by volume however, at this concentration the reaction produced polymers of ~ 50 k Da. Therefore, there seems to be a minimal threshold for the concentration of the reaction. The optimal concentration among those investigated is 5 % w/v [**Figure 2.4**].

2.3.5 Effects of TBD catalyst concentration on polymerization

Table 2.1 Growth of polymer M_w based on change in TBD concentration.

% W/V	TBD mol %	Time (h)	Mw (g/mol)	PDI
5	0.1	0.25	254712	2.4
5	0.1	24	357642	2.28
5	5	0.25	16299	3.5
5	5	24	23959	2.09
10	0.1	0.25	173057	2.94
10	0.1	24	221532	2.2
10	5	0.25	11426	2.78
10	5	24	33918	5.54

Polymerization parameters of -80 °C, no initiator. M_w measured by GPC.

After evaluating the effects that the solvent concentration is able to impart on the M_w of the polymer, we investigated the effects that catalyst concentration plays on the reaction using the parameters of 5% & 10% w/v, -80 °C, no initiator, 24 h reaction time, and TBD concentrations of 5%, 2.5%, 1%, .5%, .1% mol of lactide. We theorized that changing the

concentration of organocatalyst would have the most effect on polymerization. This is due in part

to the work described by Goodman *et. al.* and our experience working with the fast-acting

catalyst [92]. We theorized that the catalyst would create more active centers at higher

concentrations leading to smaller polymer molecular weights. We were able to achieve a high

M_w by lowering the catalyst concentration from 5% to 0.1% mol of L-lactide, (29,000 (PDI 2.09)

and 357,000 (PDI 2.28) g/mol, respectively). Likewise, by comparing the M_w achieved at 0.1%

mol catalyst concentrations to the M_w achieved in solvent concentrations of 5 and 10 % w/v

(357,000 (PDI 2.28) and 221,000 (PDI 2.20) g/mol, respectively) we can confirm that decreasing

the concentration of the reaction provides the highest molecular weight possible [**Table 2.1 and**
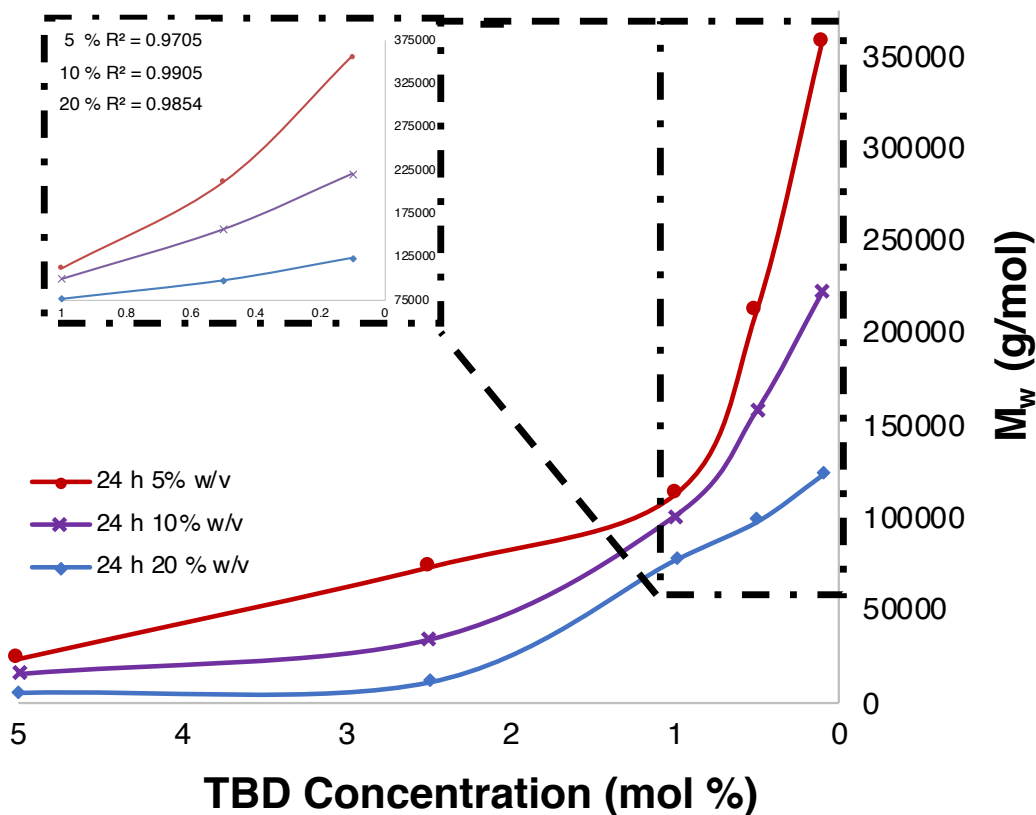
Figure 2.5 Growth of polymer M_w with change in catalyst mol % and W/V %.

As the catalyst concentration was lowered to 0.1% percent the polymer molecular weight
increased both at 5, 10, 20 % w/v reactions after 24h.

Figure 2.5]. Additionally, we attempted to polymerize the reaction using 0.01 % mol of the organocatalyst however, at 5% w/v, we only achieved molecular weights of ~ 87,700 g/ mol after 24 h. Likewise, when polymerizing the reaction at 10 % w/v at 0.01 % TBD we observed that the polymer M_w was approximately equal to that achieved by using 0.5% TBD, ~120 k Da. Therefore, there appears to be a minimum amount catalyst concentration needed to polymerize the largest polymers possible and the optimal TBD concentration among those studied is 0.1 %.

2.3.6 Controlled polymerization using initiator to synthesize polymers with defined Mw

While synthesis of HMW PLLA is beneficial for scaffold fabrication, we were also interested in showing that our system could be utilized to create defined polymers. For this reason, we investigated if we could use benzyl alcohol to synthesize polymers with a defined number of repeat units [**Table 2.2**]. We were able to demonstrate that this cold polymerization method can not only be used to synthesize HMW PLLA with $M_w > 300$ k Da, but can also be used to synthesize polymers with defined M_w, approximately the theoretical value up to 140 k Da. Although we achieved high molecular weight PLLA, when we attempted to polymerize PLLA with a L-lactide to initiator mol ratio of > 1000:1, respectively, we were not able to replicate the molecular weight of > 300 k Da. In most cases our polymerizations stalled around ~ 180 k Da with PDIs close of 1.8 – 2.5.

Table 2.2 Controlled growth of PLLA using anhydrous benzyl alcohol as initiator.

% W/V	TBD mol %	Time (h)	[I]/L- lactide	$M_{w, theo}$ (g/mol)	$M_{w, GPC}$ (g/mol)	PDI
5	0.1	24	70	10089	9940	1.16
5	0.1	24	175	25223	24200	1.22
5	0.1	24	350	50446	62002	1.38
5	0.1	24	700	100891	98403	1.41
5	0.1	24	1000	144130	142935	1.55
5	0.1	24	1500	216195	186200	1.72

Polymerization parameters -80 °C, with initiator. M_w measured by GPC.

2.3.7 Cold polymerization of general lactone polymers: PLGA, PCL using TBD organocatalyst

In order to demonstrate the versatility of our cold polymerization method we synthesized PLGA, PCL, and PGA utilizing our established method with minor modification when polymerizing PGA. What we discovered was that when polymerizing PLGA the reaction occurred extremely fast and polymerized high M_w polymers of approximately 101 k Da PDI 1.8. NMR determined the ratio of glycolide to L-lactide varied with an average of 43:57. The synthesis of PCL using the cold polymerization method in combination with the TBD catalyst produced polymers with a range of M_w 30 – 60 k Da. Although not considered high molecular weight this is higher than previously reported values for the synthesis of PCL using TBD organocatalyst[206].

2.3.8 Synthesis of HMW PSLA polymer with controlled ratio of spirolatide to L-lactide
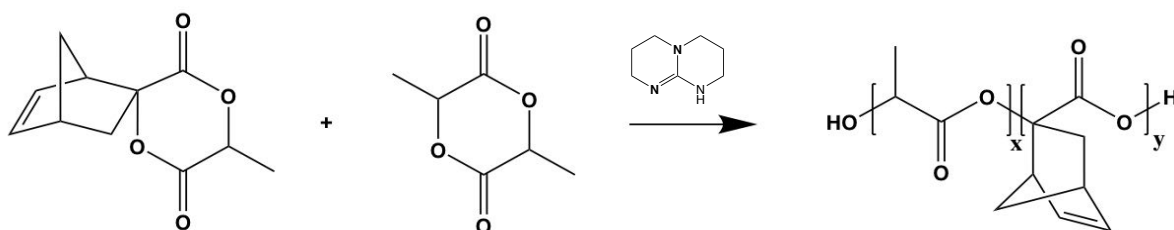
Figure 2.6 Synthesis scheme of PSLA polymerization with TBD.

PLSA with controlled feed ratio between spirolactide and L-lactide to synthesize PSLA with tailorable degree of functional norbornene groups in the polymer backbone.

Previously, Hillmeyer *et. al* described the synthesis of PSLA with varying ratios of L-lactide to spirolactide demonstrating M_n of < 35 k Da for all permeations [200]. To demonstrate the range of polymerization methods for lactones and derivatives we polymerized the permeations of spirolactide and L-lactide without the use of an initiator under our predetermined conditions [**Figure 2.6**]. We determined that our method can be used to create HMW PSLA polymers with a M_w > 300 k Da (~ 10 times previously published) [**Table 2.3**]. We did observe a trend of lower

molecular weight at the higher ratios of spirolactide to L-lactide (1:0, 1:1, 1:2, and 1:3).
However, all permeations achieved HMW with values near or > 100 k Da. We postulate, that the
reactivity and self-polymerization efficiency of spirolactide impedes the reaction leading to
lower MW polymers. After evaluating the co-polymerization via NMR, we were able to
determine that the formed polymers closely matched the theoretical ratio values. Additionally, it
is important to note that this is the first time the polymer has been reported with such a HMW,
allowing us to utilize the polymer for fabrication of nanofibrous scaffolds fibrous meshes.

Table 2.3 Growth of PSLA polymer M_w based on change in TBD concentration.

% W/V	TBD mol %	Time (h)	Monomer Ratio (Spiro:L-Lactide)	Repeat Ratio$_{theo}$ (spiro:L-lactide)	Actual Ratio$_{theo}$ (spiro:L-lactide)	$M_{w, GPC}$ (g/mol)	PDI
5	0.1	24	1 : 0	1 : 1	1 : 1	98200	1.31
5	0.1	24	1 : 1	1 : 3	1 : 4	151052	1.4
5	0.1	24	1 : 2	1 : 5	1 : 6	174599	1.38
5	0.1	24	1 : 3	1 : 7	1 : 8	180010	1.41
5	0.1	24	1 : 5	1 : 11	1 : 13	336629	1.58
5	0.1	24	1 : 10	1 : 21	1 : 21	318230	1.70
5	0.1	24	1 : 20	1 : 41	1 : 41	263940	1.81

Polymerization parameters of -80 °C, with no initiator, and a controlled ratio between
spirolactide and L-lactide. M_w measured by GPC.

2.3.9 HMW PSLA Fabricated into Biomimetic Scaffolds and Electrospinning

To demonstrate the utility of the PSLA polymer we fabricated fibers through two
different means, TIPS and electrospinning. We first began by showing that PSLA polymer could
indeed form fibers at a high molecular weight. By creating a 10% w/v polymer solution in THF
with the PSLA ratios we induced TIPS between glass slides and characterized the resulting films
via SEM. We observed that although all the polymers were of proper MW those with ratios
below 1:5 did not form the nanofiber morphology. Therefore, we focused on the PSLA$_{1:5}$ to
fabricate three-dimensional scaffolds and the electrospun fibers. Using the PSLA$_{1:5}$ we fabricated
disk-shaped 3D scaffolds with porous and interconnected morphology. Most, importantly we

were able to visualize that the scaffolds retained the favorable nanofibrous morphology [**Figure 2.7**]. We then explored the PSLA$_{1:5}$ polymer for its potential to be electrospun and create a fibers mesh. Through this method we were able to demonstrate that indeed the PSLA$_{1:5}$ polymer can be formed into a fibrous mesh that has the potential to serve for numerous tissue engineering purposes. Above all, we are able to demonstrate that we are able to synthesize HMW PSLA polymers via cold polymerization with the TBD organocatalyst to fully explore the potential of this attractive polymer.
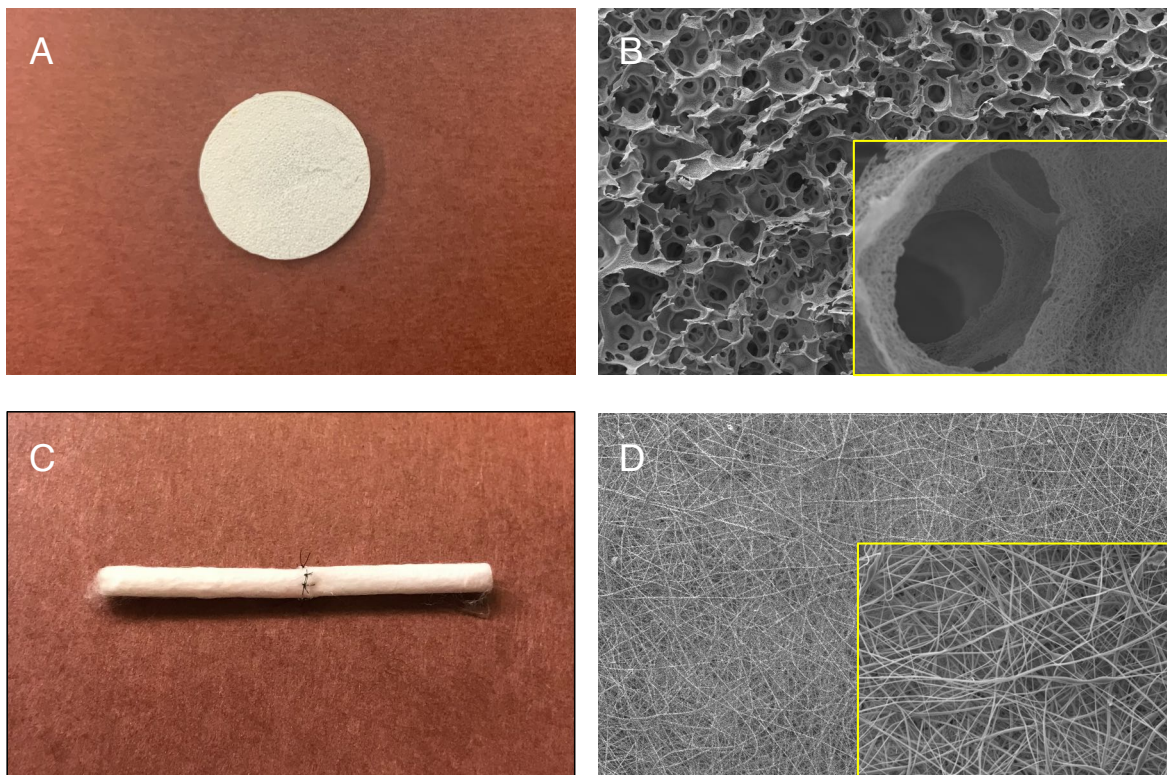
ratio 300 k Da M$_w$.

h TIPS and Sugar Leaching B) Magnified
y and porosity via (SEM) C) Gross image
D) Magnified image of PSLA fibers

2.3.10 Cold polymerization of PLLA and PSLA with alternative guanidine catalysts

Additionally, we tested the cold polymerization method using a varity of guanidine derived catalysts to demonstrate the efficiency of cold polymerization. Here we utilized DBN , MTBD, and DBU in a similar manner to polymerize PLLA. All three catalyst have been previously shown to effectively catalyze the polymerization of PLLA at room temperature and higher temperature (up to 80°C). However, none of these catalyst has been previously shown to catalyze the polymerization of PLLA under such extreme low temperatures (-80°C). Surprisingly we discovered that utilizing these catalysts the polymerization occurred in the same manner producing high molecular weight polymers with two of the 3 catalysts (DBN and MTBD). Of these DBN demonstrated superior properties of catalysing polymerization of HMW PLLA with very narrow PDI similar to living polymerization. For this reason, we utilized DBN to catalyse the polymerization of PSLA and showed that it too can polymerize HMW PSLA but with improved PDI [**Table 2.4**].

Table 2.4 Polymerization of PLLA and PSLA using DBN, MTBD, DBU.

Polymer Synthesized	Catalyst	% W/V	TBD mol %	Time (h)	$M_{w, GPC}$ (g/mol)	PDI
PLLA	DBN	5	0.5	24	250911	1.08
PLLA	DBN	10	0.5	24	144000	1.05
PLLA	MTBD	5	0.5	24	152358	1.23
PLLA	MTBD	10	0.5	24	125464	1.33
PLLA	DBU	5	0.5	24	60195	1.05
PLLA	DBU	10	0.5	24	22327	1.06
PSLA$_{1:5}$	DBN	5	0.5	24	220828	1.58
PSLA$_{1:5}$	DBN	10	0.5	24	122925	1.64

Polymerization parameters of -80 °C, with no initiator, and a controlled ratio between spirolactide and L-lactide. M_w measured by GPC.

2.4 Discussion

Researchers working to develop biomaterials for biomedical applications such as tissue engineering scaffolds are interested in synthesizing HMW polymers cheaply and with ease. Currently, acquiring HMW polymers requires purchasing from manufacturers that utilize expensive systems raising the cost of the final product. Additionally, HMW polymers from lactones such as PLLA that can form the favorable biomimetic nanofibrous architecture that contains functionality (NH$_2$, SH, or Alkene) are not commercially available. Therefore, a cheap and facile method to synthesize HMW PLLA polymers and derivatives with desired functionality with equipment readily available to most labs has been the focus in this work.

Traditionally, PLLA synthesis involves the ROP of L-lactide catalyzed by the tin catalyst stannous octoate[67, 199]. In an academic laboratory, the reaction is typically carried out in small scales using reaction vessels that severely limit the growth of the polymer. This is because the polymerization is carried out in a bulk reaction, and as the PLLA increases in MW, it becomes viscous; when the polymer reaches ~ 10-15 k Da, the polymer becomes too viscous to stir continuously. Therefore, the interactions within the polymer chains become limited and the polymer throttles. Additionally, the polymer releases water that can become entrapped in the viscous polymer and cause hydrolytic cleavage of the growing chains. In our experience, laboratory polymerization of PLLA rarely produces polymers in molecular weight larger than 50 k Da. Furthermore, the reactions are time-consuming and utilize toxic metal catalysts. In industry, these issues are remedied by using large reactors with powerful rotors and vacuums to remove the water released, thereby producing polymers with high molecular weight. However, these polymers are not tailorable (i.e., able to be end-functionalized), the cost is prohibitively expensive, and the lead time is several weeks.

For these reasons, our facile and rapid method of developing high molecular weight PLLA is an attractive method when compared to the traditional synthesis stated above. This method uses no heat, uses small amounts of an organocatalyst, and can, be performed at low concentrations (% w/v) to facilitate the growth of the polymer. As we have shown in the study, in this method, PLLA is rapidly polymerized with an organocatalyst reducing the toxicity over the tin catalyst. Most importantly, this method is facile, cheap, and scalable as we have produced batches of 5 g, which serve most laboratories' immediate needs. The reaction requires limited space and can be performed with the equipment readily available in most labs, thereby making this method accessible to most researchers.

In our experience, we achieved the same conversion and polymer molecular weight as those reported in the literature. Initially, when the reaction was performed at room temperature, a green/yellow tint was observed, leading us to believe there was a possible degradation of the catalyst due to the release of nitrogen. When the reaction was performed at 4°C, we noted the disappearance of the green/yellow tint, higher efficiency of the monomers consumed, and an increase in molecular weight of the polymer. These observations led us to believe that temperature played a role in stabilizing the reaction and increasing the molecular weight. Therefore, we began by focusing on the general procedures reported in the literature (15 % w/v, 1 % organocatalyst, and the use of benzyl alcohol as an initiator) to synthesize HMW PLLA and explored the effects that temperature would have on the polymer weight. Importantly, the PDI of the reaction demonstrated near living polymerization results similar to those reported using atom transfer radical polymerization (ATRP), or reversible addition fragmentation chain transfer (RAFT) when the polymer was below 100 k Da.

This extreme cold temperature was chosen because - 20 °C and - 80 °C freezers are commonly available and because the temperatures are far from the melting temperature of DCM. This ensured that the reaction would not solidify due to the temperature used in our method. After determining the optimal polymerization condition for the reaction with the TBD organocatalyst to be -80 °C, various parameters were investigated to determine the effect on the polymer growth. To accomplish this, we focused on three primary parameters: concentration of polymerization (w/v %), the concentration of organocatalyst used, and addition of benzyl alcohol as an initiator where we saw clear trends as we optimized the parameters.

Of interest and note was that we did not require an initiator to initiate the polymerization. To our knowledge, the use of TBD organocatalyst to polymerize lactone polymers has used an initiator to induce the polymerization. Here we report that when we utilized an initiator, we saw smaller polymers than when we did not include an initiator. We hypothesize that this is due to the fast-acting TBD catalyst activating numerous reactive centers at once in addition to those provided by the initiator concentration, the chains with the initiator can only grow in one direction as opposed to in a bifunctional manner with no initiator, and purity and dryness of the initiator; thereby limiting how large the chains can grow. Although we have reached a molecular weight limitation utilizing an initiator, we believe that this system is still superior over tin catalyzed ROP reactions, which can only polymerize PLLA in the 40-50 k Da range under standard laboratory conditions. In contrast, this this novel TBD catalyzed cold polymerization reaction can achieve defined polymers up to ~ 140 k Da.

Polymers synthesized from lactones such as PLLA have been the gold standard in biomedical applications such as tissue engineering in the fabrication of scaffolds and implants due to their favorable properties that include biodegradability, biocompatibility, and the ease of

processing[17, 18]. PLLA has been widely utilized for the development of scaffolds suitable for various tissue regeneration, such as blood vessels, cartilage, bone, and dental pulp[9, 18, 38, 54, 161, 207]. The utility and advantage of PLLA have been amplified by imparting biomimetic properties onto the scaffolds through the development of nanofibrous architecture[4, 68]. This feature is feasible when the polymer reaches a certain high molecular weight and is processed through a method known as thermal-induced phase separation (TIPS)[55, 68]. When combining a porogen made from sugar and the TIPS technique, a HMW PLLA can be processed into a porous, interconnected, and nanofibrous scaffold to improve cell attachment, proliferation, and differentiation for a wide range of tissues[59, 194, 207]. This is due to the unique fiber morphology that mimics the extracellular matrix (ECM) collagen and provides similar physical and mechanical properties in which cells naturally occupy[40, 102, 208].

In an attempt to optimize and improve the biomimetic properties of tissue engineering scaffolds, researchers made considerable effort introducing growth factors, biomolecules, and peptides that will enhance the microenvironment[2, 17, 56, 209]. Adding these signals by conjugating them to the polymers can prevent them from being washed away. However, PLLA and most other polymers used for tissue engineering scaffolds lack functionality in the backbone. For this reason, poly(spirolactide-co-lactide) (PSLA) synthesized from L-lactide and spirolactide, a derivative of L-lactide with a norbornene ring substituting a methyl group, with a high degree of backbone functionality that can be post-modified via thiol-ene click chemistry is of interest for tissue engineering scaffolding. The tailorable of norbornene rings in the polymer produced can be easily modified via thiol-ene and tetrazine click chemistry and most importantly at $PSLA_{1:5}$ and higher ratios we are able to fabricate the favorable nanofibrous architecture. Previously, PSLA has never reached a molecular weight higher than 30 k Da, which is not suitable for the

fabrication of tissue engineering scaffolds. In this work, we were able to demonstrate the broad nature of the extreme cold polymerization to synthesize HMW PSLA copolymers suitable for tissue engineering.

2.5 Conclusion

In this work, we have developed a facile and rapid method of synthesizing HMW polymers in an economical and reproducible manner. Cold temperature polymerization can be used to provide HMW for multiple applications. We demonstrate how this method can be utilized to polymerize PLLA and the functional polymer PSLA for tissue engineering platforms. Never before has PSLA been synthesized with a high molecular weight. In this work, the HMW PSLA polymer was shown that it too could be fabricated with biomimetic porous, interconnected, and nanofibrous architecture and be easily post-modified to enhance the biomimetics. For these reasons, we believe that this polymerization method will change how polymer scientists will synthesize PLLA and PSLA, allowing for a higher degree of specification and thereby expanding their use in tissue engineering.

Chapter 3. Biomimetic Tubular Scaffold with Tunable Conjugation of Heparin and Modulated

Degradation for Rapid *in situ* Regeneration of a Small Diameter Neoartery

R. Navarro[#], L. Jiang[#], O. Yang, P. Qiu, L. Zhiyong, B Yang, Y. E. Chen, P.X. Ma, "Biomimetic tubular scaffold with tunable conjugation of heparin and modulated degradation for rapid *in situ* regeneration of a small diameter neoartery." [#]Both authors contributed equally to this work. *Under Review* in Journal of Biomaterials.

3.1 Introduction

3.1.1 Cardiovascular disease and the need for vascular grafts

Cardiovascular disease (CVD) remains a severe burden on global healthcare, accounting for 17.7 million deaths, almost a third of all global deaths, in 2015 [149]. As this figure is predicted to increase to over 23 million deaths by 2030, CVD has become a pandemic that will continue to be a health issue for the foreseeable future[149, 150]. In addition to CVD's impact on human health and life, the monetary cost of CVD has been estimated to be around $530 billion in direct and indirect costs [150]. Of all the deaths caused by CVD, over 50 percent have been attributed to vascular damage induced by accumulation of vascular plaque, which leads to blocked and hardening vessels that deteriorate over time and may cause lesions. For these reasons, much effort has been put forth to develop suitable replacement vessels from allografts, xenografts, and synthetic grafts. However, these sources do not satisfy the demand for replacement vessels, particularly small diameter vessels (< 6 mm ID)[164, 171, 193]. This is due to limited supply of available allografts, biocompatibility issues with xenografts, and thrombosis issues associated with synthetic grafts smaller than 6 mm in diameter. Therefore, scientists have turned to tissue

engineering as a means to produce suitable substitutes particularly for small diameter vessels[167, 168, 210].

3.1.2 Tissue engineered vascular grafts

While synthetic grafts have served as off the shelf replacement for blood vessels, these grafts suffer from several limitations: thrombosis has been observed in small diameter (<6 mm) grafts, thereby limiting their use to large arterial blood vessels; these grafts are made from nondegradable polymers which prevent generation of natural tissue; and the implanted material becomes susceptible to wear and tear over time [169, 171]. Tissue engineering has been seen as a promising way to address these limitations and create a vascular graft that is biocompatible, biodegradable, and promotes mature native tissue formation. Recently, biomimetic scaffolds that are porous, interconnected and contain nanofibrous architecture have been synthesized [38, 50, 54, 161]. These poly(lactic acid) (PLLA) scaffolds have been shown to develop mature vascular tissue *in vitro* and when implanted subcutaneously. This is due to the enhanced biomimetic nature of the scaffold which allowed for enhanced penetration of vascular smooth muscle cells (VSMCs) into the construct promoting the desired VSMC contractile phenotype [54, 161, 194]. The nanofibrous architecture is able to mimic the natural extracellular protein in physical properties [27, 65, 68].

3.1.3 Concerns with tissue engineering scaffolds

Despite these advances, much work is still needed for tissue engineering scaffolds to regenerate viable vascular replacements. For example, PLLA is hydrophobic itself and may not provide the ideal surface for cell interactions. The degradation rate of PLLA is slow and may not optimally match the vessel regeneration. In addition, PLLA may not have the desired anti-thrombogenic properties [86, 93, 98, 177, 196, 211]. Researchers have attempted to incorporate heparin onto scaffolds, but due to the little chemical functionality of the polymers used to fabricate the

scaffolds, very little to no conjugation of heparin is possible, which requires the formation of covalent or physical covalent bonds through the surface chemical groups [160, 170, 181, 184, 191, 195]. In addition, it is not just important that we can tailor the scaffolds with biological motifs or regulatory signals, but the polymers themselves must allow us to process them into biomimetic architecture in order to retain the favorable architecture. This requires the use of HMW polymers as described in Chapter 1. Therefore, making many polymers unsuitable for tissue engineering when compared to HMW PLLA, which has been previously shown to be conducive for vascular tissue engineering. In this work, we developed a high molecular weight poly(spirolactic-co-lactic acid) (PSLA), which provides the high chemical functionality in the backbone to achieve the desired density of heparin conjugation that would prevent thrombosis when implanted *in situ* and the MW necessary for biomimetic scaffold fabrication. In addition, the high level of functionality allowed us to demonstrate how to tailor the degradation, mechanical properties, and the surface hydrophilicity. We investigated the ability of these biologically activated scaffolds for blood vessel replacement in rat models and demonstrated their ability to promote vascular tissue regeneration *in vivo*.

3.2 Materials and methods

3.2.1 Materials

L-lactide was graciously donated by Altasorb® and recrystallized in ethyl acetate before use. Poly(L-lactic acid) (PLLA, Resomer L207S) with an inherent viscosity of 1.6 dl/g was purchased from Boehringer Ingelheim (Ingelheim, Germany). Heparin was purchased from Fisher Scientific and modified with L-cysteine. Polyethylene glycol modified at one end with thiol (PEG-SH) of a MW of 10 kDa was purchased from Layson Bio. Polycaprolactone 70-80 k Da (PCL), N-Bromosuccinimide (NBS), triethylamine (TEA), Luperox® A98 benzoyl peroxide,

benzene, mineral oil, Span 80®, ethyl acetate, hexane, benzyl alcohol, magnesium sulfate (MgSO₄), sodium thiosulfate, triazabicyclodecene (TBD), L-cysteine, fructose, tetrahydrofuran (THF) and dichloromethane (DCM) were purchased from Sigma-Aldrich Company (USA) and used as received.

3.2.2 Spiro[6-methyl-1,4-dioxane-2,5-dione-3,2'-bicyclo[2.2.1]hept[5]ene] synthesis

PSLA was synthesized following [**Figure 3.1**]. L-Lactide was modified based on a method previously reported [202]. Briefly, L-Lactide was combined with NBS (1.1 eq.) in benzene (20 % w/v) and heated to reflux. Benzoyl peroxide dissolved in benzene was added dropwise and the reaction was monitored by thin layer chromatography (TLC) until completion. The reaction was vacuum filtrated and condensed and the resulting solid was dissolved in DCM, washed in sodium thiosulfate solution, and concentrated. The solid was recrystallized from ethyl acetate and hexane twice to yield white crystals, (3S, 6S)-3-Bromo-3,6-dimethyl-1,4-dioxane-2,5-dione (bromo-lactide) **(1)**. The white crystals were dissolved in DCM in a flask under nitrogen and cooled in an ice bath. TEA (1.1 eq) was added in dropwise and allowed to react for 1 h at 0° C and 1 h at 25° C. The reaction was washed with 1M HCl three times and condensed. The crystals were further purified by liquid chromatography on silica gel and recrystallization in ethyl acetate to yield white crystals, (6S)-3-Methylene-6-methyl-1,4-dioxane-2,5-dione (methylene lactide) **(2)**. To freshly distilled cyclopentadiene (2.2 eq.) **2** was added (1 eq.) and refluxed overnight in benzene under argon. The reaction was condensed and purified by liquid chromatography in 50/50 hexane:DCM (r_f = 0.31) followed by recrystallization in ethyl acetate to yield white crystals, Spiro[6-methyl-1,4-dioxane-2,5-dione-3,2'-bicyclo[2.2.1]hept[5]ene] (spiro-lactide) **(3)**.

Figure 3.1 Synthesis route of PLLA-based copolymer poly(spirolactide-co-lactic acid).

A) Addition of bromine from NBS followed by the elimination of the bromine using TEA to produce exomethylene lactide (1) B) Diels-Alder addition of freshly distilled cyclopentadiene to exomethylene lactide yielding spirolactide C) Polymerization of PSLA from L- lactide and spirolactide.

3.2.3 General procedure for the ring-opening polymerization

In a reaction flask spirolactide was added in a 1:3 ratio with L-lactide and purged three times via a standard vacuum/nitrogen gas treatment before dissolving in anhydrous DCM at 5% w/v. The flask was cooled to - 80 °C for 1 h and was then injected with 0.5 % mol TBD catalyst dissolved in DCM. The reaction was allowed to react for 24h and the polymer formed was precipitated in ethyl ether, re-dissolved in DCM and precipitated in ethyl ether and stored under

vacuum. The copolymer produced is referred to in the remainder of this work as poly(spirolactic-co-lactic acid) (PSLA).

3.2.4 Monomer, polymer and scaffold characterization

Nuclear magnetic resonance characterization: All monomers (L-lactide, exomethylene lactide and spirolactide) and polymers formed were characterized via 500 MHz ^{1}H and ^{13}C (Varian Inova 500) by dissolving in CDCl$_3$.

Ultraviolet–visible spectroscopy: All monomers and polymers formed were characterized by first dissolving in DCM and using a quartz cuvette to obtain spectrum from 200 - 700 nm (up to 350 shown) (Hitachi U-2910).

Fourier-transform infrared spectroscopy: Monomers, polymers, and modified tubular scaffolds were characterized by directly placing the sample on the diamond crystal sample holder to obtain the spectrum from 600 – 4000 nm (Thermo-Nicolet IS-50).

Scanning electron microscopy (SEM) observation: Empty scaffolds were sputter-coated with gold for 150 seconds and observed under a scanning electronic microscope (JEOL JSM-7800FLV).

Gel permeation chromatography: Polymers formed were dissolved in anhydrous tetrahydrofuran and the molecular weight of the polymers were determined by comparing to polystyrene standards (*Shimadzu GPC*).

3.2.5 Bilayer nanofibrous tubular scaffold fabrication

A tubular scaffold with favorable nanofibrous architecture and tunable physical properties, such as pore size, interconnectivity, internal diameter, and wall thickness was fabricated using a method incorporating a sugar template and thermally induced phase separation (TIPS).

Molds for the tubular scaffold were fabricated in a facile, economic, and reproducible method by using aluminum foil cut to 5 cm wide strips. The aluminum foil was wrapped around a metal rod with the desired external diameter (1.85 mm) and the sugar spheres were then deposited inside the aluminum mold while submerged in hexane to prevent moisture from agglomerating the sugar spheres. The sugar template spheres were fabricated through an emulsion method developed by Ma *et. al*[17, 64]. The sugar spheres were separated using sieves to recover spheres ranging from 60 – 150 μm in diameter. A mandrel with the desired internal diameter (1.0 mm) was placed in the center and the sugar spheres annealed to the desired interconnectivity by placing in a 37 °C incubator for 7 minutes followed by vacuum drying the scaffold.

TIPS was carried out according to procedures developed by Ma et al[61, 68]. The aluminum foil was removed, and the sugar template was dipped into a 10 % w/v polymer solution consisting of 50 % PLLA (inherent viscosity of 1.6 dl/g) and 50 % PSLA dissolved in THF, and then quickly cooled to - 80 °C in order to allow for phase separation. The scaffolds where maintained at this temperature for 24 h. PCL dissolved in trifluoroethanol (TFE) was then electrospun immediately after brushing with a mixture of 90:10 Hexane to THF (15 kV, 10 cm, 2 mL/h, w/rotation). This mixture created a tacky surface in which the electrospun PCL fibers could anneal to. The scaffolds were then placed in hexane for 24 h to remove excess THF and TFE and were subsequently placed in DDH_2O to remove the sugar spheres. After the sugar is completely washed away, the mandrel was easily removed, and the scaffold was cut to the desired length.

3.2.6 Surface modification with anticoagulant molecules

Tubular scaffolds were modified through UV-light induced thiol-ene click-chemistry with the desired molecules to be conjugated. Briefly, methoxy-PEG-SH 2k (50 mg), heparin modified with L-cysteine (100 mg), and tetramethylethylenediamine (TEMED) were dissolved in DDH$_2$O. The UV-initiator, Irgacure 2959, was dissolved in 100 μL of dimethyl sulfoxide (DMSO) and added to the solution. The scaffolds were quickly soaked in ethanol then added to the PEG/Heparin solution prior to being exposed UV-light. The scaffolds were then washed in methanol and DDH$_2$O to remove excess TEMED and Irgacure 2959 before being lyophilized. The scaffolds were then sterilized with ethylene oxide (Anproline Gas Sterilizer) and stored at -20 °C.

3.2.7 Contact angle measurements of thin-films

Thin-films were fabricated through TIPS process of a 10% polymer solution on a silicon surface to determine the wetness and change of hydrophilicity due to the conjugation of heparin. Films from both PSLA/PLLA blend and PLLA were fabricated, and a subfraction of each type were further modified with increasing concentration of heparin to produce films with the following permeations: PLLA no heparin, PLLA w/ Heparin (50 mg), PSLA, PSLA with increasing heparin concentration 10 mg, 50 mg, and 100 mg and a PEG575 gel as a positive control, n = 3 each and a standard error of ± 2°. The films were attached to a glass side using double sided tape and the advancing contact angle of a drop of water was measured utilizing Rame-Hart 200-F1 contact angle goniometer.

3.2.8 "In vitro" degradation

Flat three-dimensional scaffolds were fabricated in a Teflon® mold utilizing the sugar template previously discussed to determine the degradation rate of the interior *loose layer* in the

tubular scaffolds with or without being modified with heparin [38, 161]. Scaffolds from the PSLA/PLLA blend and PLLA were fabricated using this method and cut into a 2 mm thick disk. As a control, PLLA scaffolds were included with and without heparin conjugated as well as PSLA/PLLA blend scaffolds with and without heparin conjugated, n = 5. The scaffolds were placed in a pre-weighed 20 mL vial and then weighed to determine the mass of the scaffold at day 0. To each 20 mL vial containing a scaffold, 10 mL of 1 M PBS pH 7.4 was added and incubated at 37 °C. The PBS was removed at predetermined times, the scaffolds were lyophilized, and the mass was taken and recorded. The scaffolds were then submerged in fresh PBS and incubated at 37 °C. Images were taken at day 0 and day 35 to track the change in mass loss and degradation.

3.2.9 In situ implantation of tubular scaffold as a replacement for descending aorta in rat

A scaffold 10 mm in length and 1 mm in inner diameter were *in situ* implanted into Sprague Dawley (SD) rats, 2 - 4 month-old, weighing 200 - 400 g (Charles River Laboratories, Boston, MA) as abdominal aorta interposition grafts to evaluate the viability and effectiveness of the tubular scaffolds and to determine the remodeling in vivo. All procedures were approved by the Institutional Animal Care and Use Committee at The University of Michigan. After anesthesia with Ketamine (80mg/kg) and Xylazine (8mg/kg), heparin was administered 150 units/kg intravenously through the tail vein. The animal was placed in the supine position on a warming pad (37°C) and a midline laparotomy was performed. The infrarenal aorta was dissected and clamped using two microclamps. The vascular scaffold was implanted in an end-to-end interrupted anastomotic pattern using 9-0 prolene sutures under a microscope. The abdomen was then closed in multiple layers. Lovenox was given 100 units/kg twice a day subcutaneously for anticoagulation.

3.2.10 Doppler and ultrasound visualization and analysis of in situ graft

At a predetermined time of 1, 2, and 3 months after implantation, animals were examined using a Vevo 770® Micro-ultrasound System (Visual- Sonics, Toronto, Canada) equipped with the RMV-704 scanhead (spatial resolution 40 mm) to determine graft patency and blood flow. The diameter of the graft at the midpoint was measured from both transverse and longitudinal axis ultrasound images. Grafts were explanted at 1 w, 2 w, 1, 2, and 3 months post-operatively.

3.2.11 Histological observation of remodeled tissue engineered blood vessels (TEBVs)

The TEBVs were washed with PBS prior to being fixed with 3.7% formaldehyde in PBS and left overnight to react. Subsequently they were dehydrated through the use of ethanol, embedded in paraffin, and sectioned at a thickness of 5 mm. Sections were deparaffinized, rehydrated with a graded series of ethanol, and stained with H-E, Masson's trichrome, and Verhoeff-Van Gieson method.

3.3 Results

3.3.1 Synthesis of spirolactide and poly(spirolactide-co-lactictide)

A high molecular weight co-polymer derived from L-lactide that is biodegradable and can be easily modified via thio-lene click chemistry leading to tunable properties was successfully synthesized [**Figure 3.2**]. L-Lactide was used as the starting material in the synthesis of spirolactide and then copolymerized in a 1:3 ratio between spirolactide to L-lactide. The resulting polymer, poly(spirolactide-co-lactictide), had a molecular weight of M_w = 179 kg mol^{-1} PDI of 1.6 (measured by GPC). The monomers and polymer were thoroughly characterized using NMR, UV-VIS, and FTIR to demonstrate that we have successfully synthesized them [**Figure 3.2 D - G**] and compared with previous published results to confirm our findings [200, 202].

This PSLA was blended with PLLA at a 50:50 ratio (w/v %) and used in the fabrication of the

tubular scaffolds, referred as PLLA/PSLA.
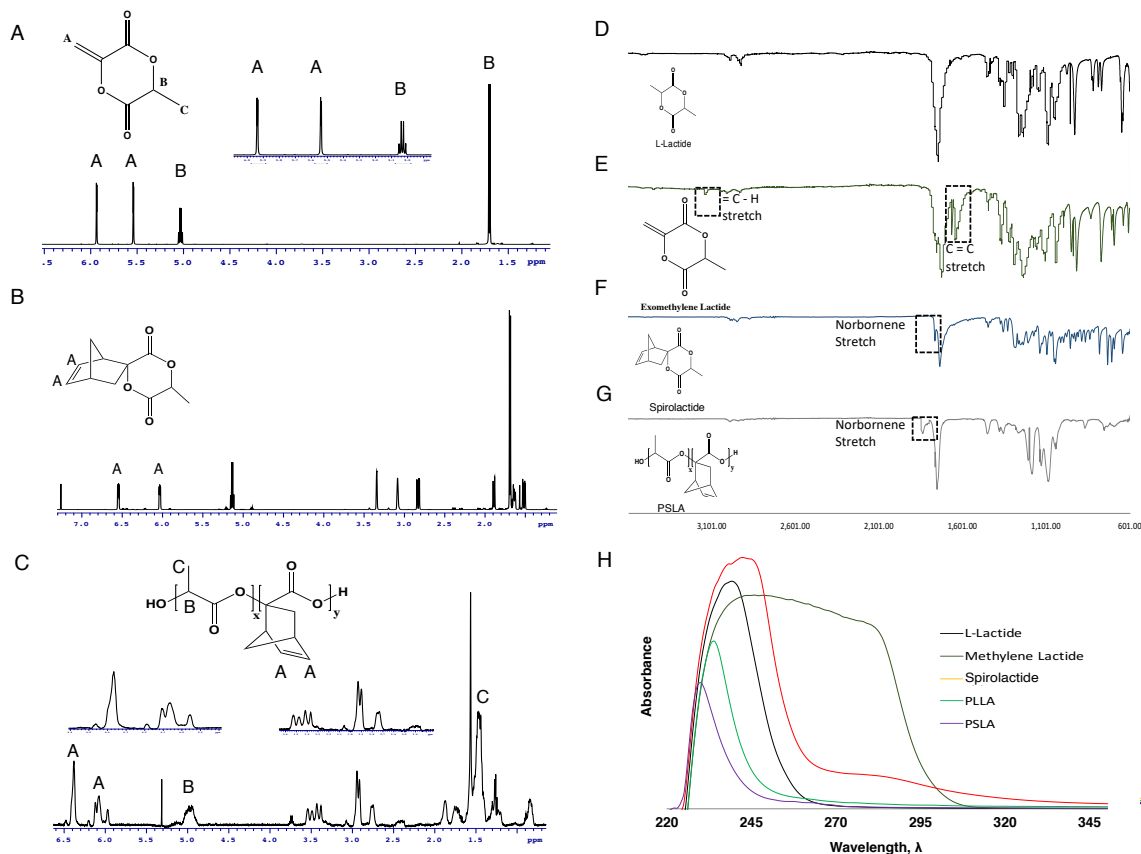
Figure 3.2 Characterization of PSLA and precursor monomers.

A) Addition of bromine from NBS followed by the elimination of the bromine using TEA to produce exomethylene lactide (1) B) Diels-Alder addition of freshly distilled cyclopentadiene to exomethylene lactide yielding spirolactide C) Polymerization of PSLA from L- Lactide and Spirolactide D - H) FTIR characterization depicting stretches of key functional groups L-lactide, exomethylene lactide, spirolactide, and PSLA to compare absorption peaks and trends H) UV – Vis absorbance of monomers, PLLA, and PSLA to compare absorption peaks and trends.

3.3.2 Nanofibrous tubular scaffold fabrication

A tubular scaffold was fabricated using the 50/50 PLLA/PSLA blend via thermally

induced phase separation (TIPS) and porogen leaching methods [**Figure 3.3 A - C**]. With this

chosen polymer blend and utilizing our previously developed sugar leeching and TIPS

techniques, we developed a highly porous and interconnected tubular scaffold that retained the favorable nanofibrous architecture (pore size of 60-150 μm; interconnectivity of ~30 μm), similar to those of PLLA. Most significantly, the tubular scaffolds could now be easily modified with anticoagulant molecules.
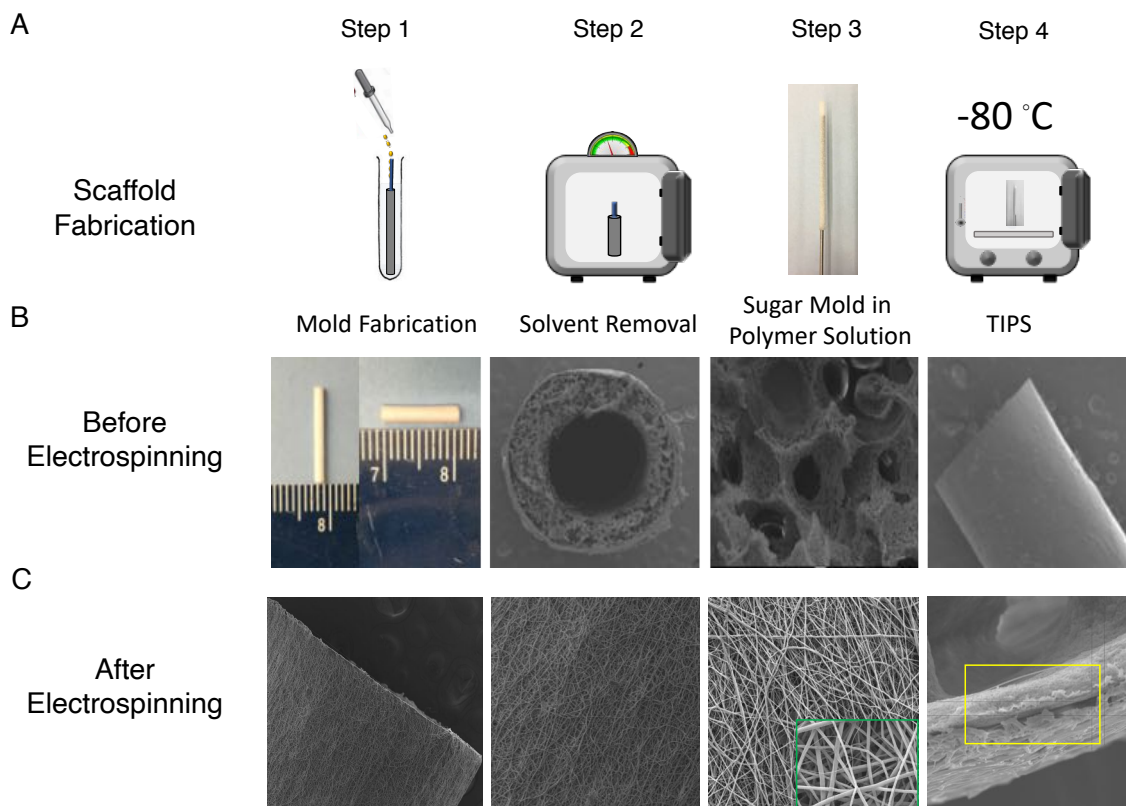
Figure 3.3 Fabrication of a tubular scaffold that can be easily post-modified.

A) Fabrication method for sugar template annealed on mandrel for the fabrication of porous and interconnected network B) Overview and SEM characterization of PSLA/PLLA *loose layer* that is highly porous, interconnected, and nanofibrous C) Visualization of PCL *dense layer* that is electrospun to provide enhanced mechanical support.

3.3.3 Conjugation of anticoagulant molecules on tubular scaffold

The above tubular scaffolds were modified with anticoagulant molecules (heparin and PEG) via thiol-ene click chemistry between the norbornene ring on the PSLA and a thiol group [**Figure 3.4 A**]. Characterization of this conjugation via FTIR demonstrated that the click

reaction between the thiol and the norbornene ring was successful because of the presence of the thiol-ene clicked peak at 800 nm and the absence of the double bond peak at around 1630 nm [**Figure 3.4 B**]. The scaffolds were visualized by SEM to demonstrate preservation of the favorable biomimetic physical properties after the surface modification (unobstructed lumen, porous and interconnected, and nanofibrous architecture) [**Figure 3.4 C**]. The conjugation was visualized through confocal microscopy by the conjugation of SH-PEG-FITC onto the PLLA/PSLA scaffolds and comparing these results to PLLA scaffolds treated in the same manner [**Figure 3.4 D**]. Compared to the control scaffold fabricated from pure PLLA, the scaffold comprised of the advanced functional polymer blend were highly modified with the fluorescent polymer (SH-PEG-FITC) and elucidated by confocal microscopy.

3.3.4 Thin-film contact angle measurement

Heparin conjugated films showed increased wettability with contact angles ranging from 25 – 40° as compared to the unmodified PLLA (100°) and PLLA/PSLA blend (110°) films. This indicates the highly hydrophilic property of the heparin conjugated materials. Both films with 50 mg heparin and with 100 mg heparin were able to absorb the water droplet after 3 and 1 min respectively [**Figure 3.4 E**].

3.3.5 Scaffold "in vitro" degradation

Three dimensional scaffolds were fabricated and conjugated with heparin to determine the mass loss of the porous layer. Four groups were made: two containing unmodified PLLA/PSLA blend and PLLA and two containing conjugated heparin. The fabricated scaffolds were incubated in PBS at 37°C and loss of mass was observed over time. Visually, the PLLA/PSLA group conjugated with heparin began to fall apart at day 10, with all scaffolds breaking apart into large and small pieces by day 28. In comparison, the PLLA group remained
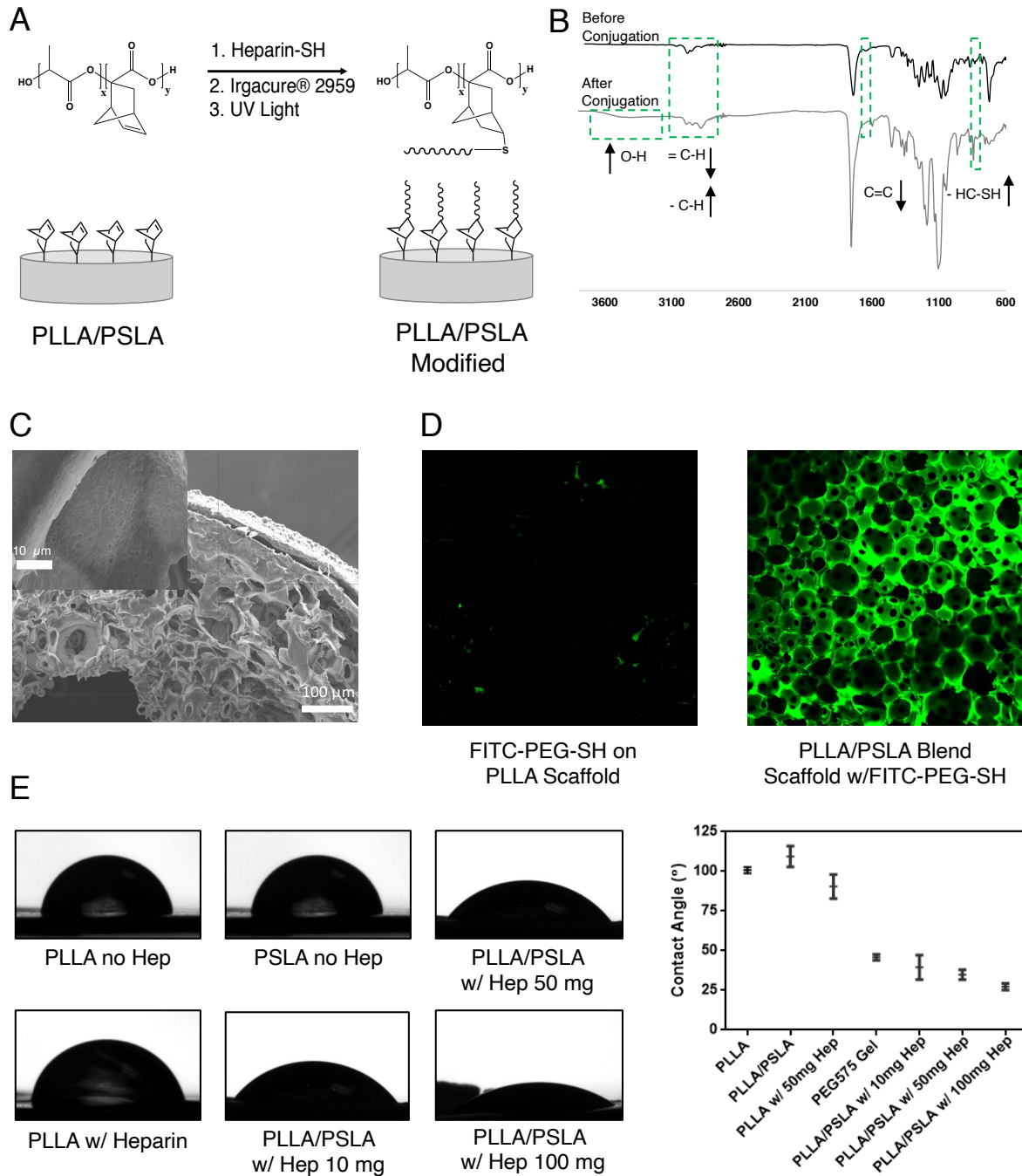
Figure 3.4 Post-modification via thiol-ene click chemistry and characterization.

A) Post-Modification scheme of PSLA polymer with heparin via thiol-ene click chemistry B) FTIR demonstrating pre and post-medication changes in spectrum stretching C) SEM visualization of tubular scaffold post modification D) Confocal Image of PLLA and PSLA modified with FITC-PEG-SH E) Change of Hydrophilicity observation, quantification, and comparison of PLLA, PSLA unmodified, and PSLA films with increasing concentration of heparin.

intact and only a small amount of scaffold was lost after 35 d [**Figure 3.5 A - B**]. This was also

observed by quantifying mass loss during this time: the PLLA scaffold lost only ~ 15 % of its

initial mass, the PLLA/PSLA with no heparin and the PLLA scaffold with heparin lost ~ 20-25

%, and the PLLA/PSLA scaffold with conjugated heparin lost ~ 52 % of the total mass. The

nanoarchitecture observed at day 0 and at day 35 showed that the nanofibers and overall
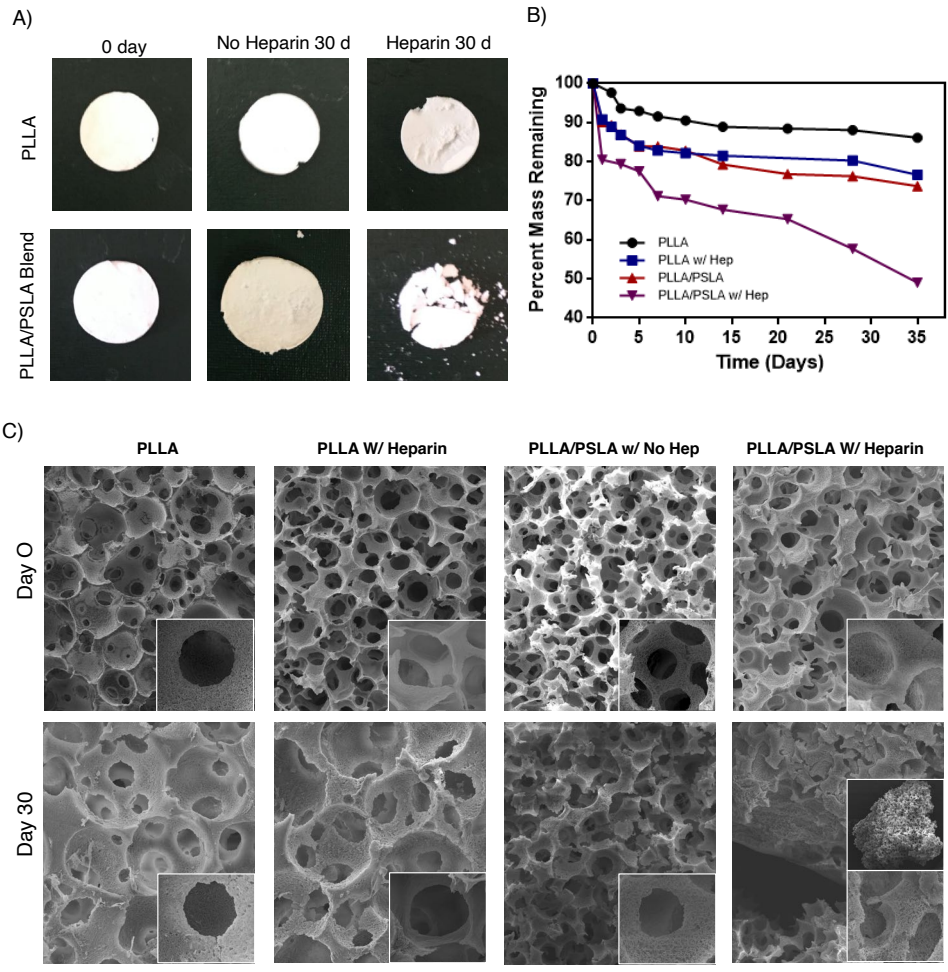
Figure 3.5 Degradation and mass loss of PLLA/PSLA scaffolds after heparin conjugation.

A) visualization of PSLA scaffold conjugated with heparin began disintegrate at week 3 with all other groups intact at end of experiment while PLLA scaffolds show minimal degradation B) quantification of scaffold mass loss over time due to heparin conjugation on PLLA/PSLA scaffolds compared to PLLA and PLLA/PSLA scaffolds with no heparin conjugated C) SEM characterization of scaffold degradation at day 35.

morphology had changed considerably in the heparin modified PLLA/PSLA blend but did not change significantly in the other groups [**Figure 3.5 C**].

3.3.6 Implantation "In situ" of tubular scaffolds in rat models

Engineered scaffolds of ~ 10 mm in length were implanted *in situ* into female rats of approximately 200 – 400 g to assess the ability of the tubular scaffolds to serve as vascular grafts and form tissue engineered blood vessels [**Figure 3.6 A**]. The scaffolds were implanted using standard surgical technique and practices. The rats were sacrificed at predetermined times of 1w, 2w, 1m, and 3m. All rats survived to time of sacrifice with no signs of bleeding, rupture, or mechanical failure of the vessel [**Figure 3.6 B**]. Most importantly, there was no discoloration of the vessel, darkening of surrounding tissue, and fascia had grown around the regenerated vessels signifying an absence of either necrosis or trigger of an immune response. Additionally, the tissue excised at three months looked similar to that of the natural vasculature [**Figure 3.6 C - E**]. After implantation, the scaffolds were observed for blood flow obstruction internal diameter changes, wall size changes, and any arising thrombosis issues via laser Doppler ultrasound and ultrasound imaging [**Figure 3.6 F - G**]. Through these means, we determined that blood flowed unobstructed, the wall size and internal diameter remained nearly identical. Additionally, the *loose layer* began to degrade at 2 weeks and remodeling began within 1 month as observed by a slight increase in diameter of the *in situ* implanted graft [**Figure 3.6 H**]. Likewise, we were able to determine that the *in situ* implanted scaffolds did not form aneurysms or hyperplasia.

3.3.7 Characterization and assessment of explanted tissue engineered vessels

The porous and interconnected scaffolds were infiltrated by native cells after as little as one week, resulting in the degradation of the polymer and the remodeling of the inner layer. After one month of *in situ* implantation, the interior of the scaffold had mostly degraded, been
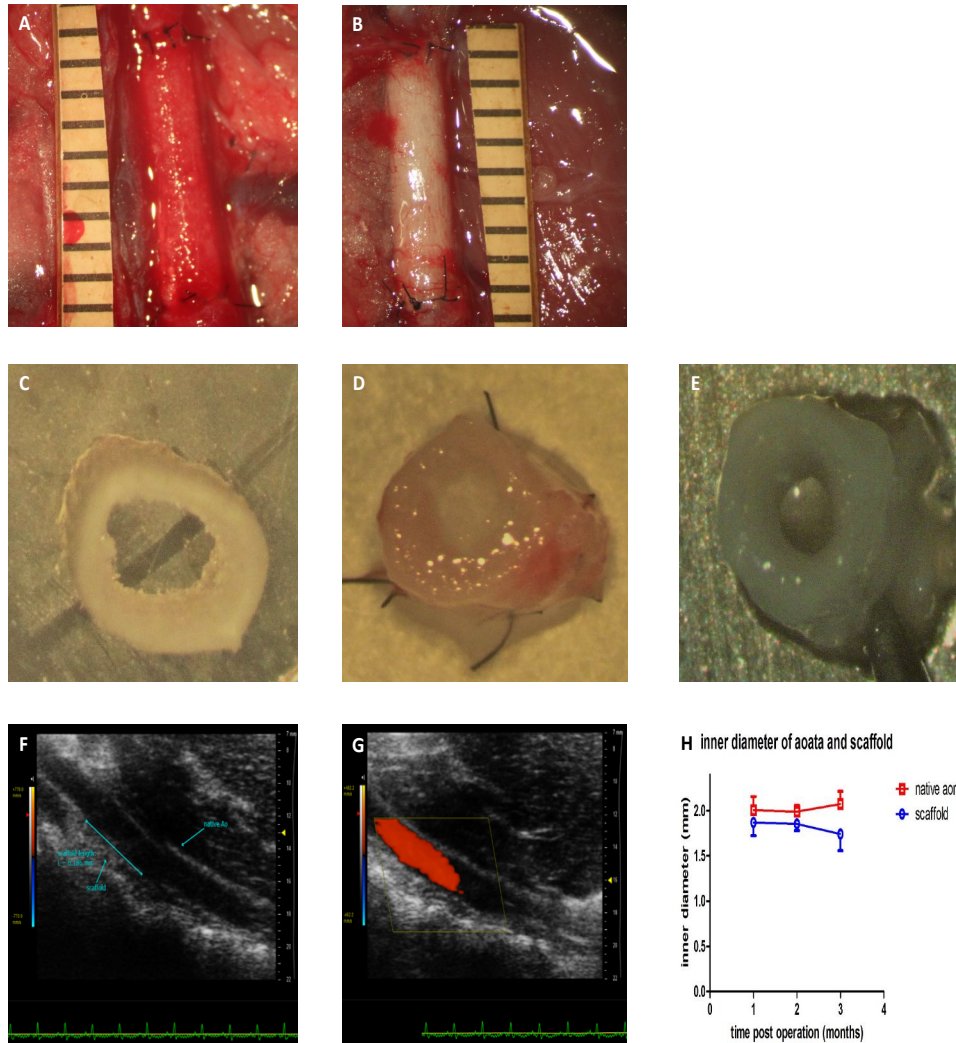
Figure 3.6 Scaffold evaluation post-implantation *in situ.*

A – B) Operative images for the implanted scaffolds (A: immediately after implant; B: 3 months post-operation). C – E) Morphologies of nanofibrous vascular scaffolds before rat abdominal aortic interpositional implant (C), 3 months post-operation (D) and native rat abdominal aorta (E). F – G) Ultrasound images of the implanted scaffold 3 months post-operation. H) Comparison of native aorta vs TEBVs over 3-month period.

replaced with native cells forming complex tissue configuration [**Figure 3.7**]. Hematoxylin and eosin staining (H&E) of the vascular graft at 1 w, 2 w, 1 mo, and 3 mo demonstrated the effectiveness of the scaffold design to promote cellular infiltration, migration and proliferation. Through these images proliferating and migrating cells were observed within the scaffold and
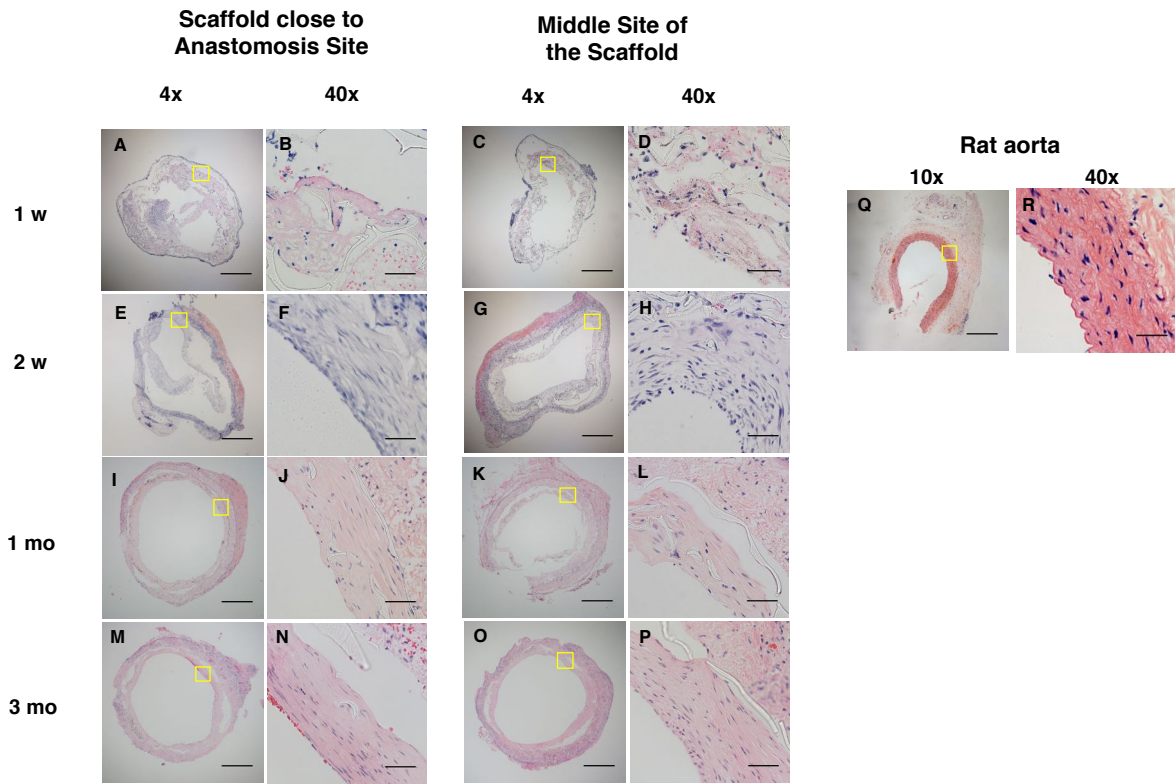
Figure 3.7 Comparison of vascular muscular reconstruction at anastomosis and middle sites of implanted scaffolds by H&E staining.

(A, B): 10x and 40x magnification from anastomosis site of scaffold at 1 week's post-operation. (C, D): 10x and 40x magnification from middle site of scaffold at 1 week's post-operation. (E, F): 10x and 40x magnification from anastomosis site of scaffold at 2 weeks' post-operation. (G, H): 10x and 40x magnification from middle site of scaffold at 2 weeks' post-operation. (I, J): 10x and 40x magnification from anastomosis site of scaffold at 1 month's post-operation. (K, L): 10x and 40x magnification from middle site of scaffold at 1 month's post-operation. (M, N): 10x and 40x magnification from anastomosis site of scaffold at 3 months' post-operation. (O, P): 10x and 40x magnification from middle site of scaffold at 1 week's post-operation. (Q, R): 10x and 40x magnification from rat's native aorta. (Scale bar: For A, C, E, G, I, K, M, O, Q=400um; For B, D, F, H, J, L, N, P, R=40um).

tissue was formed with cells orientated in a laminar fashion, similar to natural vasculature. The

deposition of collagen and elastin in the newly formed tissue at 1 and 3 months was illustrated

using Masson's Trichrome and Verhoeff-Van Gieson staining methods [**Figure 3.8**]. The

staining demonstrated that a high quantity of collagen was deposited after one month and a high

quantity of elastin was deposited after three months, with both ECM proteins approaching native
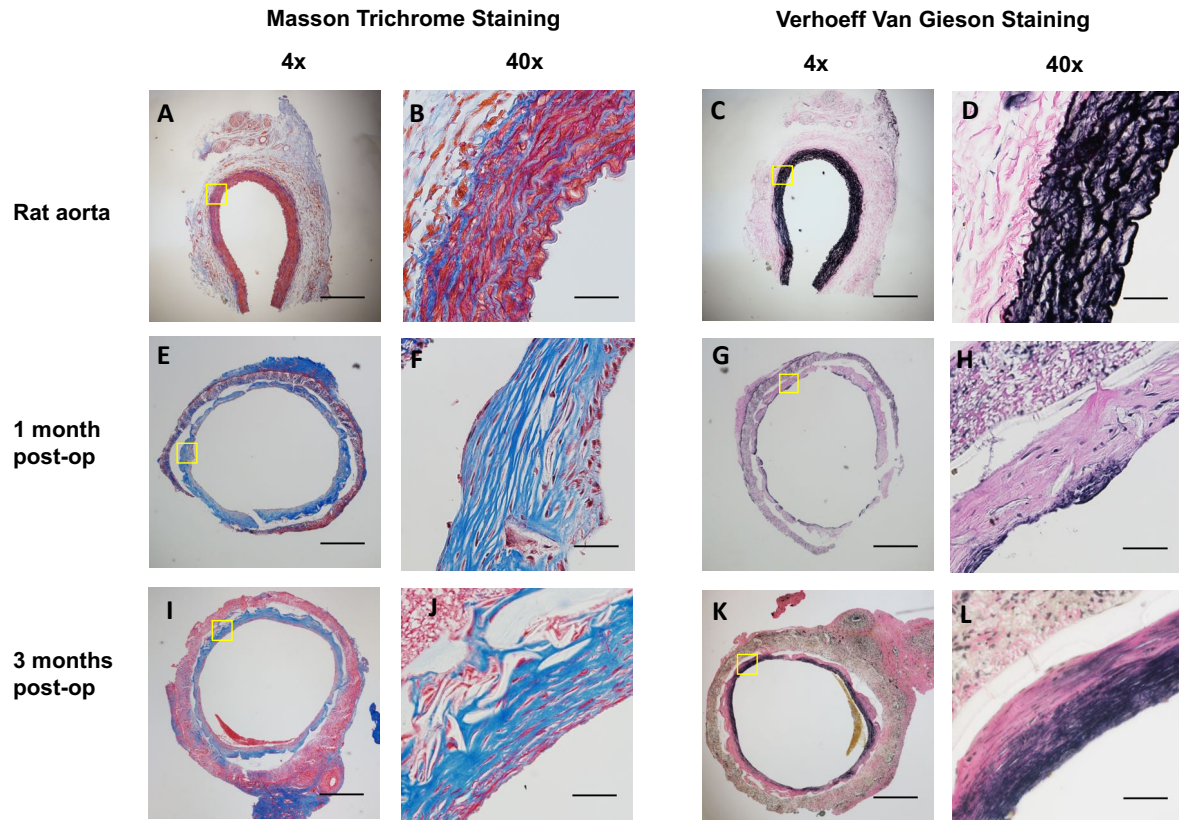
Figure 3.8 Comparison of vascular extracellular matrix reconstruction of implanted scaffolds after 1 and 3 months implantation.

(A, B): 10x and 40x magnification from rat's native aorta by Masson trichrome staining. (E, F): 10x and 40x magnification from implanted scaffold at 1 month's post-op by Masson trichrome staining. (I, J): 10x and 40x magnification from implanted scaffold at 3 months' post-op by Masson trichrome staining. (C, D): 10x and 40x magnification from rat's native aorta by Verhoeff Van Gieson staining. (G, H): 10x and 40x magnification from implanted scaffold at 1 month's post-op by Verhoeff Van Gieson staining. (K, L): 10x and 40x magnification from implanted scaffold at 3 months' post-op by Verhoeff Van Gieson staining. (Scale bar: for A, C, E, G, J, K=400um; For B, D, F, H, J, L=40um).

tissue levels. Immunofluorescence staining was utilized to illustrate SM22, a marker protein secreted by smooth muscle cells, showing cells occupying the remodeled scaffold to be smooth muscle cells. This indicates that smooth muscle cells have infiltrated the scaffold and regenerated the rat aorta at 1 mo and 3 mo post-op [**Figure 3.9**]. Endothelization of the vascular graft is important for long-term viability and for the formation of mature tissue. Immunohistochemistry
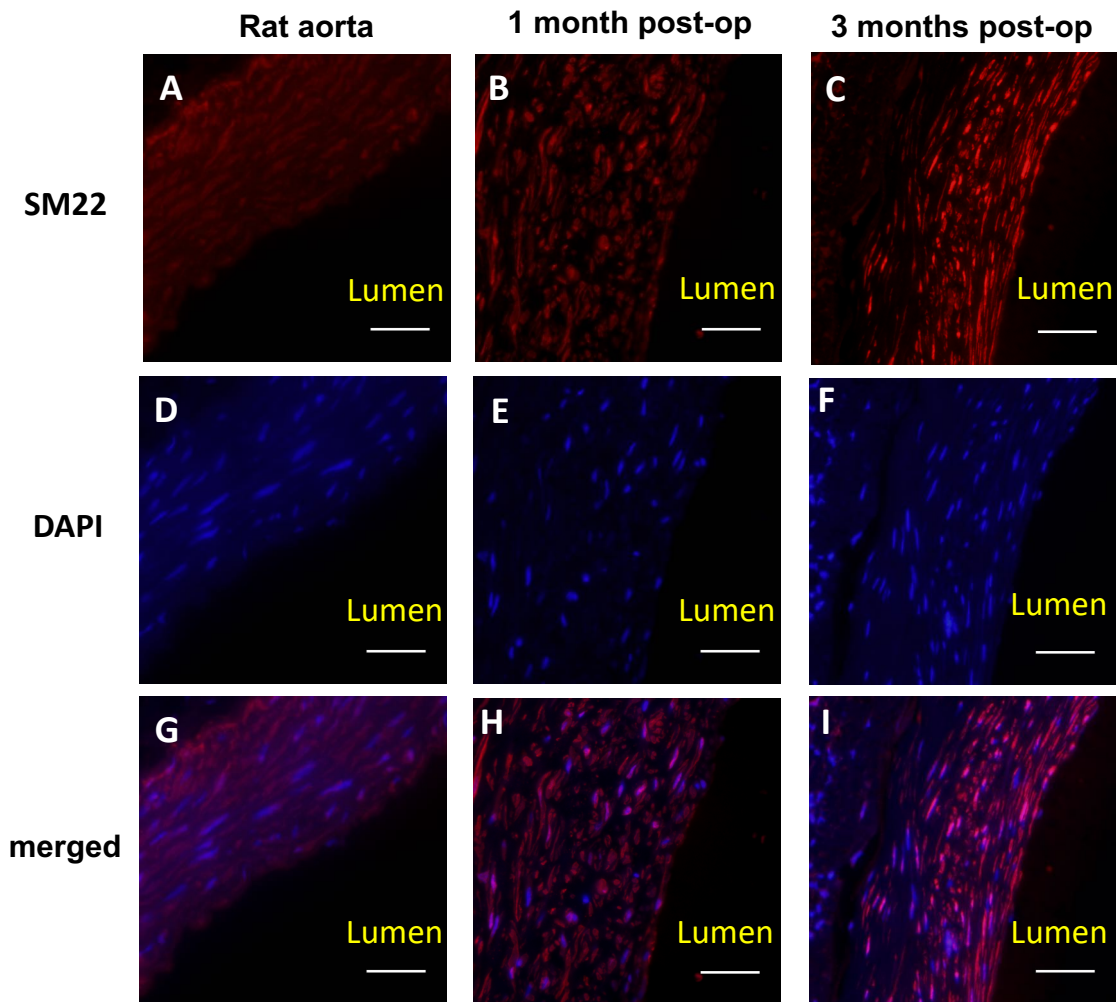
Figure 3.9 Immunofluorescence of smooth muscle cell marker SM22 indicates smooth muscle cells infiltration and reconstruction in rat aorta, 1 mo post-op and 3 mo post-op in scaffolds.

A) flourescence of SM22 in rat's native aorta D) DAPI shows nuclei in rat's native aorta G) Merged of flourescence and DAPI in rat's native aorta B) Flourencesce of SM22 in implanted scaffold at 1 mo post-op E) DAPI shows nuclei in implanted scaffold at 1 mo post-op H) Merged image of flourencesce and DAPI in implanted scaffold at 1 mo post-op C) Flourecense of SM22 in implanted scaffold at 3 mo post-op F) DAPI shows nuclei in implanted scaffold at 3 mo post-op I) merged of fluorescence and DAPI in implanted scaffold at 3 mo post-op. (Scale bar= 40um).

was done using von Willebrand factor (vWf) to demonstrate the effectiveness of the scaffold's

ability for endothelization, with incomplete endothelization at 2 weeks and complete

endothelization at one and three months [**Figure 3.10**].
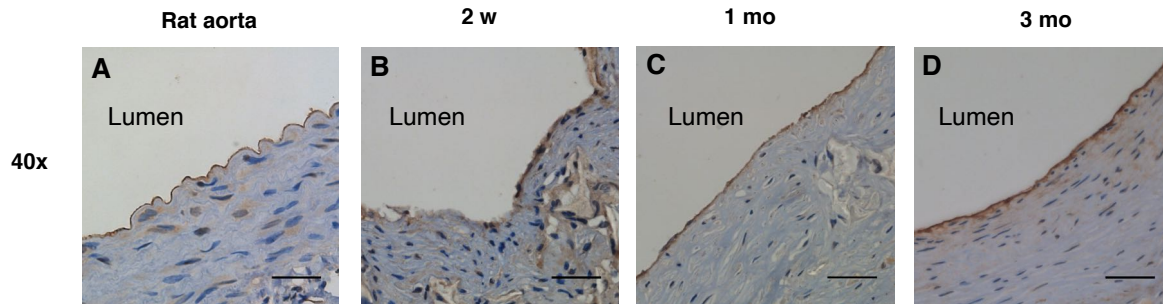
Figure 3.10 Immunohistochemistry of endothelial marker vWF of implanted scaffolds indicate endothelial cells reconstruction.

(A): Rat's native aorta; (B): 2 weeks' post-op; (C): 1 month's post-op; (D): 3 months' post-op. (Scale bar= 40um).

3.4 Discussion

The goal of this study was to create a functional blood vessel that is regenerated by the body through a cell-free off-the-shelf tubular scaffold that is biocompatible, anticoagulant, and with tailorable degradation rate. Current methods that entail the use of cultured cells to create small-diameter TEBVs for cardiac and peripheral revascularization procedures are not suitable for most clinical applications due to the immediacy when the vessel is commonly needed. Cell-free tissue engineering vascular grafts, like the one described in this study, allow for the elimination of the prohibitive lead-time required for cell culture and enable immediate implantation [167, 212].

Considerable effort has been devoted to imparting biomimetic properties through the physical architecture of the scaffold. Techniques such as TIPS and electrospinning produce nanofibrous morphology that mimics the native extracellular matrix environment both in size of the fiber, and mechanical forces exuded on the cell[38, 68, 177, 193, 213-215]. Previously, our lab developed large-diameter scaffolds fabricated from a sugar leaching template and TIPS from

72

PLLA that showed superior cellular attachment, proliferation, and migration[38]. Additionally, the nanofibrous architecture of the scaffold was shown to be conducive in mature vascular tissue formation through the differentiation of cardiovascular progenitor cells into smooth muscle cells with contractile phenotype both *in vitro* and in subcutaneous implantation mouse models [50, 54, 161]. Because of these desirable attributes, these methods for scaffold production were used as a starting point to build upon in this study. We scaled the previously developed tubular scaffold to fit a rat model and included a PCL layer to withstand hemodynamic stresses and suturing.

There has been a large variety of polymers utilized to fabricate tissue engineering scaffolds. Both slow degrading polymers, such as polycaprolactone (PCL), and faster degrading polymers, such as poly(urethane), poly(glycolic acid), and poly(glycerol sebacate) have been used in scaffold designs[37, 160, 177, 178, 196]. Rapidly degrading and slow degrading tissue engineering scaffolds have been shown to have distinct advantages and disadvantages. While slow degrading polymers have been shown to improve the durability of tissue engineering scaffolds, they often lead to calcification within formed tissue due to their long degradation times[86, 190, 197]. Similarly, rapidly degrading polymers have been shown to provide faster cell migration, proliferation, and matrix production, but suffer from the formation of aneurysms and lack of structural support [37, 177, 178, 196.]

In this study we took advantage of the beneficial properties of both slow and rapidly degrading polymers to create a bilayered scaffold with a porous inner layer fabricated from PLLA/PSLA blend, a highly functional material that can be easily modified via thiol-ene click chemistry. Three dimensional porous and interconnected scaffolds with the nanofibrous architecture were fabricated and were easily post-modified.

In this work we also demonstrated that PLLA/PSLA blend can be modified with hydrophilic polymers or macromolecules, such as heparin, to modulate the scaffold hydrophilicity. Typically, PLLA has a degradation time of 6-12 months *in vitro*. However, the PLLA/PSLA blend demonstrated a mass retention of ~ 50 % at 1 month when modified with heparin (100 mg). Not surprisingly, this shows that the increased hydrophilicity also increased degradation rate. In addition, heparin is anticoagulant helping to decrease risk of thrombus formation. Furthermore, heparin has been shown to facilitate cell adhesion [170, 181, 191, 195].

In previous studies, heparin has been introduced by dipping the scaffold in a solution of heparin. With that method retention of heparin is minimal after scaffold implantation as it is washed away due to heparin's hydrophilic nature and high solubility. As previously mentioned, PLLA and most polymers used to fabricate tubular scaffolds lack functionality in the backbone. The only points of attachment on those polymers are at the ends of the polymers due to their chemical structure, therefore very little heparin can be attached onto the scaffold[216]. We demonstrated that PLLA alone cannot be conjugated with heparin and PSLA-containing scaffold can be stably conjugated with heparin. Through the use of the PLLA/PSLA blend we were able to create a scaffold that not only contains the favorable physical attributes but can also be tailored with varying degrees of heparin to tailor surface hydrophilicity and optimize degradation rate.

The scaffolds were then implanted in situ and demonstrated biocompatibility 3 months post-op. Integration into the surrounding in situ environment was favorable. Excellent cellular migration was observed within the scaffold likely facilitated by the highly porous and interconnected architecture. The scaffolds were rapidly remodeled with most of the PLLA/PSLA inner layer degraded within a month.

Collagen and elastin play key roles in vascular tissue matrix and function. In native arteries, collagen mainly contributes arterial tensile strength, while elastin provides elasticity and compliance[193, 216]. Historically, elastin production during *in situ* vascular tissue engineering has been a major challenge[193, 217]. Excitingly, larger amounts of collagen and elastin were secreted with native-like structure in the engineered blood vessels in this study. The regenerated blood vessels functioned well in the rat models.

3.5 Conclusions

We have developed a new polymer system that allows the design of rapid and facile fabrication of tissue engineering scaffolds with tunable compositions and functionalities. By conjugating varying amounts of heparin, we were able to achieve broad ranges of hydrophilicity, degradation rate, and anti-thrombogenicity. The new PLLA/PSLA system also allows the fabrication of scaffolds with porous and nanofibrous features that are advantageous for cell migration, attachment, proliferation and smooth muscle regeneration. By combining the advantageous physical structures with the chemical functionalities, a superior bilayer scaffold was developed to achieve endothelization of blood vessels reconstructed with native-like collagen-rich and elastin-rich ECM. Importantly, after the degradation of the scaffold, the neo vessel achieved 3-month patency in a rat blood vessel replacement mode.

Chapter 4. Fabrication of Biomimetic Scaffolds from Poly(Exomethylene-co-Lactic Acid) for Facile and Click-Chemistry Functionalization for Tissue Engineering

R. Navarro, K. Rambhia, R. Kannan, W.B. Swanson, Z. Zhang, A. Adiwidjaja, J. Rieland, P.X. Ma., "Fabrication of biomimetic scaffolds from Poly(exomethylene-co-lactic acid) for facile and click-chemistry functionalization for tissue engineering" In Preparation.

4.1 Introduction

4.1.1 Biomimetic scaffolds for tissue engineering

Developing advanced biomimetic scaffolds for tissue and regenerative engineering has been an engineering challenge and goal for material scientists for the last 30 years [2, 17, 49, 64, 68, 205]. Scaffolds that closely mimic the microenvironment of the extracellular matrix (ECM) are deemed to have biomimetic properties. These scaffolds have shown the best results advantages in tissue engineering, producing tissue that often more closely resembles that of the native construct[17, 65, 209, 218]. This has been accomplished by imparting biomimetic properties to scaffolds, such as forming nanofibers, creating porous and interconnected architecture, matching mechanical properties, as well as incorporating biomolecules, growth factors (GFs), and minerals [64, 188, 204, 209, 218, 219]. As a result, scaffolds that include one or more of these biomimetic features allow for enhanced cell attachment, proliferation, and even facilitate stem cell differentiation [107, 204, 209, 219].

Of particular interest and importance is the nanofibrous and porous architecture typically seen in the ECM. Ma *et. al*. and others have previously demonstrated the impact of developing scaffolds with similar nanofibrous architecture, as seen in the native ECM [20, 38, 51, 61, 65, 68, 219-221].

A range of configurations (tubular, three-dimensional disks, and spongy microspheres) that contain this particular architecture have been engineered, and subsequently utilized for tissue engineering, including cardiovascular [38, 54, 160, 161] , bone [204, 209, 217], cartilage [107, 220, 222], and dental [59, 60, 207, 223, 224] tissue regeneration. The nanofibrous and porous biomimetic architectures was shown to advantageously enhance regeneration and therefore should be a key feature to be included when developing novel polymeric tissue engineering scaffolds.

4.1.2 Modification of scaffolds for tissue engineering

Polymers frequently used for scaffold fabrication lack chemical functionality in the backbone, therefore means for further functionalization to enhance the microenvironment are limited. To circumvent the lack of functionality, scaffolds can be fabricated by blending polymers that bear chemical motifs that permit further modificaiton together as well as subjecting the fabricated scaffold to aminolysis or plasma treatment, [64, 91, 105, 107, 225]. Aminolysis utilizes a relatively strong base to catalyze the attack on the carbon of the carbonyl with an amine containing molecule resulting in an amide or peptide bond. Plasma treatment uses electrons in the air directed at the scaffold surface to break bonds on the surface of a film or scaffold. When performed in the presence of O_2 or N_2, there are radicals formed can react with the gas present and yield hydroxyls, carboxylic acids, and amines which can be used for further functionalization. However, the plasma treatment only alters the surface as it does not penetrate deeply, the radicals are short-lived, and both plasma treatment and aminolysis can affect nanofiber morphology, as well as affect the mechanical properties of the scaffold. Polymers that contain acrylates, amines, or other functional groups have been blended to yield scaffolds that can be post modified. However, due to a lack of commercially available functional HMW polymers such as PLLA or facile and low-cost methods to synthesize these polymers.

Biomaterial scientists have to utilize low molecular weight polymers, which can disrupt the biomimetic nanofibrous architecture, as well as affect the mechanical properties [107]. Therefore, considerable effort has been expended in developing novel chemistries that can address this.

4.1.3 Click-chemistry in tissue engineering

Click-chemistry is a technique that has been used to improve the quantitative yield of the conjugation of the desired molecule to biomaterials (Huisgen *et. al.* in 1967, Sharpless *et. al.* in 2001). It is a facile method of conjugating substrates through the use of a primary alkyne and azide group coordinated by a copper catalyst. The reaction is highly selective with efficient yields and can be carried out at physiological conditions. Copper-free click chemistry is a modified method with the same specificity, yield efficiency, and capability of being performed under physiological conditions, but without the use of the copper catalyst. This process is possible due to the ring strain of the cyclooctyne driving the addition of the nucleophilic azide to form a 5-membered ring. In addition to these two methods of click-chemistry, the field has expanded to include epoxides that use ring strain and hydrazone and oxime. The latter involves nucleophilic addition by attacking a carbonyl carbon. Hence, click-chemistry is a technique that continues to evolve in the ability to produce new reactions that can occur at physiological conditions (37 ºC, aqueous environment, 7.4 pH) and are more inclusive of biological molecules while preserving their structure and function.

4.1.4 A novel "click-chemistry like" approach in tissue engineering

Introducing a high density of functional groups with click-chemistry reactivity in the scaffold is one of the approaches to impart additional biomimetic cues. It would be ideal to have a scaffold that can be conjugated under physiological conditions if needed with high conjugation efficiency and bioactivity, as seen in click-chemistry. Here we hypothesized that a copolymer

synthesized from L-lactic acid with segments containing a pendent lactic acid ring structure (formed from Exomethylene lactide (EML)) that is highly reactive, specific, tailorable that can be processed into tissue engineering constructs could provide a cost-effective and facile alternative to currently surface modification techniques and strategies. Click-chemistry like reactivity can address the problem by rapidly conjugating regulatory signals without denaturing sensitive proteins or growth factors in a high yield quantitative manner. Exomethylene lactide, derived from L-lactide, is a low-cost monomer that can provide the similar conjugation parameters as click-chemistry tools at a fraction of the cost when polymerized. The copolymer can be processed into biomimetic scaffolds with the favorable physical morphology but can also be facilely modified in a *click-chemistry fashion* with amine containing molecules.

To achieve this, we developed and synthesized a novel copolymer using HEMA-PLLA (HPLLA) and exomethylene lactide (EML) through a free radical polymerization. The unique conformation of EML when polymerized, creates a flat ring structure tightly packed together (separated by one methylene group), which induces neighbor dipole-dipole interaction leading to ring strain that can be disrupted when in contact with an amine containing molecule [226]. This causes immediate cleavage of the ring producing an amide bond between the carboxylic acid of the EML pendent and that of the amine-containing molecule to conjugated. Therefore, the novel biomimetic tissue engineering scaffolds fabricated contain a high degree of functional groups that are readily available for conjugation with available amines in biomolecules and regulatory signals that contain free amines such as peptides, hormone, and proteins. The scaffolds studied were efficiently and expediently modified and showed excellent cell viability indicating that this system can be used to impart biomimetic motifs for various tissue engineering applications

without the need for catalyst, heat, toxic chemicals or experienced material scientist as they effectively conjugated rapidly in facile in a click chemistry fashion.

4.2 Materials and methods

4.2.1 Materials

L-Lactide was graciously donated by Altasorb® and recrystallized in ethyl acetate before use. Poly(L-lactic acid) (PLLA, Resomer L207S) with an inherent viscosity of 1.6 dl/g was purchased from Boehringer Ingelheim (Ingelheim, Germany). NH_2-PEG-Methoxy 2kDa & 5kDa, 4-arm PEG-NH_2 10kDa, COOH-PEG-NH_2 was purchased from Layson Bio. N-Bromosuccinimide (NBS), Triethylamine (TEA), fluorescein isothiocyanate (FITC), Luperox® A98 Benzoyl Peroxide, Azobisisobutyronitrile (AIBN) (recrystallized in methanol before use), aminehexanol, Hydroxyethylmethacrylate (HEMA), L-Cysteine, Benzene, Mineral oil, Span 80®, ethyl acetate, hexane, N-Boc-Serinol, Magnesium Sulfate ($MgSO_4$), Sodium Thiosulfate, Fructose, tetrahydrofuran (THF) and dichloromethane (DCM) were purchased from Sigma-Aldrich Company (USA). All reagents were used as received unless otherwise noted.

4.2.2 Preparation of (6S)-3-Methylene-6-methyl-1,4-dioxane-2,5-dione (EML) and general procedure for the polymerization of poly(Exomethylene Lactide).

L-Lactide was modified and polymerized as previously reported by Hillmyer *et. al* [202]. Briefly, L-Lactide was combined with NBS (1.1 eq.) in benzene (20 % w/v) and heated to reflux. Benzoyl peroxide dissolved in benzene was added dropwise and the reaction was monitored by thin layer chromatography (TLC) until completion. The reaction was vacuum filtrated and condensed and the resulting solid was dissolved in DCM, washed in sodium thiosulfate solution, and concentrated. The solid was recrystallized from ethyl acetate and hexane twice to yield white

crystals, (3S, 6S)-3-Bromo-3,6-dimethyl-1,4-dioxane-2,5-dione (bromo-lactide). The white crystals were dissolved in DCM in a flask under nitrogen and cooled in an ice bath. TEA (1.1 eq) was added in dropwise and allowed to react for 1 h at 0° C and 1 h at 25 °C. The reaction was washed with 1M HCl three times and condensed. The crystals were further purified by liquid chromatography on silica gel and recrystallization in ethyl acetate to yield white crystals, (6S)-3-Methylene-6-methyl-1,4-dioxane-2,5-dione (exomethylene lactide) (EML). Exomethylene Lactide was polymerized using 1 mol % AIBN in dioxane under inert environment at 70° C. After polymerization was complete, the polymer was precipitated in methanol, filtered, and dried under vacuum.

4.2.3 Synthesis of HEMA-PLLA

HEMA-PLLA was synthesized through ring-opening polymerization (ROP) as previously described by Zhang *et al* [107]. Briefly, HEMA was used as the polymerization initiator with L-Lactide and the ROP catalyzed by stannous octoate in degassed environment at 150 °C to produce a polymer (M_w = 65 k Da, measured by GPC).

4.2.4 Synthesis of 2-Methylene-1,3-dioxepane (MDO)

MDO was synthesized according to the previously described method by Bailey *et. al.* [227, 228]. Briefly, chloroacetaldehyde dimethyl acetal and butanediol were reacted in a 1:1 ratio with Dowex® 50WX2 until all the methanol is distilled and collected and 2-Chloromethyl-1,3-Dioxapane is formed. The reaction was vacuum filtrated to remove the 50WX2 distilled under vacuum to isolate and then dissolved in THF and reacted with 2 mol ratio of potassium tert-butoxide in an ice bath and catalyzed with aliquot® 336 overnight. The reaction was concentrated, dissolved in ethyl ether, and purified by filtration using aluminum oxide. MDO was concentrated and isolated by vacuum distillation and stored at -20 °C.

4.2.5 Synthesis of poly(exomethylene-co-Lactic acid) (PELA)

PELA was polymerized at various ratios of HPLLA to EML 10:1, 25:1, 50:1, 75:1, and 100:1 by adding HPLLA and EML at the desired ratios and 0.5 mol ratio of MDO (relation to EML and HPLLA) into a reaction vessel which was then purged via vacuum with N_2 three times to reduce the oxygen concentration. Anhydrous Dioxane was then added to bring the concentration to 20 % w/v followed by the addition of 1% mol AIBN dissolved in anhydrous Dioxane. The reaction was then heated to 70 °C and stirred for 3 d. The reaction was removed from the heat and allowed to reach room temp before precipitating in cold methanol. The polymer was filtered and dried under vacuum for 2 d before use.

4.2.6 Conjugation efficiency of PELA polymer with various amine containing molecules

The PELA polymers with varying ratios of HPLLA to EML was conjugated with various amine containing molecules to serve as models to test if it still functioned in the same manner of conjugation when synthesized as a copolymer. This was done by dissolving the PELA polymers in DCM and mixing with solutions of NH_2-PEG-Methoxy (Aq. & DCM), aminehexanol (Aq), and L-Cysteine (Aq). The two faces were then separated (aminehexanol & L-Cysteine) before precipitating in methanol, filtered, and dried under vacuum. The conjugation was characterized via FTIR and NMR.

4.2.7 General procedure for the fabrication of thin-films

Nanofibrous thin-films were fabricated by using the thermally induced phase separation (TIPS) procedure. Briefly, PELA or PLLA was dissolved to a concentration of 12.5 (PELA) or 10 % (PLLA) w/v in THF and heated to 60 °C. The solution was cast on a flat silicon wafer and covered with a glass plate, phase separation was allowed to take place at -80 °C for 48 h. The films were slowly warmed to room temperature by immersing in an ice bath until all the ice

melted, then stored flat to dry. Thickness was measured to be approximately 200um using digital calipers and morphology was observed via SEM.

4.2.8 Microporous and interconnected nanofibrous scaffold fabrication

The porous, interconnected and nanofibrous scaffolds are fabricated using a sugar leaching method and TIPS as previously reported by Ma *et. al.* [20, 61, 68, 204, 205]. Briefly, the sugar template spheres are fabricated through an emulsion method and sieved to collect spheres ranging between 250 to 425 μm. The sugar is deposited in cylindrical molds and is heat treated to achieve the desired interconnected structure and then vacuum dried. A solution of PELA or PLLA was dissolved in THF to a concentration of 15% and 10% respectively and heated to 60 °C. The solution was then added to the dry sugar template and treated to reduced pressure to force the polymer solution into the template. TIPS was then induced at -80 °C for two days followed by submerging in excess hexane overnight to remove residual THF and maintain the scaffolds free of moisture. The scaffolds were then submerged overnight in DDH$_2$O to leach away the sugar template and the scaffolds cut to the desired diameter and width.

4.2.9 General procedure for modification of PELA thin-films and scaffolds

To visually demonstrate the conjugation potential of our PELA thin-films and three-dimensional scaffolds, NH$_2$-PEG-FITC was conjugated and observed via confocal imaging. FITC-PEG-NH$_2$ was synthesized according to Liu *et al* [229]. Briefly, 4-arm PEG-NH$_2$ (0.000025 mol, 250mg) was dissolved in 500uL 0.5M carbonate-bicarbonate buffer. FITC (0.00005 mol, 16.6mg) was dissolved in a minimum amount of acetone (approx. 50uL) and added to the PEG-amine solution, it was then left to spin in the dark for 24 hours on ice. The resulting solution was dialyzed for 72 h in 1000 mL DDH$_2$O, changed every 24 hours, and lyophilized. Using the lyophilized FITC-PEG-NH$_2$, a 10mg/mL solution was made in millipore water and protected

from light. Thin films or scaffolds were soaked for 24 h and dipped one at a time in 1mL of

FITC-PEG-amine solution in the dark for 1 min, then washed extensively in 1000 mL of

millipore water before being left to dry in the dark.

4.2.10 Visualization after modification with FITC-conjugated molecules through confocal

Microscopy

To visualize the distribution of PELA conjugation sites, FITC-PEG-NH$_2$ was conjugated

as described. Thin films and scaffolds were examined using confocal laser scanning microscopy

(Nikon Eclipse C1). All the parameters for laser intensity and gain were adjusted until

fluorescent signals cannot be seen from the control group and were kept constant within a sample

group.

4.2.11 Change of surface hydrophilicity determined via contact angle

PELA thin-films containing 5 & 25 mg of PEG conjugated unto the surface and

unconjugated PELA and PLLA samples where used. Contact angle measurements were taken

with a Rame-Hart 200-F1 contact angle goniometer. DI water was used as probe liquid.

Advancing contact angle was obtained by measuring the angle while the water was slowly added

to the surface from a ~10 µL droplet in contact with the sample and a micrometer syringe. Three

measurements were performed per sample, and the standard error is ±2°.

4.2.12 Mass loss quantification in vitro

Three-dimensional scaffolds made from PELA and PLLA, prepared as previously

described (diameter 12.0 mm, height 2.0 mm), were conjugated with increasing NH$_2$-PEG 5k

Da: 0 mg, 1 mg, 10 mg, 25 mg, 100 mg were immersed in phosphate buffer solution (10 mL, 0.1

M, pH 7.4) in a pre-weighed 20 mL vial. The PLLA scaffolds were only introduced to a 100 mg

PEG solution or 0 mg PEG solution. The samples were kept at 37 °C with a shaking speed of 25 rpm. The buffer solution was renewed at predetermined times and the sample was lyophilized and the mass taken. Morphology change was examined visually and using SEM.

4.2.13 Quantification of thin-film and scaffold modification with amine containing molecule

In order to quantify the attachment of amine containing molecules once fabricated into thin-films (8 mm diameter) with a small molecular weight amine containing molecule. The films and scaffolds were dipped into a 0.1 mg/mL solution of dopamine, the solution was then lyophilized and reconstituted in 1 mL of DDH_2O and the UV-Vis absorption was taken using a quartz cuvette (Hitachi U-2910) for Dopamin. The concentration was determined by comparing to a concentration curve ranging from 0.1 mg to 0.0005 mg with an absorption peak at 280 nm. The concentration of amine-PEG_{5k} conjugated unto three dimensional scaffolds (2mm thick and 17 mm diameter) by dissolving 50 mg in 5 mL of DDH_2O in a pre-weighed 20 mL vial. The scaffolds where placed in the solution for 2 min in a shaker to allow the conjugation to occur. The scaffolds were removed and washed in 5 mL of DDH_2O for 30 min. The solutions were then combined in the pre-weighed 20 mL, frozen, and lyophilized. The 20 mL vial was then weighed to determine the unconjugated mass of NH_2-PEG_{5k}.

4.2.14 Polymeric nanospheres fabricated and attachment on surface PELA thin-films and scaffolds

NH_2PLLA and $NH_2PEGPLLA$ were synthesized as previously described by Ju *et. al.* [230]. These polymers and PLLA were utilized to fabricate polymeric nanospheres using a double emulsion method (water/oil/water) as previously described by Wei *et. al.* [204]. The microspheres were loaded with PEG-Rhodamine B and were characterized by SEM. The nanospheres were attached on the surface of PELA and PLLA thin-films and scaffolds in both methanol and

aqueous environment. The attachment of the nanospheres was characterized by SEM and confocal imagery.

4.2.15 General characterization of monomers and polymers

Nuclear magnetic resonance characterization. ^{1}H and ^{13}C spectra of macromonomers and copolymers were recorded with an Inova 500 NMR instrument operating at 500 MHz at room temperature. Deuterated chloroform (CDCl$_3$) was used as the solvent. Spectral analysis is carried out in VnmrJ (Version 4.2, Agilent) and MestReNova (Version 12.0.0-200080, Metrelab Research)

Ultraviolet–visible spectroscopy. All monomers and polymers formed were characterized by first dissolving in DCM and using a quartz cuvette to obtain spectrum from 200 - 700 nm (up to 350 shown) (Hitachi U-2910).

Fourier-transform infrared spectroscopy. Monomers, polymers, thin-films, and scaffolds were characterized by directly placing the sample on the diamond crystal sample holder to obtain the spectrum from 600 – 4000 nm (Thermo-Nicolet IS-50).

Scanning electron microscopy (SEM) observation. The surface morphology of thin films and three-dimensional scaffolds were examined using SEM (JEOL JSM-7800FLV) with an accelerating voltage of 15 kV. Prior to observation the samples were coated with gold for 150 s using a sputter coater (Desk II, Denton Vacuum Inc.).

Gel permeation chromatography. Polymers formed were dissolved in anhydrous tetrahydrofuran and the size of the polymer were determined comparing to polystyrene standards (*Shimadzu GPC)*.

4.2.16 Cell culture and osteogenic differentiation

Human iPSC-MSCs were obtained from the Bo Yang lab. Cells were maintained in iPSC-MSC growth media (I-media) containing α-MEM, 20% FBS, 1% Penicillin-Streptomycin, and supplemented with L-glutamine (2 mM), non-essential amino acids (NEAA), 2-mercaptoethanol (1 mM), and FGF-2 (1 ng/mL). These cells were proliferated on 0.1% gelatin coated T75 flasks under normal cell culture conditions (5% CO_2 and 37°C). Media was changed every 48-72 hours. 24 hours after seeding, growth medium was replaced with osteogenic medium, consisting of high glucose DMEM with 10% FBS, 1% Penicillin-Streptomycin, and supplemented with ascorbic acid (50 μg/ml), β glycerophosphate (10 mM), and dexamethasone (100 nM).

4.2.17 Scaffold sterilization and cell seeding

Scaffolds were vacuum sterilized in 70% ethanol in 48-well suspension cell culture plates at 20-25 in Hg for 30 mins. Then scaffolds were washed three times in 1X PBS and two times in growth medium (10% α-MEM, 10% FBS, 1% Penicillin-Streptomycin) for 30 mins/wash on a shaker (5% CO_2 and 37°C). For some studies scaffolds were soaked in FBS or 1 μg/mL BMP-2 in place of the third PBS wash. Human iPSC-MSCs were seeded at 5×10^5 in 12 μL per scaffold and incubated with 1x PBS in surrounding wells for 2 hours. I-media was added after 2 hours and cells maintained or differentiated as described earlier.

4.2.18 Proliferation assay

Cell proliferation was measured by a colorimetric method using a 3-(4, 5-dimethylthiazol-2-yl)-5-(3-carboxymethoxyphenyl) 2-(4-sulfonphenyl)-2H-tetrazolium (MTS tetrazolium) compound (Cell-Titer 96 Aqueous One Solution Cell Proliferation Assay; Promega, Madison, WI). The cells were cultured at 5×10^3/well in a 96-well plate using I-media. Then 200

µL of 10% MTS reagent in I-media was added to per well and incubated for 2 hours in normal culture conditions. The incubated solution was transferred to a new 96-well plate and absorbance at 490nm was measured by a 96-well spectrophotometer on days 1-5.

4.2.19 Confocal imaging of cells on PELA scaffolds

After 3 days of *in vitro* culture, human iPSC-MSCs on PLLA and PELA scaffolds were washed in 1x PBS, 100X Triton X, and 1X PBS again. Cells were then stained with Phalloidin (Alexa Fluor™ 555) (Invitrogen) and counterstained with 4′,6-diamidino-2-phenylindole (DAPI). Human iPSC-MSC seeded scaffolds were examined using Confocal Laser Scanning Microscopy (CLSM) (Nikon Eclipse C1).

4.2.20 Calcium quantification

Cells were washed 3 times with distilled water and incubated in 500 µL of 0.5N hydrochloric acid (HCl) overnight on a shaker at 4°C to extract calcium. HCl supernatant was stored at -20°C prior to sample analysis. Calcium quantification was determined with Pointe Scientific Calcium Liquid Reagents according to the manufacturer's manual. Absorbance was measured at 570 nm. A calcium standard was used to calculate the calcium content in each sample.

4.2.21 RNA extraction and qRT-PCR

Total RNA was extracted using TRIzol. A cDNA library was created with SuperScriptII Reverse transcription reagents (Applied Biosystems) and real time qPCR was performed using TaqMan Universal PCR Master Mix (Applied Biosystems). qRT-PCR was performed using primers for Runx2 (Hs01047973_m1) and GAPDH (Hs02786624_g1). GAPDH was used to normalize gene expression as an internal standard.

4.2.22 Subcutaneous implantation

Male 6~8-week-old C57BL/6 mice (Charles River Laboratories International, Inc., Wilmington, MA) were used for the subcutaneous implantation of PLLA and PELA scaffold study. Surgery was performed under general inhalation anesthesia with isoflurane as previously described [229]. Two scaffolds were implanted subcutaneously into each pocket, for a total of 4 scaffolds per animal. Two samples were implanted for each group (n=2). The mice were sacrificed at 2 weeks post-surgery and the cell-scaffold constructs were harvested. The animal procedures were performed according to the guidelines approved by the University of Michigan Committee of Use and Care of Laboratory Animals. Specimens were process for histological analysis. Samples were processed for histological analysis.

4.2.23 Histological Analysis

Both *in vitro* and *in vivo* samples were washed with PBS, fixed in 10% formalin and embedded in paraffin blocks. 5 µm sections were prepared, subsequently deparaffinized, rehydrated with a graded series of ethanol, and stained with hematoxylin and eosin (H&E), Alizarin red S, and von Kossa.

4.2.24 Statistical analysis

Performed using SPSS Statistics Premium (Version 24, IBM, Inc.). Data are reported as mean ± standard deviation. Significance is determined as $p < 0.05$.

4.3 Results

4.3.1 Synthesis of poly(exomethylene lactide-co-lactic acid), Modification, and Characterization

The polymer components EML, MDO, and HPLLA, were synthesized as previously discussed [**Figure 4.1**]. The components were shown extremely pure before polymerization
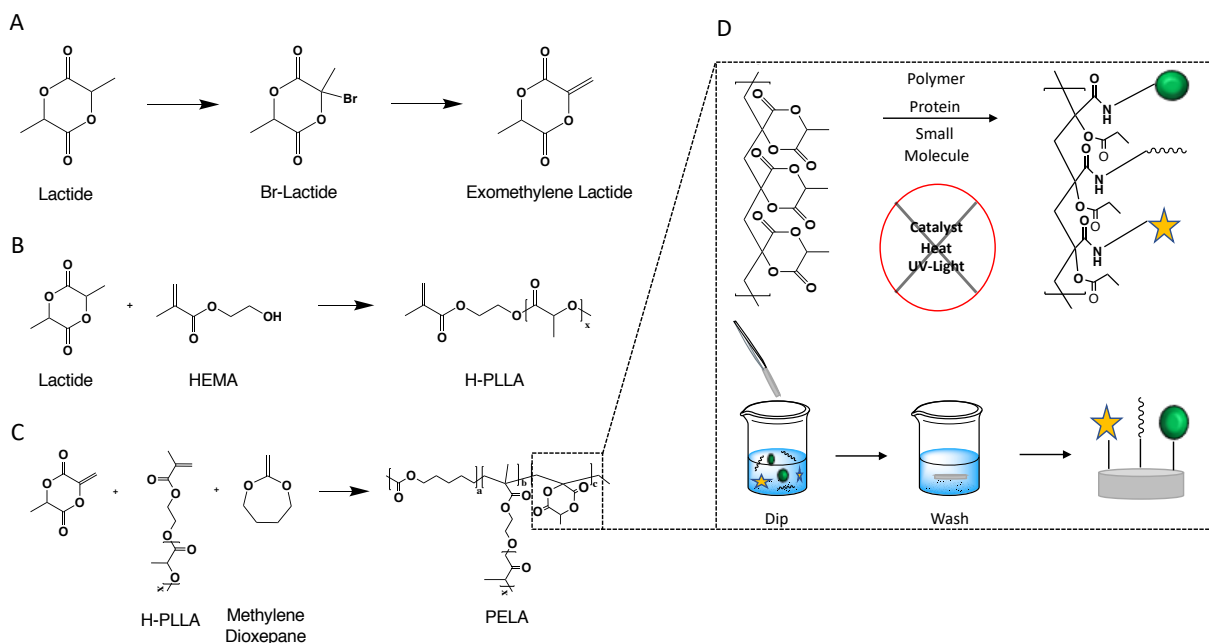
Figure 4.1 Synthesis scheme and mode of modification of PELA polymer.

A) Synthesis scheme of exomethylene lactide by brominating and debromination allylic carbon as described in 2.2.9 B) Synthesis scheme for HEMA-PLLA using a Tin catalyst (stannous octoate) in a bulk reaction C) Synthesis scheme of degradable PELA polymer using MDO to provide degradation of the carbon-carbon backbone D) Schematic depicting method of modification of both polymer before and after processing into tissue engineering scaffold.

(NMR). The PELA polymer was synthesized and characterized using NMR, GPC, DSC, and

TGA, [**Figure 4.2**]. Using these methods we were able to confirm that the novel PELA

copolymer was successfully synthesized with a molecular weight of ~ 120 k Da (molecular

weight determined via GPC) and with an incorporation of HEMA: EML outside the theoretical

values based on the feed ratios, 10:1, 25:1, 50:1, and 100:1 (determined by ^{1}H NMR) [Figure

4.2C]. In our study, we found that the 10:1 was the closest to ratio found as our theoretical value,

with 25:1 being second.

Additionally, using TGA we were able to observe 3 distinct faces of the polymer degradation, with an initial mass loss at 200 °C that is attributed to the pendent groups breaking and leaving behind a COOH, OH, and carbon-carbon backbone [Figure 1D]. The second mass loss (highest ratio) is attributed to the PLLA portion being degraded, and lastly, the third mass loss can be attributed to the degradation of the carbon-carbon backbone. These assumptions were confirmed by observations of the individual components. The intensity of each mass loss (1st and 3rd) varied depending on the ratio of HPLLA to EML.
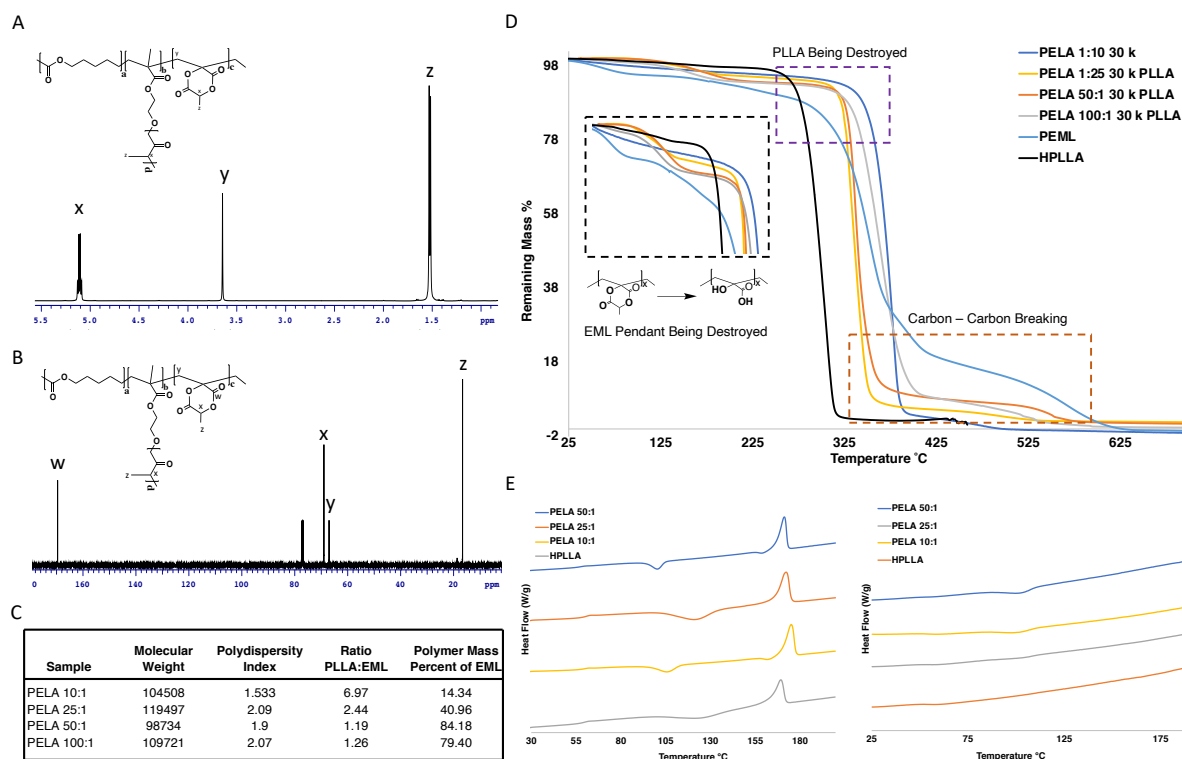
Figure 4.2 PELA polymer characterization.

A). 500 MHz ^{1}H NMR spectrum of PELA polymer in CDCl$_3$ B) 500 MHz ^{13}C NMR spectrum of PELA polymer in CDCl$_3$ C) PELA polymer ratios considered and resulting polymer MW via GPC using a styrene standard D) Thermal decomposition of PELA, HEMAPLLA, and PEML polymers depicting loss of mass E) DSC spectrum depicting glass transition of PELA.

4.3.2 PELA polymer conjugation with amine-containing molecules

Before fabrication into tissue engineering constructs, we investigated the novel PELA polymer to determine if the EML pendants are able to click with the model amine containing molecules (NH$_2$-PEG-Methoxy, aminehexanol, and L-Cysteine) chosen to demonstrate that the EML pendants can conjugate when synthesized in a copolymer. We demonstrated the stability and function of the novel PELA copolymer by showing it can be successfully modified without the need for heat or a catalyst, yet still conjugate molecules in water. In this study, we dissolved the PELA copolymer in DCM and added an amine containing molecule in either DDH$_2$O or in DCM (PEG-NH$_2$). After collecting the PELA polymers, they were modified and qualitatively characterized using FTIR. The conjugation was considered a success with the appearance of amide stretch at ~1630-1690.

4.3.3 Thin-film Fabrication and Modification Observation of Physical Properties

Thin-films from mixtures of PELA (10:1, 25:1, 50:1, 75:1, and 100:1) and PLLA were fabricated and cut to 5 mm diameter pieces and observed using SEM to verify the presence of nanofibers [**Figure 4.3**]. We further characterized the films to show the effects before and after conjugation with PEG-NH$_2$ 5 kDa. The SEM images indicated that the biomimetic nanofiber morphology was present in all the PELA films before modification and after modification; before modification the samples that contained 25:1 and 10:1 showed excellent nanofiber morphology and physical structure that was comparable to PLLA thin films. However, before modification it was evident that the films with increasing EML concentration had structural problems that presented as cracks and pores on the film surface of the samples for certain ratios (50:1 to 100:1). The samples that contained 25:1 and 10:1 showed excellent nanofiber morphology and physical structure that was comparable to PLLA thin films. After modification

the PELA films that demonstrated cracks and pores (50:1 to 100:1) showed increased porosity

and cracks; the 100:1 began to fall apart making it difficult to handle and destroying most of the

nanofiber morphology [**Figure 4.3**]. The films that demonstrated excellent morphology (25:1 &

10:1) before modification demonstrated excellent morphology, mechanical properties, and

nanofiber structure post-modification [**Figure 4.3**]. Therefore, through this study we were able to
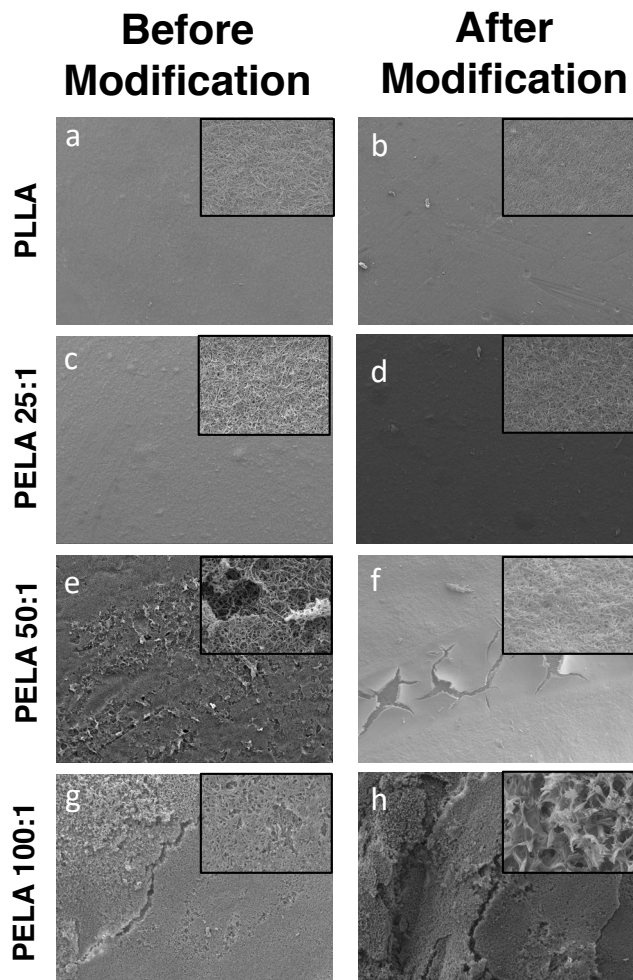
Figure 4.3 PELA/PLLA polymer thin-film fabrication and characterization through SEM before and after modification with amine-PEG$_{5000}$.

a-b) PLLA film before/ after modification demonstrating nanofibrous morphology c-d) PLLA/PELA$_{25:1}$ film before/ after modification demonstrating nanofibrous morphology c-h) PLLA/PELA films before/ after modification demonstrating loss of nanofibrous morphology.

demonstrate that the PELA copolymer could be fashioned into a two dimensional thin-film and for the first time the EML portion of the copolymer could be modified in an aqueous environment in a click-chemistry fashion, in the absence of organic solvents, heat, catalyst, or pH changes.
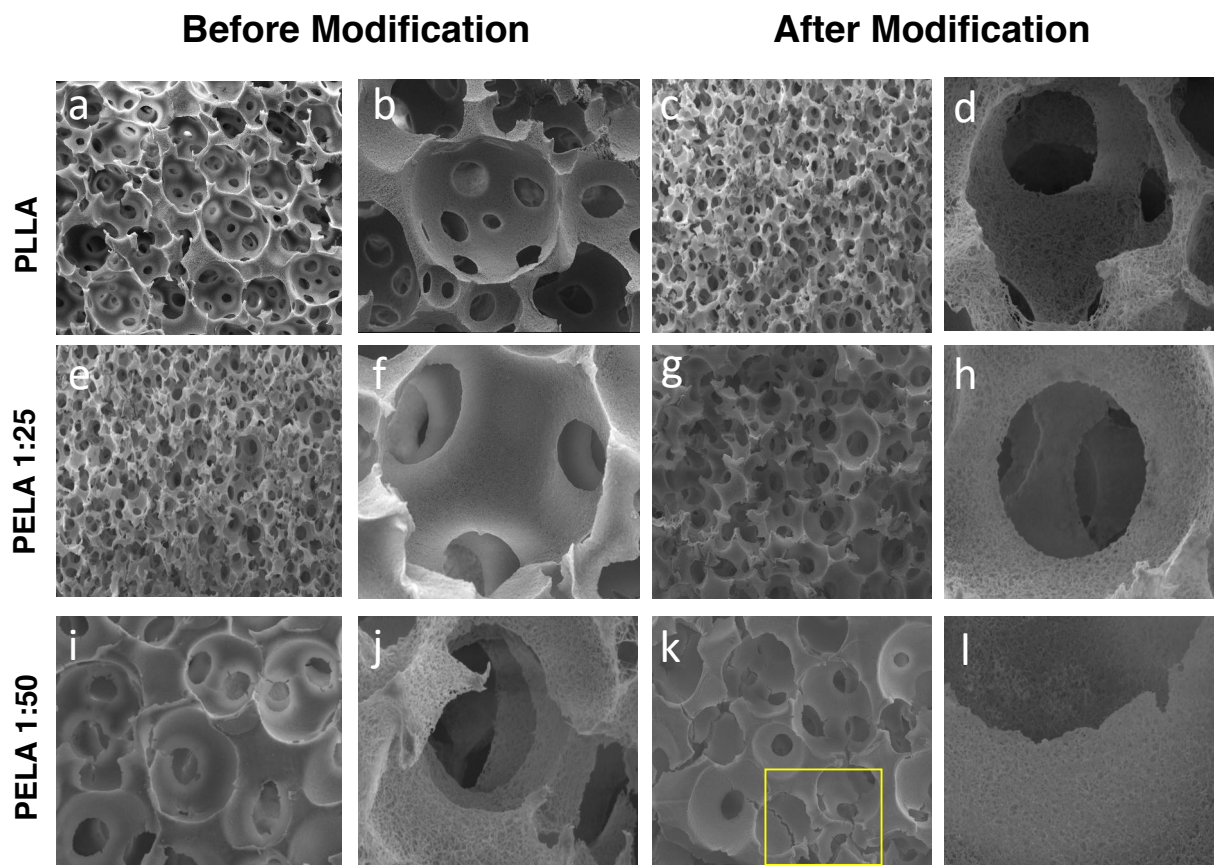
Figure 4.4 Scaffold fabrication and characterization through SEM before and after modification with amine-PEG$_{5000}$.

a-d) PLLA film before and after modification demonstrating nanofibrous and interconnected morphology e-h) PLLA/PELA$_{25:1}$ film before and after modification demonstrating nanofibrous and interconnected morphology c-h) PLLA/PELA films before and after modification demonstrating loss of porous and interconnected morphology.

4.3.4 Scaffold Fabrication and Modification and Observation of Physical Properties

Although two-dimensional structures can be a useful, the most useful tissue engineering constructs are three-dimensional due to mimicking the natural environment cells occupy. Due to the structural results observed after fabrication of the PELA thin-films, the scaffolds that we fabricated with the PELA polymers consisted of those with ratios of 10:1, 25:1, 50:1 and compared the physical and robustness of the scaffold to PLLA [**Figure 4.4**]. This is important as the scaffolds with higher EML where brittle and break apart by handling. Similarly, to the results seen in the films the scaffolds formed from PELA 10:1, 25:1 showed excellent morphology, nanofiber structure, and mechanical properties before and after modification with PEG-NH$_2$ 5k. The scaffolds fabricated from PELA 50:1 showed cracks and chips in the physical morphology before and after modification. Through this experiment we were able to demonstrate that we can fabricate a three-dimensional scaffold from PELA with similar physical and mechanical properties as those of PLLA scaffolds but can now be post modified in a facile method in the absence of toxic solvents, catalyst, or UV-light. Due to these structural and physical results all further experiments focused on the PELA 25:1 thin-film and scaffolds unless stated otherwise.

4.3.5 PELA thin-Film and scaffold conjugation with amine-containing molecules and
quantification of conjugation

After fabrication into tissue engineering constructs, we investigated the EML pendants if they are able to click with amine containing molecules. We demonstrated the stability and function of the constructs to be successfully modified without the need for heat or a catalyst, yet still conjugate molecules in water. In this study, the constructs were modified as depicted in Figure 4.1 and characterized using FTIR [**Figure 4.5A**]. The conjugation was considered a success with the appearance of amide stretch at ~1630-1690. The films and scaffolds both

demonstrated that they could be conjugated due to the formation of the amide bond formation. The PELA Thin-films and scaffolds where successfully quantified for amine molecules attached unto the surface. Films contained ~10 mg of dopamine conjugated, and scaffolds had ~25 mg of 5k-PEG-NH$_2$ conjugated, approximately 10x as much PEG compared to PLLA scaffolds. This gives us an indication to the degree of modification possible through the use of these tissue engineered constructs.
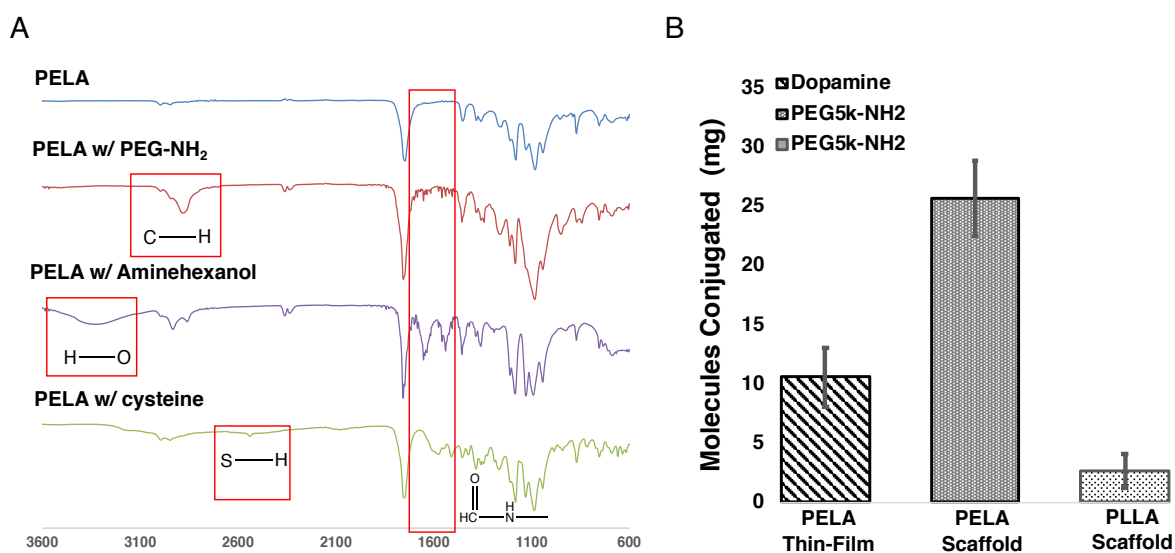
Figure 4.5 Characterization and quantification of "click-chemistry like" conjugation.

Characterization on thin-films and scaffold after conjugation with amine containing molecules A) FTIR spectrum of conjugation of amine containing molecules with PELA polymer B) Quantification of attachment of dopamine and PEG-NH$_2$ compared to PLLA scaffold, n = 5.

4.3.6 Thin-film and Scaffold Modification Visualization Through Confocal Imagery

In order to qualitatively determine the degree of modification that the PELA thin-films and scaffolds undergo they were modified with FITC-PEG-NH$_2$ both in DDH$_2$O and in methanol. This was done to mimic a potential small molecule that is insoluble in an aqueous

environment. Additionally, BSA-FITC (aq) was utilized to demonstrate that proteins through their surface amino acids of L-Lysine and L-Arginine which contain free NH_2 can be conjugated to the films and scaffolds. The films and scaffolds were soaked and modified as previously described before they were observed via confocal microscopy. Through this experiment we are able to demonstrate that the PELA thin-films and scaffolds can be easily modified with either NH_2-PEG-FITC and the BSA FITC, [**Figure 4.6A**]. The PELA scaffolds showed excellent conjugation of both dye c███████████ s c██████████████████████████ ffolds.
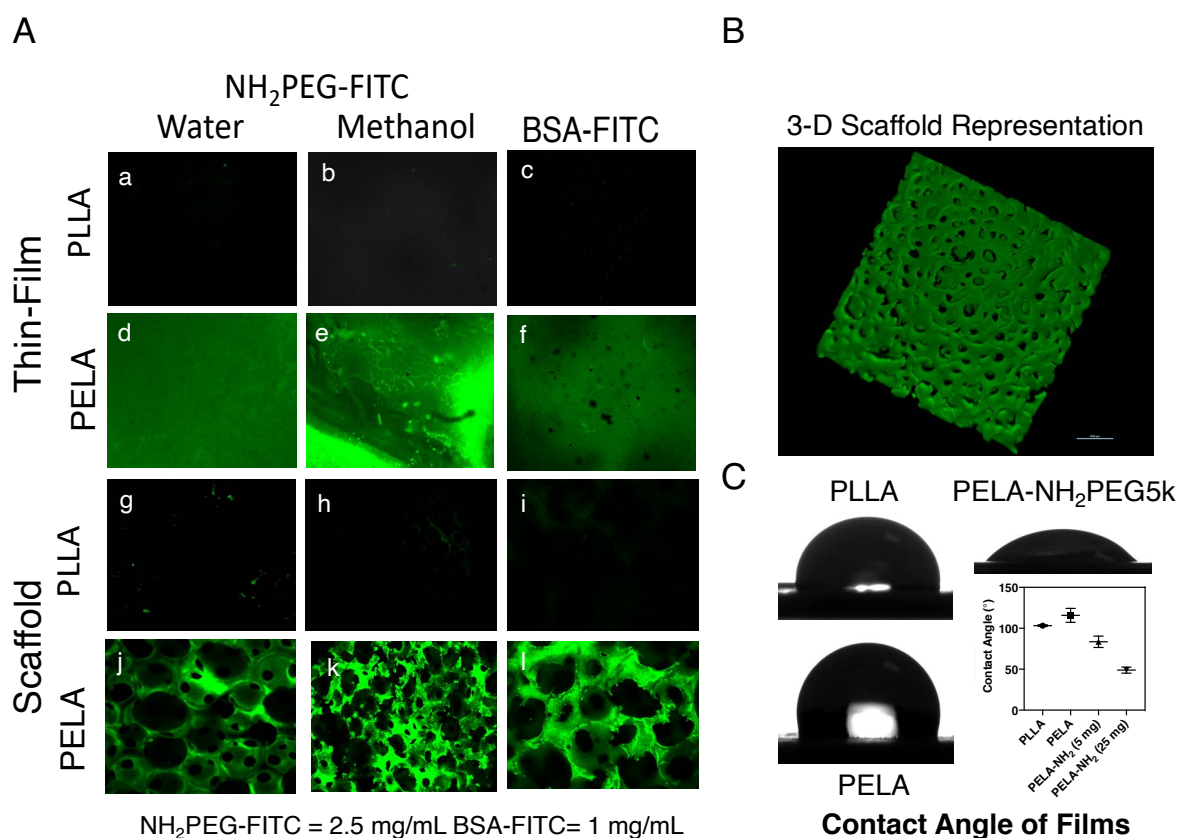
Figure 4.6 Scaffold modification with NH_2-PEG FITC & BSA-FITC, characterization, and contact Angle.

A) Modification of thin-films and scaffolds with fluorescent molecule to visualize conjugation of amine containing molecules B) Confocal 3D rendering of scaffold modified with amine-PEG-FITC C) contact angle measurement of PLLA, PLLA/PELA, PLLA/PELA thin-film conjugated with PEG-amine to demonstrate increased surface hydrophilicity.

Where only the scaffolds demonstrated limited fluorescence, which can be attributed to surface interaction and entrapment of the fluorescence molecules on the nanofibrous and porous surface of PLLA. Through three-dimensional rendering we are able to observe that the conjugation occurred throughout the entirety of the scaffold [**Figure 4.6B**].

4.3.7 Characterization of surface wettability through contact angle

The effects of modification were characterized by calculating the surface hydrophilicity of PELA thin-films before and after modification with NH_2-PEG_{5000} and comparing them to PLLA thin-films, [**Figure 4.6C**]. Through this characterization we can see that both PLLA and PELA are hydrophobic with contact angles greater than 100 ° and 110, respectively. However, once modified the PELA films surface hydrophilicity changes considerably with values ranging from 80 - 85° at 5 mg of PEG conjugation and 45 – 50 ° at 25 mg of PEG conjugated

4.3.8 Mass Loss Quantification of PLLA scaffolds and PELA scaffolds

In order to evaluate the degradation rate of the PELA scaffolds, as well as determine how the conjugation of molecules on the surface increase the hydrophilicity and affect the degradation rate PELA scaffolds were fabricated and conjugated with increasing amounts of NH_2-PEG 5k Da and the mass loss was recorded over time. Visually, the PELA group conjugated with NH_2-PEG began to fall apart at day 10, with all scaffolds breaking apart into large and small pieces by day 30 [**Figure 4.7**]. In comparison, the PLLA group remained intact and only a small amount of scaffold was lost after 35 d. This was also observed by quantifying mass loss during this time: the PLLA scaffold lost only ~ 15 % of its initial mass, the PELA with no heparin and the PLLA scaffold with heparin lost ~ 18-25 %, and the PELA with 100 mg PEG
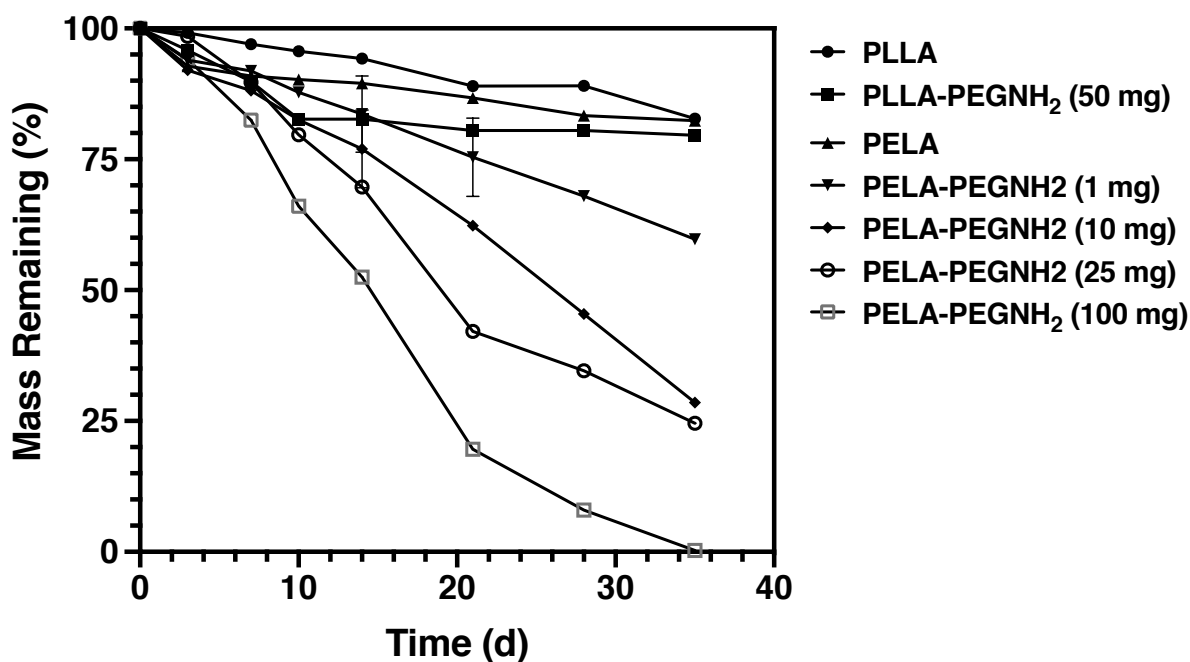
Figure 4.7 Mass loss quantification of PLLA and PELA scaffolds conjugated with PEG-NH₂. Quantification of mass remaining at predetermined time points of PELA polymer conjugated with varying amounts of PEGNH₂ compared to PLLA and PLLA with PEGNH₂.

conjugated lost ~ 99 % of the total mass. The nanoarchitecture observed at day 0 and at day 35 showed that the nanofibers and overall morphology had changed considerably in the PELA with PEG group but did not change significantly in the other groups. Therefore, we can conclude that there is an increase of hydrophilicity in the microenvironment and that the increase accelerates the rate of degradation as more PEG-NH₂ was conjugated. Through the use of this knowledge we can not only have a scaffold with biomimetic physical and mechanical properties that can be facile modified in a click-chemistry fashion but in addition we can utilize the EML pendants to tailor the degradation of the scaffold.

4.3.9 Polymeric nanospheres fabricated and attachment on PELA Thin-Films and Scaffold

Polymeric particles are another method of imparting biological cues to a tissue engineering scaffolds. Through the use of these particles, regulatory signals could be delivered to the localized environment in a controlled manner. In doing so the microenvironment can be enhanced for a prolonged duration. For this reason, polymeric particles have been utilized extensively in combination with scaffolds for tissue engineering to elicit cellular response[205, 219]. However facile methods to attach such particles in a manner in which the scaffold, the particle, or regulatory signal, which can include expensive and sensitive proteins or mRNAs, in the absence of chemicals, heat, acid/base would be a powerful tool in the tissue engineering tool kit. To show that PELA can be used to conjugate polymeric vesicles we synthesized 3 distinct polymers and fabricated them into vesicles. The three polymers were PLLA (~ 10 k Da), amine initiated PLGA (~ 10 k Da), and amine initiated PLGA with a PEG linker of 1 k Da (polymer ~11 k Da), the polymers were characterized by NMR and GPC for end group functionalization (amine presence) and molecular weight determination . NH_2-PLGA, NH_2-PEG-PLGA, and PLGA was successfully fabricated into nanospheres and loaded with NH_2PEG-Rhodamine B with a size ranging from 2-3 μm. The PELA and PLLA films were soaked for a day before conjugation with particles suspended in both water and methanol, washed to remove unconjugated spheres, and observed through SEM and confocal microscopy [**Figure 4.8A**]. Through these means we were able to determine that the PLLA films allowed minimal attachment of the amine containing particles based on the limited visualization of particles on the surface (linker and no linker) [**Figure 4.8A**]. However, there was a sizeable distinction between the number of particles on the PLLA and the PELA surface both in water and in methanol, as we were able to visualize a vast number of particles on the PELA surface [**Figure 4.8A**]. There was

A
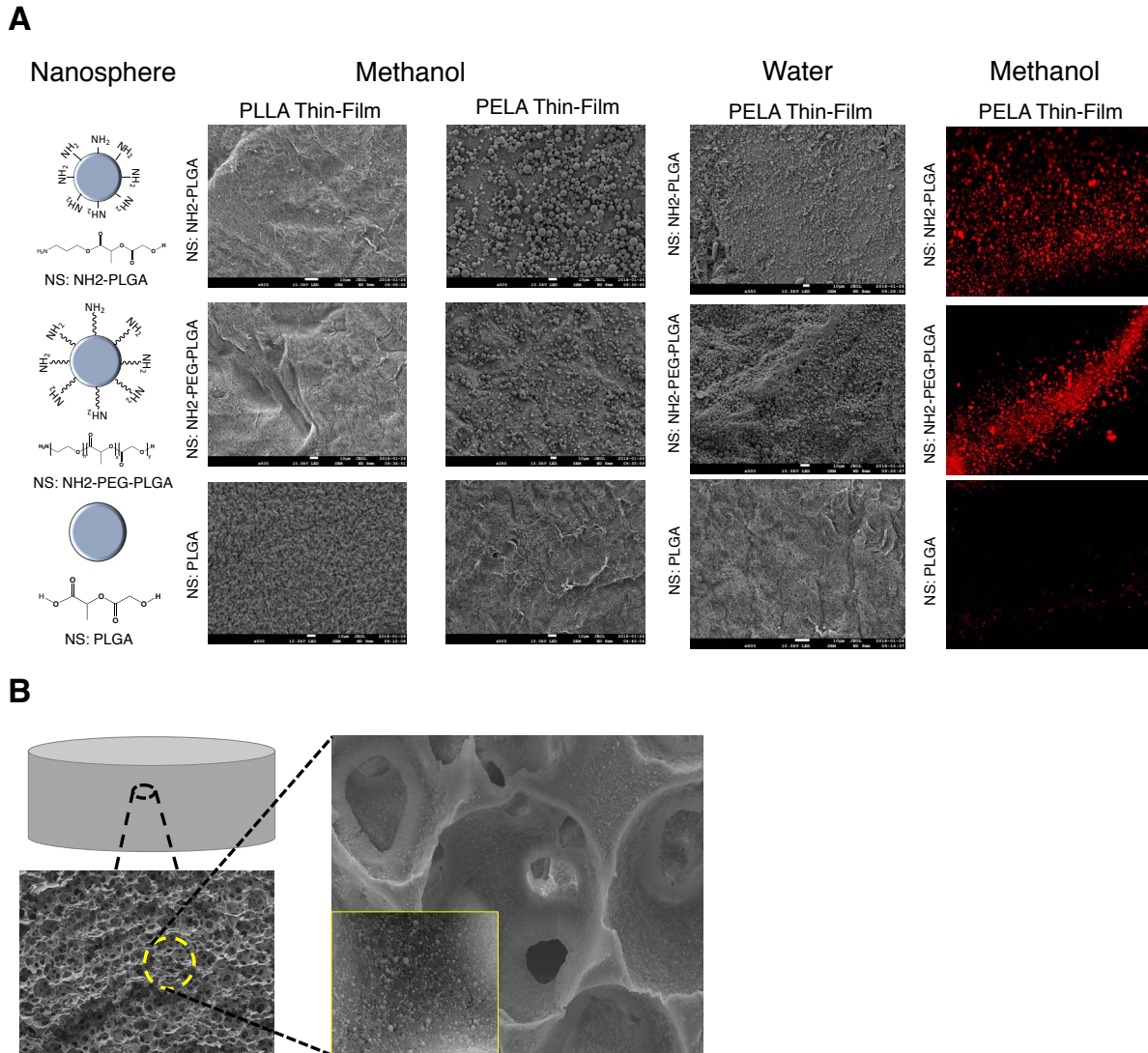
Figure 4.8 Thin Film and Scaffold Modification with Polymeric Microspheres for Sustained Drug Released.

A) Amine-functionalized polymeric particles and non-amine functionalized polymeric particles conjugated on thin films fabricated from PELA or PLLA visualized by SEM and confocal microscopy B) PELA scaffold with amine-functionalized polymeric particles.

no difference between the amine-PLGA (linker or no linker) number of particles on the surface, meaning that the linker utilized played no considerable role in the attachment. Of note is that the

PLLA particles showed minimal attachment unto the surface of the PELA film [**Figure 4.8**].

Signifying that their presence is due to entrapment and not conjugation.

In order to show that the PELA scaffolds can be utilized to attach polymeric vesicles and thereby be utilized for tissue engineering purposes, we conjugated the NH$_2$-PLGA (no linker) particles unto a PELA scaffolds and characterized in the same manner as the films. As in the films, we saw a large number of particles conjugated unto the scaffold surface and through-out the scaffold. Additionally, there was no clustering or agglomeration of the particles [**Figure 4.8 B**]. Through these experiments we are able to demonstrate for the first time to conjugate polymeric vesicles in a click-chemistry fashion in the absence of chemicals, heat, and solvents.

4.3.10 Scaffold biocompatibility "in vitro" and "in vivo" through subcutaneous implantation

Of concern was if the amine reactive EML pendants would negatively impact the scaffolds biocompatibility when cells are seeded by annealing them in place through conjugation of transmembrane proteins or molecules with free amines leading to physical deformation, diminished proliferation, or cell death. In order to demonstrate that the reactive EML pendants would not alter the cellular morphology we seeded iPS-MSCs unto the PELA and PLLA scaffolds and observed the cell morphology through SEM and confocal after staining the β-actin stained with phalloidin (red) and nuclei with DAPI (blue), [**Figure 4.9 A-B**]. Of note is that both the 50:1 and 25:1 PELA polymers were used in this experiment in order to increase the ratio of EML pendants available and demonstrate their biocompatibility. After seeding the cells for two days we were able to observe that similar to the PLLA scaffolds, the cells seeded unto the PELA scaffolds spread and formed large films consisting of cells. The scaffolds porosity assisted in the cells moving through the scaffold and there was no discernable difference between the PELA and the PLLA scaffold, [**Figure 4.9A**]. Using confocal imagery after staining the nucleus and β-

actin we are able to confirm again, that the morphology of cell was not altered due to the interaction with the amine reactive PELA copolymer. Both the cells in PLLA and PELA showed mature development of β-actin, a protein that is known to be a part of the cytoskeleton and contributes to the cellular elongation seen in the SEM, [**Figure 4.9B**].

Additionally, the cell survival was confirmed after 5 days post-seeding through an MTS proliferation assay. Using this assay, we are able to confirm that the PELA polymers and
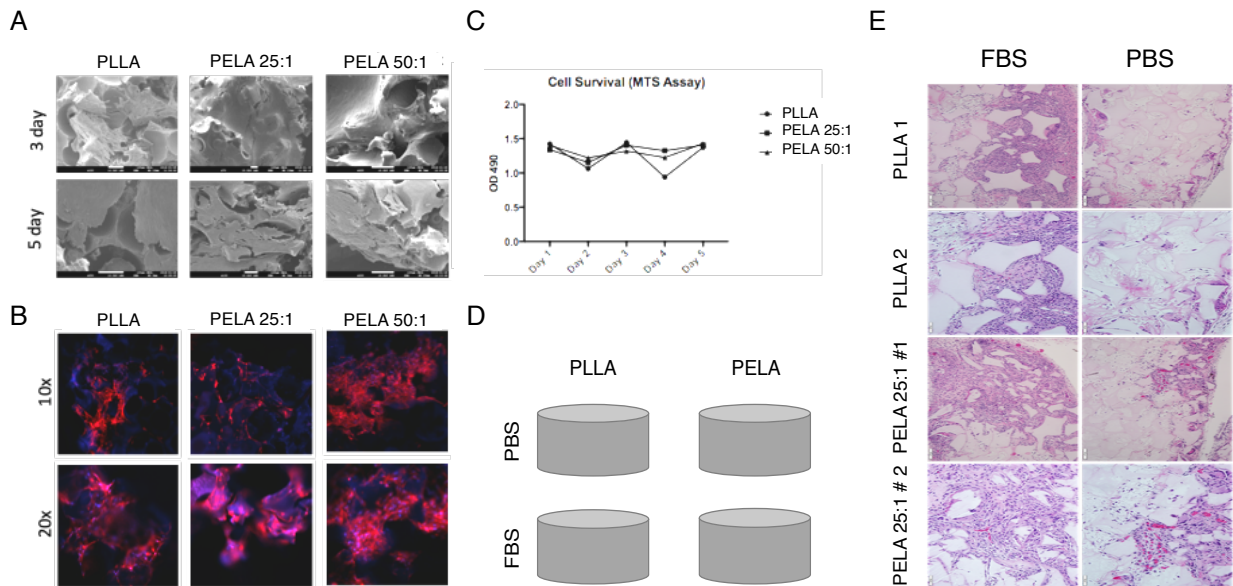
Figure 4.9 Cytocompatibility of PELA scaffolds compared to PLLA scaffolds.

A) SEM characterization of 3 day and 5 day cell seeding on PELA and PLLA scaffolds to demonstrate biocompatibility B) 3 day proliferation of iPS-MSCs. β-actin stained with phalloidin (red) and nuclei with DAPI (blue). Images at 10x (top) and 20x (bottom) C) 5 day MTS proliferation assay D) schematic illustration of PBS and FBS soaked PLLA and PELA 1:25 scaffolds E) Subcutaneously implantation of scaffolds in mice for 2 weeks characterization via H&E staining to demonstrate host cell infiltration. Scale bars at 20 μm.

scaffolds have no discerning cytotoxicity and are as biocompatible as the PLLA scaffolds *in vitro*. To demonstrate the PELA scaffolds biocompatibility *in vivo*, we implanted PELA scaffolds soaked in FBS, or non-soaked, and subcutaneously implanted them into the back of a mouse. At the end of 2 weeks the scaffolds were compared to the results of PLLA scaffolds

implanted in the same manner and stained with H & E. After the 2 weeks, we were able to conclude that the PELA scaffolds are indeed biocompatible *in vitro* and can be used as tissue engineering constructs. Both the PELA and PLLA scaffolds that were not soaked in FBS had less cells migrated into the scaffold. However, the FBS soaked PELA scaffold showed improved cellular penetration in the scaffolds. When compared qualitatively we can conclude that the PELA scaffolds conjugated with proteins in FBS are more biocompatible than PLLA scaffolds *in vivo*. Taken together, with the previous results we can determine that the PELA polymer can be utilized to fabricate a biomimetic scaffold that be further optimized in a click-chemistry fashion as a tissue engineering construct.

4.4 Discussion

Polymer scaffolds are an invaluable tool in tissue regeneration, providing a three-dimensional template similar to that of the native extracellular matrix (ECM) for cells to grow and proliferate into the desired tissue. Tissue regeneration is optimized in tissue quality and time to regeneration when scaffolds mimic the natural ECM. Of importance is the biomimetic physical architecture that has been previously developed by Ma and coworkers [49, 59, 161], where a three-dimensional fibrous architecture that is porous and interconnect is developed through a sugar leaching method and TIPS. Scaffolds with these features have been utilized and shown to be conducive for an array of tissue engineering applications and therefore offer a base starting point when developing novel scaffolds and biomaterials.

Recently, considerable effort has been spent to enhance the scaffold's biomimetic nature beyond physical characteristics by imparting biological motifs or regulatory signals that can trigger biologic responses. This has been a chemical and engineering challenge requiring an experienced material scientist due to the complicated procedures, toxic chemicals, solvents, as

well as the cost and time required. Additionally, these procedures can have deleterious effects due to trace chemicals left after implantation and can disrupt either the biomimetic architecture or the mechanical properties of the scaffold. Therefore, novel methods to develop scaffolds with biomimetic architecture that can be functionalized with such biological signals easily, efficiently, and economically are the focus of this work.

To achieve this, we have developed a novel copolymer derived from L-Lactide, poly(exomethylene-co-lactic acid) (PELA), that can be fabricated into films and scaffolds with the aforementioned biomimetic architecture that is conducive for tissue formation, contains excellent mechanical properties, and can be easily conjugated with amine containing molecules. The selectivity for amine containing molecules (nucleophiles) is quite broad, achieving conjugation with weak and strong nucleophiles such as tris(hydroxymethyl)aminomethanol (weak pKa ~ 7.77) to guanidine (strong pKa ~13.8) in aqueous environments[231]. To demonstrate the broad nature of the reaction we conjugated various molecules, amino acids (R & K) (pK$_a$ 8 – 12), serinol (pK$_a$ 9.0), dopamine (~ pK$_a$ 8.9, tetraethylpentamine (pK$_a$9.68), with a range of pK$_a$'s and determined that we achieved conjugation of the amine containing molecule via an amide formation in aqueous environments [232-234]. Additionally, this is further explored through the use of NH$_2$-PEG$_{5K}$, as it is conjugated unto the PELA constructs both in water and in anhydrous methanol [**Figure 4.6**]. The pKa in water is reported at approximately 10 where in anhydrous methanol the pKa is estimated to be 30 % of the value seen in an aqueous environment [235, 236]. Therefore, we can postulate that the conjugation of the nucleophilic addition is not dependent on the pK$_a$ (strong nucleophile) but on the amine of the amine containing molecule being free to form an amide bond.

After fully characterizing the copolymer chemical structure and reactivity [**Figure 4.2**], we set out by demonstrating that indeed the polymer could be fabricated into fibrous architecture by the development of two-dimensional thin-films [**Figure 4.3**]. Two-dimensional structures are utilized in material science and tissue engineering as a simple platform to investigate physical and mechanical properties, hydrophilicity (contact angle), conjugation efficiency, and biocompatibility. Through the use of thermally induced phase separation (TIPS), we fabricated films of the PELA polymers. We demonstrated that the polymer with less than 25:1 (EML to HPLLA) ratio indeed produced the biomimetic fibrous architecture with excellent mechanical property [**Figure 4.3c**]. This copolymer was further shown to be able to be used in the development of three-dimensional scaffolds [**Figure 4.4**]. The scaffolds developed using this copolymer (PELA$_{25:1}$) were made porous by the addition of a sugar porogen and thereby incorporating the favorable biomimetic morphology [**Figure 4.4 e-f**].

In the presence of an amine-containing molecule, the thin-films and scaffolds were rapidly modified in a click-chemistry approach via amide-bond formation in the absence of catalyst, heat, or organic solvents and without producing toxic byproducts [**Figure 4.3-4.4**]. For the first time, demonstrating that the EML pendants can be conjugated in water and methanol[230]. This is as crucial as the PEML stability, and reactivity was never evaluated previously in an aqueous environment our studies demonstrated that indeed the PELA polymer could serve for tissue engineering construct that can be conjugated under these circumstances and post-fabrication [230]. Most importantly, we were able to demonstrate that the mechanical properties and physical morphology of the scaffolds were not altered after modification, as it can be seen in the PELA$_{25:1}$ thin films [**Figure 4.3d**] and scaffolds [**Figure 4.4g-h**] conjugated with PEG-NH$_2$ demonstrated no change when visualized under SEM.

Importantly we demonstrated that the molecules were conjugated on the surface and not just fouled unto the surface [**Figure 4.5A**]. Additionally, the mass of molecules that can be conjugated unto the surface was determined through the use of dopamine (~10 mg) on the thin-films and NH_2-PEG_{5k} (25 mg) on the scaffolds [**Figure 4.5B**] - demonstrating that the PELA polymer can be conjugated in a *click-chemistry like* fashion and can be loaded with a known maximum mass of regulatory signals for films and scaffolds. The conjugation efficiency was further visualized through confocal microscopy of NH_2-PEG-FITC and BSA-FITC unto PELA thin-films and scaffolds and comparing it PLLA films and scaffolds [**Figure 4.6A**]. A clear difference in fluorescence was seen with the PELA constructs compared to the PLLA that only demonstrated fluorescence due to entrapment of the NH_2-PEG-FITC and BSA-FITC.

The tissue engineering constructs demonstrated increased wettability, tailorable degradation, as well as excellent biocompatibility *in vitro* and *in vivo*. These superior attributes make scaffolds developed from this novel copolymer a promising tool for tissue engineering by providing a construct that can be optimized with biomimetic characteristics. By determining the contact angle, we demonstrated that we could tailor the hydrophilicity of the surface [**Figure 4.6 C**], thereby having effects on the rate of degradation and biocompatibility. Likewise, to achieve complete polymer degradation, specifically in the carbon-carbon backbone, a cyclic ketene acetal was used. MDO is a unique molecule that is polymerized via free radical polymerization and structure switches to produce an ester in the backbone [**Figure 4.1**]. Through the use of this polymer, we were able to show complete degradation of the scaffolds that had 100 mg of NH_2-PEG_{5k} introduced after 35 days [**Figure 4.7**].

An alternative method to enhance the microenvironment is through the temporal and spatial control release of regulatory signals. This can be achieved through the use of polymeric

vesicles which have been shown to achieve such control release of growth factors, therapeutic agents, and proteins amongst others [63, 66, 205, 237-240]. However, incorporating such polymeric vesicles unto scaffolds has been problematic due to the use of solvents, heat, or chemical treatment that alter the particle surface, affecting the release kinetics, as well as affect the nanofibrous structure of the scaffold. Additionally, in many of these systems you can see aggregation of the particles and thereby providing uneven release of the regulatory signal through the scaffold. For this reason, using the PELA scaffold to conjugate such particles and demonstrating click-chemistry conjugation of the particles that are homogeneously disbursed is a significant finding [**Figure 4.8**]. The polymeric vesicles where shown to conjugate on the surface with high efficiency under physiological conditions and in methanol, thereby demonstrating broad use.

Taken together, we were able to demonstrate that the PELA polymer can be utilized to fabricate a tissue engineering scaffold with biomimetic physical characteristics. The constructs can be modified easily with biological motifs or regulatory signals on the surface that could trigger a biological response or in polymeric particles that can release such signals in a controlled released with spatial orientation. The biocompatibility and translational relevance of the biomimetic properties imparted on the PELA scaffolds were evaluated *in vitro* and *in vivo*. Culminating in *in vivo* studies with PELA scaffolds conjugated with proteins from FBS media that enhanced the host cell-penetration and remodeling over PLLA scaffolds. Proving that the PELA polymer fabricated into tissue-engineered scaffolds could serve as a tissue engineering construct and provide enhanced biocompatibility *in vivo* over other scaffolds.

4.5 Conclusion

Scaffolds are an invaluable tool in tissue and regenerative engineering with their clinical use expanding as biomimetic features are optimized. By building on previously described biomimetic physical characteristics we were able to develop scaffolds that can be easily enhanced in a click-chemistry fashion. In this work, we investigated a novel copolymer, PELA, with reactivity towards amines derived from L-Lactide, and fabricated it into scaffolds for tissue engineering for the first-time with biomimetic architecture. The scaffolds fabricated from this polymer contained biomimetic physical (nanofibrous, porous and interconnected) and mechanical properties. Most importantly, the scaffolds were shown to be facilely modified in an aqueous environment in a *click-chemistry fashion* in the absence of organic solvents, chemicals, UV-light, while retaining the biomimetic properties post-modification. Additionally, the scaffolds were shown to be biocompatible both *in vitro* and *in vivo* similarly to PLLA scaffolds. Taken together, we believe we have developed a novel scaffold platform that can be utilized for numerous tissue engineering applications and can be scaled for use by scientists outside of materials science due to the ease of modification. Future studies can broaden the use of the PELA polymer by looking at the reactivity of nucleophiles beyond amines, thereby broading the use of the polymer for biomedical application.

Chapter 5. Conclusions & Future Works

5.1 Thesis summary

Through the work presented in this thesis, we were able to demonstrate that tissue engineering techniques and methods can be simplified and made available for broad general use by groups who would traditionally abstain from using such approaches. Tissue engineering is an interdisciplinary field that requires more insight than what material scientists can provide. As described through the tissue engineering triad [Figure 1.1], the best possible tissue engineering constructs rely on biomaterials, cells (endogenous or exogenous), and regulatory signals to induce a cellular response. Therefore, it is expected that this knowledge and expertise will be drawn from more than only a material scientist and include the expertise and understanding of life scientists as well as physicians. However, due to the complexity, expertise needed, and cost of the equipment required to synthesize biodegradable polymers and fabricate tissue engineering constructs, groups outside materials and polymer science traditionally abstain from utilizing such techniques. Therefore, it is imperative that the material scientist simplify and demystify polymerization methods and tissue engineering construct fabrication in a manner - easily, tailorable, and economically - which can be utilized by a broad range of disciplines. Through this work, we put forth methods to synthesize rapidly tailorable and biodegradable polymers and methods to fabricate scaffolds with biomimetic physical architecture with minimal footprint, efficiently and economically, and tailored for the desired applications.

Developing HMW polymers in a rapidly, facile, and economical fashion with limited footprint and without traditional equipment utilized in material science laboratories provided the foundation for work provided in this thesis. Through the use of a novel synthesis method, we were able to demonstrate how HMW polymers from lactones can be synthesized for tissue engineering scaffolding. Additionally, through this method, we can synthesize polymers that are well defined in MW and end-functionalized if need be. Most, importantly we were able to synthesize HMW polymers of the PSLA polymer, which has a tailorable degree of functionality in the backbone, thereby producing scaffolds that can be easily modified with regulatory signals. As mentioned, this synthesis method has a very low footprint, requiring no dedicated hood space, hotplates, or specialized glassware. We utilize culture tubes and freezers commonly available in life science laboratories with minimal space required (culture tube is 20 cm in length by 2.5 cm in diameter) and can produce batches of HMW polymer of up to 10 g in as fast as one hour. The amount of polymer produced by this one-pot synthesis reaction in our experience is ideal scale for most laboratories.

The importance and use of the PSLA polymer in tissue engineering was demonstrated for the first time in the literature by the work in this thesis through the development of tubular scaffolds for *in situ* implantation in rat models. The highly functional polymer was modified with heparin to tailor the degradation rate, surface hydrophilicity, and biocompatibility. In collaboration with Professor Bo Yang, a cardiovascular surgeon and researcher, we successfully implanted the scaffolds into rat models and observed them for three-months. After the predetermined time, the reconstructed scaffolds were explanted and evaluated. The scaffolds exceeded our expectations, demonstrating excellent reconstruction of the inner layer with mature vascular tissue, and deposition of collagen and elastin. Additionally, the scaffolds demonstrated

no sign of aneurism, hyperplasia, or lethal thrombi formation. This work demonstrated the potential of the PSLA polymer with its tailorable functionality to serve as a biodegradable polymer for Tissue Engineering.

Modifying scaffolds and biomaterials with regulatory signals can lead to positive outcomes with regards to tissue formation such as cellular response (proliferation, differentiation, and mature tissue formation), ECM formation, and enhancing biocompatibility. Therefore, incorporating these signals can be an essential tissue engineering approach to improve the desired outcome. However, the post-modification of scaffolds can be a daunting experience, even for a material scientist. Modification techniques and approaches are not always effective, conjugation chemistries such as EDC-chemistry, aminolysis, and plasma treatment can experience difficulties. These problems can involve conjugation efficiency, disruption of the scaffold's properties (nanofibrous structure & mechanical properties), and the potential to denature and damage the molecules that are being conjugated. Advance conjugation techniques and methods such as click-chemistry tools have been shown to be ideal for preventing and diminishing the negative effects of traditional conjugation methods. However, these tools can be prohibitively costly and require an experienced materials chemist to conjugate the click-chemistry tools to the molecules that are being joined together. Therefore, these approaches are not a solution as a means to simplify and broaden the use of tissue engineering techniques beyond traditional material laboratories. For this reason, the PELA polymer can solve these problems, as it is able to be modified and conjugated by amine-containing regulatory signals by click-chemistry. We consider this a significant outcome of this work – as groups wishing to study specific effects due to a regulatory signal can do so without the need of material scientists.

Taken together, the development of both the synthesis methods to form HMW polymers such as PLLA and PSLA and the development of copolymers which are easily modified (PELA), combined with previously described scaffold fabrication methods make it possible to fabricate scaffolds that contain biomimetic physical architecture in a facile and rapid manner. Most importantly, we believe that through the work presented in this document, we have simplified processes in the tissue engineering field, opening the door for groups outside the materials discipline to utilize tissue engineering tools and have achieved the aim of the work.

5.2 Proposed Future Work

While the focus of this work was to demonstrate how we can simplify and thereby broaden the use of tissue engineering techniques as well as show how the biodegradable polymers we developed can be used in tissue engineering. There are still many areas to continue to explore and make an impact on this work. We specifically want to highlight three distinct areas which we are exploring 1) demonstrating living like polymerization properties of cold polymerization leading to ultra-high molecular weight (>1,000,000) 2) development of a fast degradable dense outer layer to match the degradation of the inner layer 3) Exploring the use of the PELA polymer as a biodegradable polymer to fabricate polymeric particles as cancer. The work and approach will be summarized in the following sections.

5.2.1 Synthesis of Ultra high molecular weight PLLA through guanidine catalyst

In the literature the TBD catalyzed reaction is referenced as a semi-living reaction [92]. In the literature, the TBD catalyzed reaction is referenced as a semi-living reaction 92. However, this has not been fully explored as of now. In our work, we have seen that the catalyst remains active after one-month in the reaction vessel. We demonstrated its viability as we can induce polymer chain growth through the addition of additional monomer or decreasing the viscosity of

the reaction by lower the w/v % of the polymer concentration. We are pursuing these avenues as a means to increase the HMW currently achieved (350 k Da). The goal is to demonstrate living polymerization properties and achieve MWs of > 1000 k Da. We believe that this benchmark will extend the use of what we can currently utilize the synthesized polymer for 3-D printing or fabrication of degradable cups and straws.

5.2.2 Tunable degradation of the outer layer dense-layer

Currently, we are developing a replacement of the outer "dense-layer" that was deposited by electrospinning PCL. Although, the PCL fibers provided exceptional mechanical properties that ensured the scaffold could sustain the hemodynamic forces as well as the suturing process. The polymer degrades very slowly (2-3 years) and can be problematic by causing calcification in the reconstructed vessel[192, 197]. Therefore, the ideal polymer to fabricate the outer-dense layer would provide the mechanical strength to endure the suturing processes but can be tailored to degrade at defined times. We are attempting to solve the issue by two routes 1) Electrospinning PSLA fibers, which are strong and nonelastic to provide the mechanical strength 2) Development of fast-degrading elastic polymers from MTC (methyl trioxocane) and MDO.

In this approach, through the fabrication of the PSLA polymer, we create fibers that mechanical strong (3x M Pa vs PLLA) but with very little elasticity. The fibers developed in this fashion have been demonstrated to contain the mechanical strength to endure suturing. We postulate that through these tailorable polymers, we can modulate the degradation of the outer layer and provide tailorable degradation rates similar to the inner layer. Additionally, through the use of MDO and MTC, we are synthesizing an elastic copolymer with increased hydrophilicity due to the ratio of MTC. We postulate that through the use of fibers fabricated from this MTC/MDO copolymer we will achieve tailorable degradation rate by modulating the feed ratio

114

and retain the favorable elastic properties we observe with PCL. Through these methods, we aim to enhance our current scaffold design and ensure that we provide a scaffold that can be 100 % tailored for the duration we designate.

5.2.3 Fabrication of polymeric particles from PELA polymer

Being able to functionalize the surface of a material can be beneficial in drug delivery to either shield the particle to prevent an immune response or to incorporate binding motifs. Therefore, a high density of chemical functionality on the material is beneficial as we can conjugate an increasing amount of binding or shielding motifs. However, traditional chemical functional groups can experience poor conjugation efficiency. Hence, a polymeric particle fabricated from PELA can prove to be beneficial to improve the conjugation efficiency between binding and shielding motifs. Using our polymerization method detailed in chapter 4, we can modulate the density of reactive EML groups on the surface of the polymeric particle. In this manner, we can modulate the density of motifs we wish to attach. Most importantly, the PELA polymer can be dissolved in DCM, and processes by well-established and facile methods outline by Ma and coworkers [36, 68, 205, 241]. As proof of concept, the particles have been conjugated with a cell-adhesion peptide specific for SKBR-3 breast cancer cells and have been shown to have a high rate of particle uptake compared to particles without the binding motif. These particles also lead to higher cell death compared to our control groups when loaded with cancer therapeutic. Thereby demonstrating that this highly reactive polymer can be utilized for numerous applications in tissue engineering and regenerative medicine.

Chapter 6. Bibliography

1.   Breuer, C. K.; Shin'oka, T.; Tanel, R. E.; Zund, G.; Mooney, D. J.; Ma, P. X.; Miura, T.; Colan, S.; Langer, R.; Mayer, J. E.; Vacanti, J. P., Tissue engineering lamb heart valve leaflets. *Biotechnol Bioeng* **1996,** *50* (5), 562-7.

2.   Burdick, J. A.; Mauck, R. L.; Wiley online library., Biomaterials for tissue engineering applications a review of the past and future trends. Springer: Wien ; New York, 2011; pp. 1 online resource (x, 564 p.). http://dx.doi.org/10.1002/9783527646821.

3.   He, D.; Dong, W.; Tang, S.; Wei, J.; Liu, Z.; Gu, X.; Li, M.; Guo, H.; Niu, Y., Tissue engineering scaffolds of mesoporous magnesium silicate and poly(epsilon-caprolactone)-poly(ethylene glycol)-poly(epsilon-caprolactone) composite. *Journal of materials science. Materials in medicine* **2014,** *25* (6), 1415-24.

4.   Smith, L. A.; Ma, P. X., Nano-fibrous scaffolds for tissue engineering. *Colloids Surf B Biointerfaces* **2004,** *39* (3), 125-31.

5.   Song, Y.; Feijen, J.; Grijpma, D. W.; Poot, A. A., Tissue engineering of small-diameter vascular grafts: a literature review. *Clin Hemorheol Microcirc* **2011,** *49* (1-4), 357-74.

6.   Wobma, H.; Vunjak-Novakovic, G., Tissue Engineering and Regenerative Medicine 2015: A Year in Review. *Tissue Eng Part B Rev* **2016,** *22* (2), 101-13.

7.   Kim, B. S.; Mooney, D. J., Development of biocompatible synthetic extracellular matrices for tissue engineering. *Trends Biotechnol* **1998,** *16* (5), 224-30.

8.   Lutolf, M. P.; Hubbell, J. A., Synthetic biomaterials as instructive extracellular microenvironments for morphogenesis in tissue engineering. *Nat Biotechnol* **2005,** *23* (1), 47-55.

9.   Ma, H.; Hu, J.; Ma, P. X., Polymer scaffolds for small-diameter vascular tissue engineering. *Adv Funct Mater* **2010,** *20* (17), 2833-2841.

10.   Agrawal, C. M.; Ray, R. B., Biodegradable polymeric scaffolds for musculoskeletal tissue engineering. *J Biomed Mater Res* **2001,** *55* (2), 141-50.

11.   Holland, T. A.; Mikos, A. G., Biodegradable polymeric scaffolds. Improvements in bone tissue engineering through controlled drug delivery. *Adv Biochem Eng Biotechnol* **2006,** *102*, 161-85.

12.   Kim, J.; Yaszemski, M. J.; Lu, L., Three-dimensional porous biodegradable polymeric scaffolds fabricated with biodegradable hydrogel porogens. *Tissue Eng Part C Methods* **2009,** *15* (4), 583-94.

13.   Luderer, F.; Begerow, I.; Schmidt, W.; Martin, H.; Grabow, N.; Bunger, C. M.; Schareck, W.; Schmitz, K. P.; Sternberg, K., Enhanced visualization of biodegradable polymeric vascular scaffolds by incorporation of gold, silver and magnetite nanoparticles. *J Biomater Appl* **2013,** *28* (2), 219-31.

14.   Nam, Y. S.; Park, T. G., Porous biodegradable polymeric scaffolds prepared by thermally induced phase separation. *J Biomed Mater Res* **1999,** *47* (1), 8-17.

15.   Albertsson, A. C.; Ljungquist, O., Degradable Polyesters as Biomaterials. *Acta Polym* **1988,** *39* (1-2), 95-104.

16.   Ma, P. X., Scaffolds for tissue fabrication. *Materials Today* **2004,** *7* (5), 30-40.

17.   Ma, P. X., Biomimetic materials for tissue engineering. *Adv Drug Deliver Rev* **2008,** *60* (2), 184-198.

18.   Liu, X.; Ma, P. X., Polymeric scaffolds for bone tissue engineering. *Ann Biomed Eng* **2004,** *32* (3), 477-86.

19.   Haddad, T.; Noel, S.; Liberelle, B.; El Ayoubi, R.; Ajji, A.; De Crescenzo, G., Fabrication and surface modification of poly lactic acid (PLA) scaffolds with epidermal growth factor for neural tissue engineering. *Biomatter* **2016,** *6* (1), e1231276.

20.   Huang, Y. X.; Ren, J.; Chen, C.; Ren, T. B.; Zhou, X. Y., Preparation and properties of poly(lactide-co-glycolide) (PLGA)/ nano-hydroxyapatite (NHA) scaffolds by thermally induced phase separation and rabbit MSCs culture on scaffolds. *J Biomater Appl* **2008,** *22* (5), 409-32.

21.   Sachlos, E.; Czernuszka, J. T., Making tissue engineering scaffolds work. Review: the application of solid freeform fabrication technology to the production of tissue engineering scaffolds. *Eur Cell Mater* **2003,** *5*, 29-39; discussion 39-40.

22.   Mauney, J. R.; Adam, R. M., Dynamic reciprocity in cell-scaffold interactions. *Adv Drug Deliv Rev* **2015,** *82-83*, 77-85.

23.   Murphy, C. M.; O'Brien, F. J.; Little, D. G.; Schindeler, A., Cell-scaffold interactions in the bone tissue engineering triad. *Eur Cell Mater* **2013,** *26*, 120-32.

24.   Spector, M., Novel cell-scaffold interactions encountered in tissue engineering: contractile behavior of musculoskeletal connective tissue cells. *Tissue Eng* **2002,** *8* (3), 351-7.

25.   Gentile, P.; Chiono, V.; Carmagnola, I.; Hatton, P. V., An overview of poly(lactic-co-glycolic) acid (PLGA)-based biomaterials for bone tissue engineering. *Int J Mol Sci* **2014,** *15* (3), 3640-59.

26.   Li, X. W.; Li, H.; Zhao, Y. Y.; Tang, X. Y.; Ma, S. F.; Gong, B.; Li, M. F., Facile synthesis of well-defined hydrophilic polyesters as degradable poly(ethylene glycol)-like biomaterials. *Polymer Chemistry* **2015,** *6* (36), 6452-6456.

27.   Wei, G.; Ma, P. X., Nanostructured Biomaterials for Regeneration. *Adv Funct Mater* **2008,** *18* (22), 3566-3582.

28.   Cortizo, M. S.; Molinuevo, M. S.; Cortizo, A. M., Biocompatibility and biodegradation of polyester and polyfumarate based-scaffolds for bone tissue engineering. *J Tissue Eng Regen Med* **2008,** *2* (1), 33-42.

29.   Kim, J. A.; Lim, J.; Naren, R.; Yun, H. S.; Park, E. K., Effect of the biodegradation rate controlled by pore structures in magnesium phosphate ceramic scaffolds on bone tissue regeneration in vivo. *Acta Biomater* **2016,** *44*, 155-67.

30.   Mkhabela, V.; Ray, S. S., Biodegradation and bioresorption of poly(varepsilon-caprolactone) nanocomposite scaffolds. *Int J Biol Macromol* **2015,** *79*, 186-92.

31.   Tesfamariam, B., Bioresorbable vascular scaffolds: Biodegradation, drug delivery and vascular remodeling. *Pharmacol Res* **2016,** *107*, 163-171.

32.   Mo, X.; Weber, H.-J., Electrospinning P(LLA-CL) Nanofiber: A Tubular Scaffold Fabrication with Circumferential Alignment. *Macromolecular Symposia* **2004,** *217* (1), 413-416.

33.   Smith, L. A.; Liu, X.; Ma, P. X., Tissue Engineering with Nano-Fibrous Scaffolds. *Soft Matter* **2008,** *4* (11), 2144-2149.

34.   Feng, G.; Zhang, Z.; Dang, M.; Zhang, X.; Doleyres, Y.; Song, Y.; Chen, D.; Ma, P. X., Injectable nanofibrous spongy microspheres for NR4A1 plasmid DNA transfection to reverse fibrotic degeneration and support disc regeneration. *Biomaterials* **2017,** *131*, 86-97.

35.   Kuang, R.; Zhang, Z.; Jin, X.; Hu, J.; Gupte, M. J.; Ni, L.; Ma, P. X., Nanofibrous spongy microspheres enhance odontogenic differentiation of human dental pulp stem cells. *Adv Healthc Mater* **2015,** *4* (13), 1993-2000.

36. Liu, Z.; Chen, X.; Zhang, Z.; Zhang, X.; Saunders, L.; Zhou, Y.; Ma, P. X., Nanofibrous Spongy Microspheres To Distinctly Release miRNA and Growth Factors To Enrich Regulatory T Cells and Rescue Periodontal Bone Loss. *ACS nano* **2018,** *12* (10), 9785-9799.

37. Dahl, S. L.; Kypson, A. P.; Lawson, J. H.; Blum, J. L.; Strader, J. T.; Li, Y.; Manson, R. J.; Tente, W. E.; DiBernardo, L.; Hensley, M. T.; Carter, R.; Williams, T. P.; Prichard, H. L.; Dey, M. S.; Begelman, K. G.; Niklason, L. E., Readily available tissue-engineered vascular grafts. *Sci Transl Med* **2011,** *3* (68), 68ra9.

38. Hu, J. A.; Sun, X. A.; Ma, H. Y.; Xie, C. Q.; Chen, Y. E.; Ma, P. X., Porous nanofibrous PLLA scaffolds for vascular tissue engineering. *Biomaterials* **2010,** *31* (31), 7971-7977.

39. Hu, J.; Ma, P. X., Nano-fibrous tissue engineering scaffolds capable of growth factor delivery. *Pharm Res* **2011,** *28* (6), 1273-81.

40. Woo, K. M.; Chen, V. J.; Ma, P. X., Nano-fibrous scaffolding architecture selectively enhances protein adsorption contributing to cell attachment. *J Biomed Mater Res A* **2003,** *67* (2), 531-7.

41. Bhatnagar, R.; Li, S., Biomimetic scaffolds for tissue engineering. *Conf Proc IEEE Eng Med Biol Soc* **2004,** *2004*, 5021-3.

42. Holzwarth, J. M.; Ma, P. X., Biomimetic nanofibrous scaffolds for bone tissue engineering. *Biomaterials* **2011,** *32* (36), 9622-9.

43.   Khalili, S.; Nouri Khorasani, S.; Razavi, M.; Hashemi Beni, B.; Heydari, F.; Tamayol, A., Nanofibrous scaffolds with biomimetic structure. *J Biomed Mater Res A* **2018,** *106* (2), 370-376.

44.   Owen, S. C.; Shoichet, M. S., Design of three-dimensional biomimetic scaffolds. *J Biomed Mater Res A* **2010,** *94* (4), 1321-31.

45.   Park, J. Y.; Park, S. H.; Kim, M. G.; Park, S. H.; Yoo, T. H.; Kim, M. S., Biomimetic Scaffolds for Bone Tissue Engineering. *Adv Exp Med Biol* **2018,** *1064*, 109-121.

46.   Park, K. E.; Jung, S. Y.; Lee, S. J.; Min, B. M.; Park, W. H., Biomimetic nanofibrous scaffolds: preparation and characterization of chitin/silk fibroin blend nanofibers. *Int J Biol Macromol* **2006,** *38* (3-5), 165-73.

47.   Park, K. E.; Kang, H. K.; Lee, S. J.; Min, B. M.; Park, W. H., Biomimetic nanofibrous scaffolds: preparation and characterization of PGA/chitin blend nanofibers. *Biomacromolecules* **2006,** *7* (2), 635-43.

48.   Yuan, N.; Rezzadeh, K. S.; Lee, J. C., Biomimetic Scaffolds for Osteogenesis. *Receptors Clin Investig* **2015,** *2* (3).

49.   Hu, J.; Sun, X.; Ma, H.; Xie, C.; Chen, Y. E.; Ma, P. X., Porous nanofibrous PLLA scaffolds for vascular tissue engineering. *Biomaterials* **2010,** *31* (31), 7971-7.

50.   Hu, J.; Xie, C.; Ma, H.; Yang, B.; Ma, P. X.; Chen, Y. E., Construction of vascular tissues with macro-porous nano-fibrous scaffolds and smooth muscle cells enriched from differentiated embryonic stem cells. *PLoS One* **2012,** *7* (4), e35580.

51.   Yang, Y.; Zhao, J.; Zhao, Y.; Wen, L.; Yuan, X.; Fan, Y., Formation of porous PLGA scaffolds by a combining method of thermally induced phase separation and porogen leaching. *Journal of Applied Polymer Science* **2008,** *109* (2), 1232-1241.

52.   Frank, A.; Rath, S. K.; Venkatraman, S. S., Controlled release from bioerodible polymers: effect of drug type and polymer composition. *J Control Release* **2005,** *102* (2), 333-44.

53.   Fuoco, T.; Finne-Wistrand, A.; Pappalardo, D., A Route to Aliphatic Poly(ester)s with Thiol Pendant Groups: From Monomer Design to Editable Porous Scaffolds. *Biomacromolecules* **2016,** *17* (4), 1383-94.

54.   Hu, J.; Wang, Y.; Jiao, J.; Liu, Z.; Zhao, C.; Zhou, Z.; Zhang, Z.; Forde, K.; Wang, L.; Wang, J.; Baylink, D. J.; Zhang, X. B.; Gao, S.; Yang, B.; Chen, Y. E.; Ma, P. X., Patient-specific cardiovascular progenitor cells derived from integration-free induced pluripotent stem cells for vascular tissue regeneration. *Biomaterials* **2015,** *73*, 51-9.

55.   Liu, X.; Ma, P. X., Phase separation, pore structure, and properties of nanofibrous gelatin scaffolds. *Biomaterials* **2009,** *30* (25), 4094-103.

56.   Soares, D. G.; Zhang, Z.; Mohamed, F.; Eyster, T. W.; de Souza Costa, C. A.; Ma, P. X., Simvastatin and nanofibrous poly(l-lactic acid) scaffolds to promote the odontogenic potential of dental pulp cells in an inflammatory environment. *Acta Biomater* **2018,** *68*, 190-203.

57.   Wang, Z.; Cui, Y.; Wang, J.; Yang, X.; Wu, Y.; Wang, K.; Gao, X.; Li, D.; Li, Y.; Zheng, X. L.; Zhu, Y.; Kong, D.; Zhao, Q., The effect of thick fibers and large pores of

electrospun poly(epsilon-caprolactone) vascular grafts on macrophage polarization and arterial regeneration. *Biomaterials* **2014,** *35* (22), 5700-10.

58. Chen, V. J.; Ma, P. X., Nano-fibrous poly(L-lactic acid) scaffolds with interconnected spherical macropores. *Biomaterials* **2004,** *25* (11), 2065-73.

59. Gupte, M. J.; Ma, P. X., Nanofibrous scaffolds for dental and craniofacial applications. *J Dent Res* **2012,** *91* (3), 227-34.

60. Kuang, R.; Zhang, Z.; Jin, X.; Hu, J.; Shi, S.; Ni, L.; Ma, P. X., Nanofibrous spongy microspheres for the delivery of hypoxia-primed human dental pulp stem cells to regenerate vascularized dental pulp. *Acta Biomater* **2016,** *33*, 225-34.

61. Ma, P. X.; Zhang, R., Synthetic nano-scale fibrous extracellular matrix. *J Biomed Mater Res* **1999,** *46* (1), 60-72.

62. Katsogiannis, K. A. G.; Vladisavljević, G. T.; Georgiadou, S., Porous electrospun polycaprolactone (PCL) fibres by phase separation. *European Polymer Journal* **2015,** *69*, 284-295.

63. Kirby, G. T. S.; White, L. J.; Rahman, C. V.; Cox, H. C.; Qutachi, O.; Rose, F. R. A. J.; Hutmacher, D. W.; Shakesheff, K. M.; Woodruff, M. A., PLGA-Based Microparticles for the Sustained Release of BMP-2. *Polymers* **2011,** *3* (1), 571-586.

64. Liu, X.; Holzwarth, J. M.; Ma, P. X., Functionalized synthetic biodegradable polymer scaffolds for tissue engineering. *Macromol Biosci* **2012,** *12* (7), 911-9.

65.   Liu, X.; Ma, P. X., The nanofibrous architecture of poly(L-lactic acid)-based functional copolymers. *Biomaterials* **2010,** *31* (2), 259-69.

66.   Makadia, H. K.; Siegel, S. J., Poly Lactic-co-Glycolic Acid (PLGA) as Biodegradable Controlled Drug Delivery Carrier. *Polymers* **2011,** *3* (3), 1377-1397.

67.   Mehta, R.; Kumar, V.; Bhunia, H.; Upadhyay, S. N., Synthesis of poly(lactic acid): A review. *J Macromol Sci-Pol R* **2005,** *C45* (4), 325-349.

68.   Smith, I. O.; Liu, X. H.; Smith, L. A.; Ma, P. X., Nanostructured polymer scaffolds for tissue engineering and regenerative medicine. *Wires Nanomed Nanobi* **2009,** *1* (2), 226-236.

69.   Gunatillake, P. A.; Adhikari, R., Biodegradable synthetic polymers for tissue engineering. *Eur Cell Mater* **2003,** *5*, 1-16; discussion 16.

70.   Brannigan, R. P.; Dove, A. P., Synthesis, properties and biomedical applications of hydrolytically degradable materials based on aliphatic polyesters and polycarbonates. *Biomater Sci* **2016,** *5* (1), 9-21.

71.   Han, H.; Zhu, J.; Zhang, F. F.; Li, F. X.; Wang, X. L.; Yu, J. Y.; Qin, X. H.; Wu, D. Q., Hydrophilic and degradable polyesters based on l-aspartic acid with antibacterial properties for potential application in hernia repair. *Biomater Sci* **2019,** *7* (12), 5404-5413.

72.   Lecomte, P.; Jerome, C., Synthesis and Fabrication of Polyesters as Biomaterials. *Polymeric Biomaterials: Structure and Function, Vol 1* **2013**, 1-36.

73.   Song, L.; Ding, A. X.; Zhang, K. X.; Gong, B.; Lu, Z. L.; He, L., Degradable polyesters via ring-opening polymerization of functional valerolactones for efficient gene delivery. *Org Biomol Chem* **2017,** *15* (31), 6567-6574.

74.   Cheng, T.; O'Rorke, R.; Ortiz, R. F.; Yan, T. Y.; Hemmer, E.; Vetrone, F.; Marks, R. S.; Steele, T. W. J., Self-assembled photoadditives in polyester films allow stop and go chemical release. *Acta Biomater* **2017,** *54*, 186-200.

75.   Dhingra, S.; Weisel, R. D.; Li, R. K., Synthesis of aliphatic polyester hydrogel for cardiac tissue engineering. *Methods Mol Biol* **2014,** *1181*, 51-9.

76.   Borgaonkar, P.; Sharma, S.; Chen, M.; Bhowmick, S.; Schmidt, D. F., A flexible approach to the preparation of polymer scaffolds for tissue engineering. *Macromol Biosci* **2007,** *7* (2), 201-7.

77.   Gonzalez-Garcia, D. M.; Marcos-Fernandez, A.; Rodriguez-Lorenzo, L. M.; Jimenez-Gallegos, R.; Vargas-Becerril, N.; Tellez-Jurado, L., Synthesis and in Vitro Cytocompatibility of Segmented Poly(Ester-Urethane)s and Poly(Ester-Urea-Urethane)s for Bone Tissue Engineering. *Polymers (Basel)* **2018,** *10* (9).

78.   Idris, S. B.; Arvidson, K.; Plikk, P.; Ibrahim, S.; Finne-Wistrand, A.; Albertsson, A. C.; Bolstad, A. I.; Mustafa, K., Polyester copolymer scaffolds enhance expression of bone markers in osteoblast-like cells. *J Biomed Mater Res A* **2010,** *94* (2), 631-9.

79.   Ye, H.; Zhang, K.; Kai, D.; Li, Z.; Loh, X. J., Polyester elastomers for soft tissue engineering. *Chem Soc Rev* **2018,** *47* (12), 4545-4580.

80. Curia, S.; Biundo, A.; Fischer, I.; Braunschmid, V.; Gubitz, G. M.; Stanzione, J. F., 3rd, Towards Sustainable High-Performance Thermoplastics: Synthesis, Characterization, and Enzymatic Hydrolysis of Bisguaiacol-Based Polyesters. *ChemSusChem* **2018,** *11* (15), 2529-2539.

81. Chang, S. H.; Lee, H. J.; Park, S.; Kim, Y.; Jeong, B., Fast Degradable Polycaprolactone for Drug Delivery. *Biomacromolecules* **2018,** *19* (6), 2302-2307.

82. Laurent, C. P.; Vaquette, C.; Liu, X.; Schmitt, J. F.; Rahouadj, R., Suitability of a PLCL fibrous scaffold for soft tissue engineering applications: A combined biological and mechanical characterisation. *J Biomater Appl* **2018,** *32* (9), 1276-1288.

83. Malikmammadov, E.; Tanir, T. E.; Kiziltay, A.; Hasirci, V.; Hasirci, N., PCL and PCL-based materials in biomedical applications. *J Biomater Sci Polym Ed* **2018,** *29* (7-9), 863-893.

84. Jain, R. A., The manufacturing techniques of various drug loaded biodegradable poly(lactide-co-glycolide) (PLGA) devices. *Biomaterials* **2000,** *21* (23), 2475-90.

85. Zund, G.; Breuer, C. K.; Shinoka, T.; Ma, P. X.; Langer, R.; Mayer, J. E.; Vacanti, J. P., The in vitro construction of a tissue engineered bioprosthetic heart valve. *Eur J Cardiothorac Surg* **1997,** *11* (3), 493-7.

86. Khosravi, R.; Best, C. A.; Allen, R. A.; Stowell, C. E.; Onwuka, E.; Zhuang, J. J.; Lee, Y. U.; Yi, T.; Bersi, M. R.; Shinoka, T.; Humphrey, J. D.; Wang, Y.; Breuer, C. K., Long-Term Functional Efficacy of a Novel Electrospun Poly(Glycerol Sebacate)-Based Arterial Graft in Mice. *Ann Biomed Eng* **2016,** *44* (8), 2402-16.

87.   Lee, K. W.; Stolz, D. B.; Wang, Y., Substantial expression of mature elastin in arterial constructs. *Proc Natl Acad Sci U S A* **2011,** *108* (7), 2705-10.

88.   Yoo, Y.-C.; Kim, H.-Y.; Jin, F.-L.; Park, S.-J., Synthesis of poly(glycolide-caprolactone) copolymers for application as bioabsorbable suture materials. *Macromolecular Research* **2013,** *21* (6), 687-692.

89.   Blocks, Stars and Combs: Complex Macromolecular Architecture Polymers via Click Chemistry. In *Click Chemistry for Biotechnology and Materials Science*, pp 89-117.

90.   Prabaharan, M.; Grailer, J. J.; Pilla, S.; Steeber, D. A.; Gong, S., Amphiphilic multi-arm-block copolymer conjugated with doxorubicin via pH-sensitive hydrazone bond for tumor-targeted drug delivery. *Biomaterials* **2009,** *30* (29), 5757-66.

91.   Kim, H.; Olsson, J. V.; Hedrick, J. L.; Waymouth, R. M., Facile Synthesis of Functionalized Lactones and Organocatalytic Ring-Opening Polymerization. *ACS Macro Letters* **2012,** *1* (7), 845-847.

92.   Simon, L.; Goodman, J. M., The mechanism of TBD-catalyzed ring-opening polymerization of cyclic esters. *J Org Chem* **2007,** *72* (25), 9656-62.

93.   Garkhal, K.; Verma, S.; Jonnalagadda, S.; Kumar, N., Fast degradable poly(L-lactide-co-ε-caprolactone) microspheres for tissue engineering: Synthesis, characterization, and degradation behavior. *Journal of Polymer Science Part A: Polymer Chemistry* **2007,** *45* (13), 2755-2764.

94.   Zhang, X.; MacDonald, D. A.; Goosen, M. F.; McAuley, K. B., Mechanism of lactide polymerization in the presence of stannous octoate: the effect of hydroxy and carboxylic acid substances. *Journal of Polymer Science Part A: Polymer Chemistry* **1994,** *32* (15), 2965-2970.

95.   Park, T. G., Degradation of poly(lactic-co-glycolic acid) microspheres: effect of copolymer composition. *Biomaterials* **1995,** *16* (15), 1123-30.

96.   Lu, L.; Garcia, C. A.; Mikos, A. G., In vitro degradation of thin poly(DL-lactic-co-glycolic acid) films. *J Biomed Mater Res* **1999,** *46* (2), 236-244.

97.   Sugiura, T.; Tara, S.; Nakayama, H.; Yi, T.; Lee, Y. U.; Shoji, T.; Breuer, C. K.; Shinoka, T., Fast-degrading bioresorbable arterial vascular graft with high cellular infiltration inhibits calcification of the graft. *J Vasc Surg* **2017,** *66* (1), 243-250.

98.   Yang, X.; Wei, J.; Lei, D.; Liu, Y.; Wu, W., Appropriate density of PCL nano-fiber sheath promoted muscular remodeling of PGS/PCL grafts in arterial circulation. *Biomaterials* **2016,** *88*, 34-47.

99.   Lee, H.; Yoon, H.; Kim, G., Highly oriented electrospun polycaprolactone micro/nanofibers prepared by a field-controllable electrode and rotating collector. *Applied Physics A* **2009,** *97* (3), 559-565.

100.   Sprott, M. R.; Gallego-Ferrer, G.; Dalby, M. J.; Salmeron-Sanchez, M.; Cantini, M., Functionalization of PLLA with Polymer Brushes to Trigger the Assembly of Fibronectin into Nanonetworks. *Adv Healthc Mater* **2019,** *8* (3), e1801469.

101. Roberts, M. J.; Bentley, M. D.; Harris, J. M., Chemistry for peptide and protein PEGylation. *Adv Drug Deliv Rev* **2002,** *54* (4), 459-76.

102. Trappmann, B.; Gautrot, J. E.; Connelly, J. T.; Strange, D. G.; Li, Y.; Oyen, M. L.; Cohen Stuart, M. A.; Boehm, H.; Li, B.; Vogel, V.; Spatz, J. P.; Watt, F. M.; Huck, W. T., Extracellular-matrix tethering regulates stem-cell fate. *Nat Mater* **2012,** *11* (7), 642-9.

103. Protein and Peptide Conjugation to Polymers and Surfaces Using Oxime Chemistry. In *Click Chemistry for Biotechnology and Materials Science*, pp 53-68.

104. Hoyle, C. E.; Bowman, C. N., Thiol-ene click chemistry. *Angew Chem Int Ed Engl* **2010,** *49* (9), 1540-73.

105. Bao, Y. S.; Zhaorigetu, B.; Agula, B.; Baiyin, M.; Jia, M., Aminolysis of aryl ester using tertiary amine as amino donor via C-O and C-N bond activations. *J Org Chem* **2014,** *79* (2), 803-8.

106. Ju, M.; Gong, F.; Cheng, S.; Gao, Y., - Fast and Convenient Synthesis of Amine-Terminated Polylactide as a Macroinitiator for <svg style="vertical-align:-0.18pt;width:15.525px;" id="M1" height="10.7" version="1.1" viewBox="0 0 15.525 10.7" width="15.525" xmlns:xlink="http://www.w3.org/1999/xlink" xmlns="http://www.w3.org/2000/svg">. **2011,** *- 2011*.

107. Zhang, Z.; Gupte, M. J.; Jin, X.; Ma, P. X., Injectable Peptide Decorated Functional Nanofibrous Hollow Microspheres to Direct Stem Cell Differentiation and Tissue Regeneration. *Adv Funct Mater* **2015,** *25* (3), 350-360.

108. Diaz, D. D.; Rajagopal, K.; Strable, E.; Schneider, J.; Finn, M. G., "Click" chemistry in a supramolecular environment: stabilization of organogels by copper(I)-catalyzed azide-alkyne [3 + 2] cycloaddition. *J Am Chem Soc* **2006,** *128* (18), 6056-7.

109. Copper-Catalyzed 'Click' Chemistry for Surface Engineering. In *Click Chemistry for Biotechnology and Materials Science*, pp 291-307.

110. Presolski, S. I.; Hong, V. P.; Finn, M. G., Copper-Catalyzed Azide-Alkyne Click Chemistry for Bioconjugation. *Curr Protoc Chem Biol* **2011,** *3* (4), 153-162.

111. Himo, F.; Lovell, T.; Hilgraf, R.; Rostovtsev, V. V.; Noodleman, L.; Sharpless, K. B.; Fokin, V. V., Copper(I)-catalyzed synthesis of azoles. DFT study predicts unprecedented reactivity and intermediates. *J Am Chem Soc* **2005,** *127* (1), 210-6.

112. Fluorogenic Copper(I)-Catalyzed Azide–Alkyne Cycloaddition Reactions and their Applications in Bioconjugation. In *Click Chemistry for Biotechnology and Materials Science*, pp 327-353.

113. Kolb, H. C.; Finn, M. G.; Sharpless, K. B., Click Chemistry: Diverse Chemical Function from a Few Good Reactions. *Angew Chem Int Ed Engl* **2001,** *40* (11), 2004-2021.

114. Copper-Free Click Chemistry. In *Click Chemistry for Biotechnology and Materials Science*, pp 29-51.

115. Yi, G.; Son, J.; Yoo, J.; Park, C.; Koo, H., Application of click chemistry in nanoparticle modification and its targeted delivery. *Biomater Res* **2018,** *22*, 13.

116. Mudgal, M. M.; Birudukota, N.; Doke, M. A., Applications of Click Chemistry in the Development of HIV Protease Inhibitors. *Int J Med Chem* **2018,** *2018*, 2946730.

117. Kalelkar, P. P.; Geng, Z.; Finn, M. G.; Collard, D. M., Azide-Substituted Polylactide: A Biodegradable Substrate for Antimicrobial Materials via Click Chemistry Attachment of Quaternary Ammonium Groups. *Biomacromolecules* **2019,** *20* (9), 3366-3374.

118. Gotsbacher, M. P.; Codd, R., Azido-Desferrioxamine Siderophores as Functional Click-Chemistry Probes Generated in Culture upon Adding a Diazo-Transfer Reagent. *Chembiochem* **2019**.

119. Deane, C., Bioorthogonal chemistry: Click on, click off. *Nat Chem Biol* **2017,** *13* (10), 1057.

120. Koo, H.; Choi, M.; Kim, E.; Hahn, S. K.; Weissleder, R.; Yun, S. H., Bioorthogonal Click Chemistry-Based Synthetic Cell Glue. *Small* **2015,** *11* (48), 6458-66.

121. Pereira, R. F.; Barrias, C. C.; Bartolo, P. J.; Granja, P. L., Cell-instructive pectin hydrogels crosslinked via thiol-norbornene photo-click chemistry for skin tissue engineering. *Acta Biomater* **2018,** *66*, 282-293.

122. Mohanty, N.; Vass, I.; Demeter, S., Copper Toxicity Affects Photosystem II Electron Transport at the Secondary Quinone Acceptor, Q(B). *Plant Physiol* **1989,** *90* (1), 175-9.

123. Aston, N. S.; Watt, N.; Morton, I. E.; Tanner, M. S.; Evans, G. S., Copper toxicity affects proliferation and viability of human hepatoma cells (HepG2 line). *Hum Exp Toxicol* **2000,** *19* (6), 367-76.

124. Arredondo, M.; Cambiazo, V.; Tapia, L.; Gonzalez-Aguero, M.; Nunez, M. T.; Uauy, R.; Gonzalez, M., Copper overload affects copper and iron metabolism in Hep-G2 cells. *Am J Physiol Gastrointest Liver Physiol* **2004,** *287* (1), G27-32.

125. Rostovtsev, V. V.; Green, L. G.; Fokin, V. V.; Sharpless, K. B., A stepwise huisgen cycloaddition process: copper(I)-catalyzed regioselective "ligation" of azides and terminal alkynes. *Angew Chem Int Ed Engl* **2002,** *41* (14), 2596-9.

126. Baskin, J. M.; Prescher, J. A.; Laughlin, S. T.; Agard, N. J.; Chang, P. V.; Miller, I. A.; Lo, A.; Codelli, J. A.; Bertozzi, C. R., Copper-free click chemistry for dynamic in vivo imaging. *Proc Natl Acad Sci U S A* **2007,** *104* (43), 16793-7.

127. Kalia, J.; Raines, R. T., Hydrolytic stability of hydrazones and oximes. *Angew Chem Int Ed Engl* **2008,** *47* (39), 7523-6.

128. Kolmel, D. K.; Kool, E. T., Oximes and Hydrazones in Bioconjugation: Mechanism and Catalysis. *Chem Rev* **2017,** *117* (15), 10358-10376.

129. Marsili, L.; Franceschi, G.; Galliani, C.; Sanfilippo, A.; Vigevani, A., New rifamycins. II. Synthesis and biological activity of oximes, hydrazones, and semicarbazones of 3-N-(piperidin-4-one)rifamycin S. *Farmaco Sci* **1982,** *37* (12), 781-6.

130. Morales, S.; Acena, J. L.; Garcia Ruano, J. L.; Cid, M. B., Sustainable Synthesis of Oximes, Hydrazones, and Thiosemicarbazones under Mild Organocatalyzed Reaction Conditions. *J Org Chem* **2016,** *81* (20), 10016-10022.

131. Verma, K. K., Spot-test detection of aryl hydrazines, hydrazones, osazones, oximes and aromatic amines. *Talanta* **1979,** *26* (3), 257-9.

132. Matson, J. B.; Stupp, S. I., Drug release from hydrazone-containing peptide amphiphiles. *Chem Commun (Camb)* **2011,** *47* (28), 7962-4.

133. Xu, W.; Ding, J.; Xiao, C.; Li, L.; Zhuang, X.; Chen, X., Versatile preparation of intracellular-acidity-sensitive oxime-linked polysaccharide-doxorubicin conjugate for malignancy therapeutic. *Biomaterials* **2015,** *54*, 72-86.

134. Xu, W.; Ding, J.; Xiao, C.; Li, L.; Zhuang, X.; Chen, X., Corrigendum to "Versatile preparation of intracellular-acidity-sensitive oxime-linked polysaccharide-doxorubicin conjugate for malignancy therapeutic" [Biomaterials 54 (2015) 72-86]. *Biomaterials* **2018,** *163*, 88.

135. Hardy, J. G.; Lin, P.; Schmidt, C. E., Biodegradable hydrogels composed of oxime crosslinked poly(ethylene glycol), hyaluronic acid and collagen: a tunable platform for soft tissue engineering. *J Biomater Sci Polym Ed* **2015,** *26* (3), 143-61.

136. Baker, A. E. G.; Bahlmann, L. C.; Tam, R. Y.; Liu, J. C.; Ganesh, A. N.; Mitrousis, N.; Marcellus, R.; Spears, M.; Bartlett, J. M. S.; Cescon, D. W.; Bader, G. D.; Shoichet, M. S., Benchmarking to the Gold Standard: Hyaluronan-Oxime Hydrogels Recapitulate Xenograft Models with In Vitro Breast Cancer Spheroid Culture. *Adv Mater* **2019,** *31* (36), e1901166.

137.   Di Tuoro, D.; Portaccio, M.; Lepore, M.; Arduini, F.; Moscone, D.; Bencivenga, U.; Mita, D. G., An acetylcholinesterase biosensor for determination of low concentrations of Paraoxon and Dichlorvos. *N Biotechnol* **2011,** *29* (1), 132-8.

138.   Lowe, A. B., Thiol-ene "click" reactions and recent applications in polymer and materials synthesis: a first update. *Polymer Chemistry* **2014,** *5* (17), 4820-4870.

139.   Wendeln, C.; Rinnen, S.; Schulz, C.; Arlinghaus, H. F.; Ravoo, B. J., Photochemical microcontact printing by thiol-ene and thiol-yne click chemistry. *Langmuir* **2010,** *26* (20), 15966-71.

140.   Saada, M. C.; Ombouma, J.; Montero, J. L.; Supuran, C. T.; Winum, J. Y., Thiol-ene click chemistry for the synthesis of highly effective glycosyl sulfonamide carbonic anhydrase inhibitors. *Chem Commun (Camb)* **2013,** *49* (50), 5699-701.

141.   Liu, Y.; Hou, W.; Sun, H.; Cui, C.; Zhang, L.; Jiang, Y.; Wu, Y.; Wang, Y.; Li, J.; Sumerlin, B. S.; Liu, Q.; Tan, W., Thiol-ene click chemistry: a biocompatible way for orthogonal bioconjugation of colloidal nanoparticles. *Chem Sci* **2017,** *8* (9), 6182-6187.

142.   Northrop, B. H.; Coffey, R. N., Thiol-ene click chemistry: computational and kinetic analysis of the influence of alkene functionality. *J Am Chem Soc* **2012,** *134* (33), 13804-17.

143.   Lv, Y.; Lin, Z.; Svec, F., "Thiol-ene" click chemistry: a facile and versatile route for the functionalization of porous polymer monoliths. *Analyst* **2012,** *137* (18), 4114-8.

144.   Xin, S.; Wyman, O. M.; Alge, D. L., Assembly of PEG Microgels into Porous Cell-
        Instructive 3D Scaffolds via Thiol-Ene Click Chemistry. *Adv Healthc Mater* **2018,** *7* (11),
        e1800160.

145.   Ruizendaal, L.; Pujari, S. P.; Gevaerts, V.; Paulusse, J. M.; Zuilhof, H., Biofunctional
        silicon nanoparticles by means of thiol-ene click chemistry. *Chem Asian J* **2011,** *6* (10),
        2776-86.

146.   Yao, X.; Zheng, H.; Zhang, Y.; Ma, X.; Xiao, Y.; Wang, Y., Engineering Thiol-Ene
        Click Chemistry for the Fabrication of Novel Structurally Well-Defined Multifunctional
        Cyclodextrin Separation Materials for Enhanced Enantioseparation. *Anal Chem* **2016,** *88*
        (9), 4955-64.

147.   Luong, N. D.; Sinh le, H.; Johansson, L. S.; Campell, J.; Seppala, J., Functional
        graphene by thiol-ene click chemistry. *Chemistry* **2015,** *21* (8), 3183-6.

148.   Wang, J.; Wang, X.; Yan, G.; Fu, S.; Tang, R., pH-sensitive nanogels with ortho ester
        linkages prepared via thiol-ene click chemistry for efficient intracellular drug release. *J
        Colloid Interface Sci* **2017,** *508*, 282-290.

149.   Matheny, M.; McPheeters, M. L.; Glasser, A.; Mercaldo, N.; Weaver, R. B.; Jerome,
        R. N.; Walden, R.; McKoy, J. N.; Pritchett, J.; Tsai, C., In *Systematic Review of
        Cardiovascular Disease Risk Assessment Tools*, Rockville (MD), 2011.

150.   Kaplan, G. A.; Keil, J. E., Socioeconomic factors and cardiovascular disease: a review of
        the literature. *Circulation* **1993,** *88* (4 Pt 1), 1973-98.

151. World Health, O. *Global status report on non-communicable diseases 2010*; 2011.

152. Falk, E.; Shah, P. K.; Fuster, V., Coronary plaque disruption. *Circulation* **1995,** *92* (3), 657-71.

153. Stary, H. C.; Chandler, A. B.; Dinsmore, R. E.; Fuster, V.; Glagov, S.; Insull, W., Jr.; Rosenfeld, M. E.; Schwartz, C. J.; Wagner, W. D.; Wissler, R. W., A definition of advanced types of atherosclerotic lesions and a histological classification of atherosclerosis. A report from the Committee on Vascular Lesions of the Council on Arteriosclerosis, American Heart Association. *Arterioscler Thromb Vasc Biol* **1995,** *15* (9), 1512-31.

154. Stary, H. C.; Chandler, A. B.; Glagov, S.; Guyton, J. R.; Insull, W., Jr.; Rosenfeld, M. E.; Schaffer, S. A.; Schwartz, C. J.; Wagner, W. D.; Wissler, R. W., A definition of initial, fatty streak, and intermediate lesions of atherosclerosis. A report from the Committee on Vascular Lesions of the Council on Arteriosclerosis, American Heart Association. *Circulation* **1994,** *89* (5), 2462-78.

155. Stary, H. C.; Blankenhorn, D. H.; Chandler, A. B.; Glagov, S.; Insull, W., Jr.; Richardson, M.; Rosenfeld, M. E.; Schaffer, S. A.; Schwartz, C. J.; Wagner, W. D.; et al., A definition of the intima of human arteries and of its atherosclerosis-prone regions. A report from the Committee on Vascular Lesions of the Council on Arteriosclerosis, American Heart Association. *Arterioscler Thromb* **1992,** *12* (1), 120-34.

156. Davies, M. J., The pathophysiology of acute coronary syndromes. *Heart* **2000,** *83* (3), 361-6.

157.   Davies, M. J., Pathophysiology of acute coronary syndromes. *Indian Heart J* **2000,** *52* (4), 473-9.

158.   Hashimoto, M.; Greenberg, M. M.; Kow, Y. W.; Hwang, J. T.; Cunningham, R. P., The 2-deoxyribonolactone lesion produced in DNA by neocarzinostatin and other damaging agents forms cross-links with the base-excision repair enzyme endonuclease III. *J Am Chem Soc* **2001,** *123* (13), 3161-2.

159.   Wu, J.; Wu, L.; Xu, X.; Xu, X.; Yin, X.; Chen, Y.; Hu, Y., Microspheres made by w/o/o emulsion method with reduced initial burst for long-term delivery of endostar, a novel recombinant human endostatin. *Journal of Pharmaceutical Sciences* **2009,** *98* (6), 2051-2058.

160.   Wu, W.; Allen, R. A.; Wang, Y., Fast-degrading elastomer enables rapid remodeling of a cell-free synthetic graft into a neoartery. *Nat Med* **2012,** *18* (7), 1148-53.

161.   Wang, Y.; Hu, J.; Jiao, J.; Liu, Z.; Zhou, Z.; Zhao, C.; Chang, L. J.; Chen, Y. E.; Ma, P. X.; Yang, B., Engineering vascular tissue with functional smooth muscle cells derived from human iPS cells and nanofibrous scaffolds. *Biomaterials* **2014,** *35* (32), 8960-9.

162.   Shinoka, T.; Shum-Tim, D.; Ma, P. X.; Tanel, R. E.; Langer, R.; Vacanti, J. P.; Mayer, J. E., Jr., Tissue-engineered heart valve leaflets: does cell origin affect outcome? *Circulation* **1997,** *96* (9 Suppl), II-102-7.

163.   Shinoka, T.; Ma, P. X.; Shum-Tim, D.; Breuer, C. K.; Cusick, R. A.; Zund, G.; Langer, R.; Vacanti, J. P.; Mayer, J. E., Jr., Tissue-engineered heart valves. Autologous valve leaflet replacement study in a lamb model. *Circulation* **1996,** *94* (9 Suppl), II164-8.

164.   Patterson, J. T.; Gilliland, T.; Maxfield, M. W.; Church, S.; Naito, Y.; Shinoka, T.; Breuer, C. K., Tissue-engineered vascular grafts for use in the treatment of congenital heart disease: from the bench to the clinic and back again. *Regenerative Medicine* **2012,** *7* (3), 409-419.

165.   Nemeno-Guanzon, J. G.; Lee, S.; Berg, J. R.; Jo, Y. H.; Yeo, J. E.; Nam, B. M.; Koh, Y. G.; Lee, J. I., Trends in Tissue Engineering for Blood Vessels. *Journal of Biomedicine and Biotechnology* **2012**.

166.   van Haaften, E. E.; Bouten, C. V. C.; Kurniawan, N. A., Vascular Mechanobiology: Towards Control of In Situ Regeneration. *Cells* **2017,** *6* (3).

167.   Li, S.; Sengupta, D.; Chien, S., Vascular tissue engineering: from in vitro to in situ. *Wires Syst Biol Med* **2014,** *6* (1), 61-76.

168.   Cleary, M. A.; Geiger, E.; Grady, C.; Best, C.; Naito, Y.; Breuer, C., Vascular tissue engineering: the next generation. *Trends Mol Med* **2012,** *18* (7), 394-404.

169.   Kurobe, H.; Maxfield, M. W.; Breuer, C. K.; Shinoka, T., Concise review: tissue-engineered vascular grafts for cardiac surgery: past, present, and future. *Stem Cells Transl Med* **2012,** *1* (7), 566-71.

170. Conklin, B. S.; Richter, E. R.; Kreutziger, K. L.; Zhong, D. S.; Chen, C., Development and evaluation of a novel decellularized vascular xenograft. *Med Eng Phys* **2002,** *24* (3), 173-83.

171. Kakisis, J. D.; Liapis, C. D.; Breuer, C.; Sumpio, B. E., Artificial blood vessel: The Holy Grail of peripheral vascular surgery. *J Vasc Surg* **2005,** *41* (2), 349-354.

172. Bos, G. W.; Poot, A. A.; Beugeling, T.; van Aken, W. G.; Feijen, J., Small-diameter vascular graft prostheses: current status. *Arch Physiol Biochem* **1998,** *106* (2), 100-15.

173. Radomski, J. S.; Jarrell, B. E.; Pratt, K. J.; Williams, S. K., Effects of in vitro aging on human endothelial cell adherence to dacron vascular graft material. *J Surg Res* **1989,** *47* (2), 173-7.

174. Hauptmann, S.; Klosterhalfen, B.; Mittermayer, C.; Ruhlmann, K. U.; Kaufmann, R.; Hocker, H., Evidence for macrophage-mediated defluorization of a Teflon vascular graft. *J Mater Sci-Mater M* **1996,** *7* (6), 345-348.

175. Weiss, W. M.; Riles, T. S.; Gouge, T. H.; Mizrachi, H. H., Angiosarcoma at the Site of a Dacron Vascular Prosthesis - a Case-Report and Literature-Review. *J Vasc Surg* **1991,** *14* (1), 87-91.

176. de Valence, S.; Tille, J. C.; Giliberto, J. P.; Mrowczynski, W.; Gurny, R.; Walpoth, B. H.; Moller, M., Advantages of bilayered vascular grafts for surgical applicability and tissue regeneration. *Acta Biomater* **2012,** *8* (11), 3914-20.

177. Soletti, L.; Hong, Y.; Guan, J.; Stankus, J. J.; El-Kurdi, M. S.; Wagner, W. R.; Vorp, D. A., A bilayered elastomeric scaffold for tissue engineering of small diameter vascular grafts. *Acta Biomater* **2010,** *6* (1), 110-22.

178. Gui, L.; Dash, B. C.; Luo, J.; Qin, L.; Zhao, L.; Yamamoto, K.; Hashimoto, T.; Wu, H.; Dardik, A.; Tellides, G.; Niklason, L. E.; Qyang, Y., Implantable tissue-engineered blood vessels from human induced pluripotent stem cells. *Biomaterials* **2016,** *102*, 120-9.

179. Wissing, T. B.; Bonito, V.; Bouten, C. V. C.; Smits, A., Biomaterial-driven in situ cardiovascular tissue engineering-a multi-disciplinary perspective. *NPJ Regen Med* **2017,** *2*, 18.

180. Wang, F.; Mohammed, A.; Li, C.; Ge, P.; Wang, L.; King, M. W., Degradable/non-degradable polymer composites for in-situ tissue engineering small diameter vascular prosthesis application. *Biomed Mater Eng* **2014,** *24* (6), 2127-33.

181. Henry, J. J. D.; Yu, J.; Wang, A.; Lee, R.; Fang, J.; Li, S., Engineering the mechanical and biological properties of nanofibrous vascular grafts for in situ vascular tissue engineering. *Biofabrication* **2017,** *9* (3), 035007.

182. Liu, J.; Qin, Y.; Wu, Y.; Sun, Z.; Li, B.; Jing, H.; Zhang, C.; Li, C.; Leng, X.; Wang, Z.; Kong, D., The surrounding tissue contributes to smooth muscle cells' regeneration and vascularization of small diameter vascular grafts. *Biomater Sci* **2018**.

183. Dong, X.; Yuan, X.; Wang, L.; Liu, J.; Midgley, A. C.; Wang, Z.; Wang, K.; Liu, J.; Zhu, M.; Kong, D., Construction of a bilayered vascular graft with smooth internal

surface for improved hemocompatibility and endothelial cell monolayer formation. *Biomaterials* **2018,** *181*, 1-14.

184. Wang, W.; Hu, J.; He, C.; Nie, W.; Feng, W.; Qiu, K.; Zhou, X.; Gao, Y.; Wang, G., Heparinized PLLA/PLCL nanofibrous scaffold for potential engineering of small-diameter blood vessel: tunable elasticity and anticoagulation property. *J Biomed Mater Res A* **2015,** *103* (5), 1784-97.

185. Lee, S. J.; Kim, M. E.; Nah, H.; Seok, J. M.; Jeong, M. H.; Park, K.; Kwon, I. K.; Lee, J. S.; Park, S. A., Vascular endothelial growth factor immobilized on mussel-inspired three-dimensional bilayered scaffold for artificial vascular graft application: In vitro and in vivo evaluations. *J Colloid Interface Sci* **2019,** *537*, 333-344.

186. Shinoka, T.; Breuer, C. K.; Tanel, R. E.; Zund, G.; Miura, T.; Ma, P. X.; Langer, R.; Vacanti, J. P.; Mayer, J. E., Jr., Tissue engineering heart valves: valve leaflet replacement study in a lamb model. *Ann Thorac Surg* **1995,** *60* (6 Suppl), S513-6.

187. Ravi, S.; Chaikof, E. L., Biomaterials for vascular tissue engineering. *Regen Med* **2010,** *5* (1), 107-20.

188. Sell, S. A.; McClure, M. J.; Garg, K.; Wolfe, P. S.; Bowlin, G. L., Electrospinning of collagen/biopolymers for regenerative medicine and cardiovascular tissue engineering. *Adv Drug Deliv Rev* **2009,** *61* (12), 1007-19.

189. Shinoka, T.; Shum-Tim, D.; Ma, P. X.; Tanel, R. E.; Isogai, N.; Langer, R.; Vacanti, J. P.; Mayer, J. E., Jr., Creation of viable pulmonary artery autografts through tissue engineering. *J Thorac Cardiovasc Surg* **1998,** *115* (3), 536-45; discussion 545-6.

190. Vaz, C. M.; van Tuijl, S.; Bouten, C. V.; Baaijens, F. P., Design of scaffolds for blood vessel tissue engineering using a multi-layering electrospinning technique. *Acta Biomater* **2005,** *1* (5), 575-82.

191. Ye, L.; Wu, X.; Mu, Q.; Chen, B.; Duan, Y.; Geng, X.; Gu, Y.; Zhang, A.; Zhang, J.; Feng, Z. G., Heparin-Conjugated PCL Scaffolds Fabricated by Electrospinning and Loaded with Fibroblast Growth Factor 2. *J Biomater Sci Polym Ed* **2011,** *22* (1-3), 389-406.

192. de Valence, S.; Tille, J. C.; Mugnai, D.; Mrowczynski, W.; Gurny, R.; Moller, M.; Walpoth, B. H., Long term performance of polycaprolactone vascular grafts in a rat abdominal aorta replacement model. *Biomaterials* **2012,** *33* (1), 38-47.

193. Ercolani, E.; Del Gaudio, C.; Bianco, A., Vascular tissue engineering of small-diameter blood vessels: reviewing the electrospinning approach. *J Tissue Eng Regen Med* **2015,** *9* (8), 861-88.

194. Xie, C.; Hu, J.; Ma, H.; Zhang, J.; Chang, L. J.; Chen, Y. E.; Ma, P. X., Three-dimensional growth of iPS cell-derived smooth muscle cells on nanofibrous scaffolds. *Biomaterials* **2011,** *32* (19), 4369-75.

195. Huang, C.; Wang, S.; Qiu, L.; Ke, Q.; Zhai, W.; Mo, X., Heparin loading and pre-endothelialization in enhancing the patency rate of electrospun small-diameter vascular grafts in a canine model. *ACS Appl Mater Interfaces* **2013,** *5* (6), 2220-6.

196. Nieponice, A.; Soletti, L.; Guan, J.; Hong, Y.; Gharaibeh, B.; Maul, T. M.; Huard, J.; Wagner, W. R.; Vorp, D. A., In vivo assessment of a tissue-engineered vascular graft

combining a biodegradable elastomeric scaffold and muscle-derived stem cells in a rat model. *Tissue Eng Part A* **2010,** *16* (4), 1215-23.

197. Li, W.; Chen, J.; Xu, P.; Zhu, M.; Wu, Y.; Wang, Z.; Zhao, T.; Cheng, Q.; Wang, K.; Fan, G.; Zhu, Y.; Kong, D., Long-term evaluation of vascular grafts with circumferentially aligned microfibers in a rat abdominal aorta replacement model. *J Biomed Mater Res B Appl Biomater* **2018,** *106* (7), 2596-2604.

198. Higutchi, C.; Sarraf, Y. S.; Nardino, E. P.; Pereira, W. M. G.; Daboin, B. E. G.; Carvalho, L. E. W.; Correa, J. A., Vascular Reconstruction Technique Using a Tubular Graft for Leiomyosarcoma of the Inferior Vena Cava: A Case Report. *EJVES Short Rep* **2017,** *36*, 5-8.

199. Kricheldorf, H. R.; Kreiser-Saunders, I.; Stricker, A., Polylactones 48. SnOct(2)-initiated polymerizations of lactide: A mechanistic study. *Macromolecules* **2000,** *33* (3), 702-709.

200. Fiore, G. L.; Jing, F.; Young, J. V. G.; Cramer, C. J.; Hillmyer, M. A., High Tg aliphatic polyesters by the polymerization of spirolactide derivatives. *Polymer Chemistry* **2010,** *1* (6), 870-877.

201. Corneillie, S.; Smet, M., PLA architectures: the role of branching. *Polymer Chemistry* **2015,** *6* (6), 850-867.

202. Jing, F.; Hillmyer, M. A., A bifunctional monomer derived from lactide for toughening polylactide. *J Am Chem Soc* **2008,** *130* (42), 13826-7.

203.   Smith, L. A.; Ma, P. X., Computer-designed nano-fibrous scaffolds. *Methods Mol Biol* **2012,** *868*, 125-34.

204.   Wei, G.; Jin, Q.; Giannobile, W. V.; Ma, P. X., The enhancement of osteogenesis by nano-fibrous scaffolds incorporating rhBMP-7 nanospheres. *Biomaterials* **2007,** *28* (12), 2087-96.

205.   Jin, Q.; Wei, G.; Lin, Z.; Sugai, J. V.; Lynch, S. E.; Ma, P. X.; Giannobile, W. V., Nanofibrous scaffolds incorporating PDGF-BB microspheres induce chemokine expression and tissue neogenesis in vivo. *PLoS One* **2008,** *3* (3), e1729.

206.   Lohmeijer, B. G. G.; Pratt, R. C.; Leibfarth, F.; Logan, J. W.; Long, D. A.; Dove, A. P.; Nederberg, F.; Choi, J.; Wade, C.; Waymouth, R. M.; Hedrick, J. L., Guanidine and amidine organocatalysts for ring-opening polymerization of cyclic esters. *Macromolecules* **2006,** *39* (25), 8574-8583.

207.   Wang, J.; Ma, H.; Jin, X.; Hu, J.; Liu, X.; Ni, L.; Ma, P. X., The effect of scaffold architecture on odontogenic differentiation of human dental pulp stem cells. *Biomaterials* **2011,** *32* (31), 7822-30.

208.   Qiang, N.; Tang, S.; Shi, X. J.; Li, H.; Ma, Y. H.; Tao, H. X.; Lin, Q., Synthesis of functional polyester for fabrication of nano-fibrous scaffolds and its effect on PC12 cells. *J Biomater Sci Polym Ed* **2016,** *27* (3), 191-201.

209.   Sun, H.; Feng, K.; Hu, J.; Soker, S.; Atala, A.; Ma, P. X., Osteogenic differentiation of human amniotic fluid-derived stem cells induced by bone morphogenetic protein-7 and enhanced by nanofibrous scaffolds. *Biomaterials* **2010,** *31* (6), 1133-9.

210. Roh, J. D.; Sawh-Martinez, R.; Brennan, M. P.; Jay, S. M.; Devine, L.; Rao, D. A.; Yi, T.; Mirensky, T. L.; Nalbandian, A.; Udelsman, B.; Hibino, N.; Shinoka, T.; Saltzman, W. M.; Snyder, E.; Kyriakides, T. R.; Pober, J. S.; Breuer, C. K., Tissue-engineered vascular grafts transform into mature blood vessels via an inflammation-mediated process of vascular remodeling. *Proc Natl Acad Sci U S A* **2010,** *107* (10), 4669-74.

211. Yu, X.; Yang, Y.; Xu, H., *Lightweight Materials from Biopolymers and Biofibers*. American Chemical Society: 2014; Vol. 1175, p 0.

212. van Luyn, M. J.; Plantinga, J. A.; Brouwer, L. A.; Khouw, I. M.; de Leij, L. F.; van Wachem, P. B., Repetitive subcutaneous implantation of different types of (biodegradable) biomaterials alters the foreign body reaction. *Biomaterials* **2001,** *22* (11), 1385-91.

213. Soletti, L.; Nieponice, A.; Guan, J.; Stankus, J. J.; Wagner, W. R.; Vorp, D. A., A seeding device for tissue engineered tubular structures. *Biomaterials* **2006,** *27* (28), 4863-70.

214. Anderson, J. M.; Rodriguez, A.; Chang, D. T., Foreign body reaction to biomaterials. *Semin Immunol* **2008,** *20* (2), 86-100.

215. Trindade, R.; Albrektsson, T.; Tengvall, P.; Wennerberg, A., Foreign Body Reaction to Biomaterials: On Mechanisms for Buildup and Breakdown of Osseointegration. *Clin Implant Dent Relat Res* **2016,** *18* (1), 192-203.

216. Song, L.; Zhou, Q.; Duan, P.; Guo, P.; Li, D.; Xu, Y.; Li, S.; Luo, F.; Zhang, Z., Successful development of small diameter tissue-engineering vascular vessels by our novel integrally designed pulsatile perfusion-based bioreactor. *PLoS One* **2012,** *7* (8), e42569.

217. Tara, S.; Kurobe, H.; Rocco, K. A.; Maxfield, M. W.; Best, C. A.; Yi, T.; Naito, Y.; Breuer, C. K.; Shinoka, T., Well-organized neointima of large-pore poly(L-lactic acid) vascular graft coated with poly(L-lactic-co-epsilon-caprolactone) prevents calcific deposition compared to small-pore electrospun poly(L-lactic acid) graft in a mouse aortic implantation model. *Atherosclerosis* **2014,** *237* (2), 684-91.

218. Hinderer, S.; Brauchle, E.; Schenke-Layland, K., Generation and Assessment of Functional Biomaterial Scaffolds for Applications in Cardiovascular Tissue Engineering and Regenerative Medicine. *Adv Healthc Mater* **2015,** *4* (16), 2326-41.

219. Wei, G.; Jin, Q.; Giannobile, W. V.; Ma, P. X., Nano-fibrous scaffold for controlled delivery of recombinant human PDGF-BB. *J Control Release* **2006,** *112* (1), 103-10.

220. Liu, X.; Jin, X.; Ma, P. X., Nanofibrous hollow microspheres self-assembled from star-shaped polymers as injectable cell carriers for knee repair. *Nat Mater* **2011,** *10* (5), 398-406.

221. Pan, Z.; Ding, J., Poly(lactide-co-glycolide) porous scaffolds for tissue engineering and regenerative medicine. *Interface Focus* **2012,** *2* (3), 366-77.

222. Liu, Q.; Wang, J.; Chen, Y.; Zhang, Z.; Saunders, L.; Schipani, E.; Chen, Q.; Ma, P. X., Suppressing mesenchymal stem cell hypertrophy and endochondral ossification in 3D

cartilage regeneration with nanofibrous poly(l-lactic acid) scaffold and matrilin-3. *Acta Biomater* **2018,** *76*, 29-38.

223.   Das, S.; Bellare, J. R., Dental Pulp Stem Cells in Customized 3D Nanofibrous Scaffolds for Regeneration of Peripheral Nervous System. *Methods Mol Biol* **2018**.

224.   Wang, J.; Liu, X.; Jin, X.; Ma, H.; Hu, J.; Ni, L.; Ma, P. X., The odontogenic differentiation of human dental pulp stem cells on nanofibrous poly(L-lactic acid) scaffolds in vitro and in vivo. *Acta Biomater* **2010,** *6* (10), 3856-63.

225.   Wang, C. C.; Lin, L. H.; Chen, C. W.; Lo, Y. C., Surface Modification of Poly(lactic acid) Fabrics with Plasma Pretreatment and Chitosan/Siloxane Polyesters Coating for Color Strength Improvement. *Polymers (Basel)* **2017,** *9* (8).

226.   Britner, J.; Ritter, H., Self-Activation of Poly(methylenelactide) through Neighboring-Group Effects: A Sophisticated Type of Reactive Polymer. *Macromolecules* **2015,** *48* (11), 3516-3522.

227.   Bailey, W. J.; Ni, Z.; Wu, S.-R., Synthesis of poly-ϵ-caprolactone via a free radical mechanism. Free radical ring-opening polymerization of 2-methylene-1,3-dioxepane. *Journal of Polymer Science: Polymer Chemistry Edition* **1982,** *20* (11), 3021-3030.

228.   Bailey, W. J.; Zhou, L. L., A New Elimination with Phase-Transfer Catalysis for Cyclic Ketene Acetals. *Tetrahedron Lett* **1991,** *32* (12), 1539-1540.

229. Liu, M.; Xie, C.; Pan, H.; Pan, J.; Lu, W., Separation of polyethylene glycols and their fluorescein-labeled compounds depending on the hydrophobic interaction by high-performance liquid chromatography. *J Chromatogr A* **2006,** *1129* (1), 61-6.

230. Ju, M.; Gong, F.; Cheng, S.; Gao, Y., Fast and Convenient Synthesis of Amine-Terminated Polylactide as a Macroinitiator for -Benzyloxycarbonyl-L-Lysine-N-Carboxyanhydrides. *International Journal of Polymer Science* **2011,** *2011*, 7.

231. Eckert, F.; Klamt, A., Accurate prediction of basicity in aqueous solution with COSMO-RS. *J Comput Chem* **2006,** *27* (1), 11-9.

232. Bryantsev, V. S.; Diallo, M. S.; Goddard, W. A., 3rd, pKa calculations of aliphatic amines, diamines, and aminoamides via density functional theory with a Poisson-Boltzmann continuum solvent model. *J Phys Chem A* **2007,** *111* (20), 4422-30.

233. Fitch, C. A.; Platzer, G.; Okon, M.; Garcia-Moreno, B. E.; McIntosh, L. P., Arginine: Its pKa value revisited. *Protein Sci* **2015,** *24* (5), 752-61.

234. Corona-Avendano, S.; Alarcon-Angeles, G.; Rosquete-Pina, G. A.; Rojas-Hernandez, A.; Gutierrez, A.; Ramirez-Silva, M. T.; Romero-Romo, M.; Palomar-Pardave, M., New insights on the nature of the chemical species involved during the process of dopamine deprotonation in aqueous solution: theoretical and experimental study. *J Phys Chem B* **2007,** *111* (7), 1640-7.

235. Rossini, E.; Bochevarov, A. D.; Knapp, E. W., Empirical Conversion of pK a Values between Different Solvents and Interpretation of the Parameters: Application to Water, Acetonitrile, Dimethyl Sulfoxide, and Methanol. *ACS Omega* **2018,** *3* (2), 1653-1662.

236. Mahato, R. I., *Biomaterials for delivery and targeting of proteins and nucleic acids*. CRC Press: Boca Raton :, 2005; Vol. Boca Raton :.

237. Kim, K. K.; Pack, D. W., Microspheres for Drug Delivery. In *BioMEMS and Biomedical Nanotechnology: Volume I Biological and Biomedical Nanotechnology*, Ferrari, M.; Lee, A. P.; Lee, L. J., Eds. Springer US: Boston, MA, 2006; pp 19-50.

238. Muzykantov, V. R., *Targeted Drug Delivery to Endothelial Adhesion Molecules*. 2013; Vol. 2013, p 27.

239. Reischl, D.; Zimmer, A., Drug delivery of siRNA therapeutics: potentials and limits of nanosystems. *Nanomedicine* **2009,** *5* (1), 8-20.

240. Rives, C. B., *Tissue engineering scaffolds for protein and DNA delivery: A platform for islet transplantation*. ProQuest: 2008.

241. Liu, X.; Won, Y.; Ma, P. X., Porogen-induced surface modification of nano-fibrous poly(L-lactic acid) scaffolds for tissue engineering. *Biomaterials* **2006,** *27* (21), 3980-7.